

**RESILIENT MODULUS AND FATIGUE LIFE
CHARACTERIZATION OF ASPHALT CONCRETE
MIXTURES USED IN THE OHIO TEST ROAD**

Special Student Study



PB99-113516

FINAL REPORT State Job No. 14663(0)

May 1998

**Submitted to
The Ohio Department of Transportation**



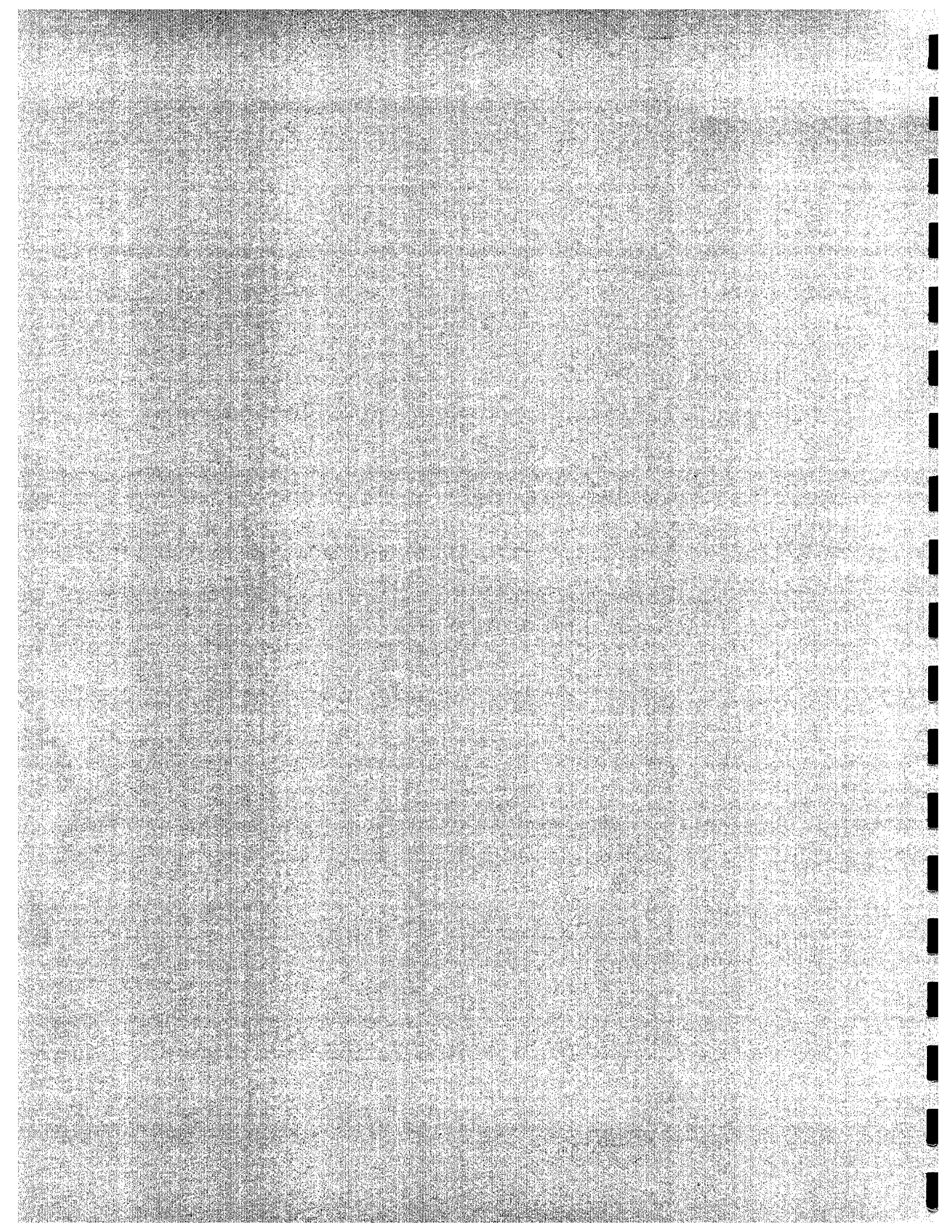
by


J. Ludwig Figueroa and Paul W. Debuty

**Department of Civil Engineering
CASE WESTERN RESERVE UNIVERSITY
Cleveland, Ohio 44106**

**Prepared in cooperation with the Ohio Department of Transportation and
the U.S. Department of Transportation, Federal Highway Administration.**

REPRODUCED BY: **NTIS**
U.S. Department of Commerce
National Technical Information Service
Springfield, Virginia 22161



1. Report No. ST/SS/98-001	 PB99-113516	3. Recipient's Catalog No.	
4. Title and Subtitle RESILIENT MODULUS AND FATIGUE LIFE CHARACTERIZATION OF ASPHALT CONCRETE MIXTURES USED IN THE OHIO TEST ROAD		5. Report Date May, 1997	
		6. Performing Organization Code	
7. Author(s) Ludwig Figueroa, Paul W. DeButy		8. Performing Organization Report No.	
		10. Work Unit No. (TRAIS)	
9. Performing Organization Name and Address Case Western Reserve University Department of Civil Engineering Cleveland, OH 44106		11. Contract or Grant No. State Job No. 14663(0)	
		13. Type of Report and Period Covered Final Report	
12. Sponsoring Agency Name and Address Ohio Department of Transportation 25 S. Front St. Columbus, OH 43215		14. Sponsoring Agency Code	
		15. Supplementary Notes	
16. Abstract <p>The performance of flexible and rigid pavements depends not only on the effects of traffic but also on environmental effects. As part of the Federal Highway Administration's (FHWA) Strategic Highway Research Program (SHRP), a test road was recently constructed on U.S. 23 just North of Delaware, Ohio. This road includes four different sets of sections to study various factors affecting pavement performance. Monitoring environmental factors is of extreme value as they affect subgrade soil and pavement layer properties and subsequently pavement life and performance.</p> <p>Five seasonal instrumentation sites as well as the responsibility for the onsite weather station for the Ohio Test Road were assigned to Case Western Reserve University. Installation and monitoring procedures for subgrade soil moisture content, pavement and subgrade temperature, and frost depth sensors as well as the monitoring of a complete weather station is discussed. The methodology to check the quality of the data is presented along with preliminary results and correlations of use in the eventual development of a mechanistic design procedure. In addition, subgrade soil and AC materials were tested to characterize important properties and to develop useful correlations. Finite element computer analyses were also conducted to determine the influence of seasonal factors on the response of flexible pavement to traffic loads.</p> <p>Specifically, equations were developed to correlate AC temperatures with hourly ambient air temperatures to ultimately determine the resilient modulus. Characteristic resilient modulus values of the fine-grained silty clays found at the site were determined as a function of the degree of saturation. Equations were established relating the AC resilient modulus to temperature for both the surface and intermediate layers. Indirect tensile strength testing was performed at two temperatures on two types of AC with the results being within generally accepted limits. Using material test results, finite element analyses were conducted on an actual pavement section using the program ILLIPAVE. Results show reasonably accurate comparisons for stress, strain, and deflections between pavements modeled with a constant average modulus and those modeled with multiple layers having moduli established by temperature. However, key parameters such as the AC radial tensile strain do not show comparisons justifiable for using uniform moduli analyses.</p>			
17. Key Words Resilient Modulus, AC Elastic Modulus, Ohio Test Road, Mechanistic Pavement Design		18. Distribution Statement No Restrictions. This document is available to the public through the National Technical Information Service, Springfield, Virginia 22161	
19. Security Classif. (of this report) Unclassified	20. Security Classif. (of this page) Unclassified	21. No. of Pages 125	22. Price



**RESILIENT MODULUS AND FATIGUE LIFE CHARACTERIZATION OF
ASPHALT CONCRETE MIXTURES USED IN THE OHIO TEST ROAD**

Special Student Study

FINAL REPORT State Job No. 14663(0)

May 1998

Submitted to
The Ohio Department of Transportation

by

J. Ludwig Figueroa and Paul W. Debuty

Department of Civil Engineering
CASE WESTERN RESERVE UNIVERSITY
Cleveland, Ohio 44106

Prepared in cooperation with the Ohio Department of Transportation and the U.S.
Department of Transportation, Federal Highway Administration.
The opinions, findings and conclusions expressed in this publication are those of the authors

PROTECTED UNDER INTERNATIONAL COPYRIGHT
ALL RIGHTS RESERVED.
NATIONAL TECHNICAL INFORMATION SERVICE
U.S. DEPARTMENT OF COMMERCE



RESILIENT MODULUS AND FATIGUE LIFE CHARACTERIZATION OF ASPHALT CONCRETE MIXTURES USED IN THE OHIO TEST ROAD

Abstract

The performance of flexible and rigid pavements depends not only on the effects of traffic but also on environmental effects. As part of the Federal Highway Administration's (FHWA) Strategic Highway Research Program (SHRP), a test road was recently constructed on U.S. 23 just North of Delaware, Ohio. This road includes four different sets of sections to study various factors affecting pavement performance. Monitoring environmental factors is of extreme value as they affect subgrade soil and pavement layer properties and subsequently pavement life and performance.

Five seasonal instrumentation sites as well as the responsibility for the onsite weather station for the Ohio Test Road were assigned to Case Western Reserve University. Installation and monitoring procedures for subgrade soil moisture content, pavement and subgrade temperature, and frost depth sensors as well as the monitoring of a complete weather station is discussed. The methodology to check the quality of the data is presented along with preliminary results and correlations of use in the eventual development of a mechanistic design procedure. In addition, subgrade soil and AC materials were tested to characterize important properties and to develop useful correlations. Finite element computer analyses were also conducted to determine the influence of seasonal factors on the response of flexible pavement to traffic loads.

Specifically, equations were developed to correlate AC temperatures with hourly ambient air temperatures to ultimately determine the resilient modulus.

Characteristic resilient modulus values of the fine-grained silty clays found at the site were determined as a function of the degree of saturation.

Equations were established relating the AC resilient modulus to temperature for both the surface and intermediate layers. Indirect tensile strength testing was performed at two temperatures on two types of AC with the results being within generally accepted limits.

Using material test results, finite element analyses were conducted on an actual pavement section using the program ILLIPAVE. Results show reasonably accurate comparisons for stress, strain, and deflections between pavements modeled with a constant average modulus and those modeled with multiple layers having moduli established by temperature. However, key parameters such as the AC radial tensile strain do not show comparisons justifiable for using uniform moduli analyses.

Table of Contents

	<u>Page</u>
Abstract	ii
Table of Contents	iv
List of Figures	vii
List of Tables	x
Chapter 1. Introduction	1
Chapter 2. Instrumentation	8
2.1 Overview	8
2.2 Sensors	8
2.2.1 Moisture Content	8
2.2.2 Temperature	12
2.2.3 Frost Depth	13
2.2.4 Ground Water Table Depth	16
2.3 Sensor Preparation	17
2.4 Monitoring Equipment	17
2.4.1 Onsite Equipment	17
2.4.2 Mobile Equipment	18
2.5 Weather Station Components	18
2.5.1 Overview	18
2.5.2 Air Temperature and Relative Humidity	19
2.5.3 Rainfall	19
2.5.4 Wind Speed and Direction	21
2.5.5 Solar Radiation	21
Chapter 3. Sensor Installation	22
3.1 Overview	22
3.2 Sub-Surface Sensor Installation	22
3.2.1 Borings	22
3.2.2 Probe Installation	22
3.2.3 Cable Installation	23
3.3 Onsite Monitoring Equipment Installation	24
Chapter 4. Sensor Monitoring Procedures and Data Analysis	25
4.1 Overview	25
4.2 CR10 Datalogger Setup	25
4.3 Data Retrieval	25

4.3.1. Onsite Unit	25
4.3.2 Mobile Units	26
4.4 Data Analysis	27
4.4.1 SMPCheck Program	28
4.4.2 Procedure	28
4.4.3 Problems	35
4.4.4 AWSCheck Program	36
4.4.5 Procedure	36
4.4.6 Problems	37
Chapter 5. Subgrade Soil and Asphalt Concrete Testing and Characterization	42
5.1 Overview	42
5.2 Subgrade and Embankment Soil Characterization	42
5.2.1 Specific Gravity	42
5.2.2 Moisture-Density Relationships	43
5.2.3 Atterberg Limits	44
5.2.4 Shelby Tube Sampling	45
5.2.5 Subgrade Soil Resilient Modulus	46
5.2.5.1 Overview	46
5.2.5.2 Sample Preparation	48
5.2.5.3 Testing Procedure	50
5.2.5.4 Results	52
5.3 Asphalt Concrete Testing and Characterization	55
5.3.1 Overview	55
5.3.2 Resilient Modulus	56
5.3.2.1 Overview	56
5.3.2.2 Testing Procedure	58
5.3.2.3 Results	59
5.3.3 Indirect Tensile Strength	61
5.3.3.1 Overview	61
5.3.3.2 Procedure	61
5.3.3.3 Results	62
Chapter 6. Flexible Pavement Analysis with ILLIPAVE	63
6.1 Overview	63
6.2 Procedure	64
6.3 Results	66
Chapter 7. Preliminary Seasonal Findings	71
7.1 Overview	71

7.2 Soil Moisture Content and Rainfall Correlations	71
7.2.1 Results and Conclusions	72
7.3 Air and Asphalt Concrete Temperature Correlations	72
7.3.1 Results and Conclusions	73
7.4 Hourly Pavement Temperature Variations	76
7.4.1 Portland Cement Concrete Temperature Variations	76
7.4.2 Results	76
7.4.3 Other Observations	77
Chapter 8. Conclusions and Recommendations	79
Literature Cited	83
Appendix A. ILLIPAVE Results	85
Appendix B. Soil Moisture Content and Rainfall Correlations	98
Appendix C. Air and Asphalt Concrete Temperature Correlations	104
Appendix D. Hourly Pavement Temperature Variations	112

List of Figures

	<u>Page</u>
1.1 Ohio Test Road Instrumentation Layout	4
2.1 Federal Highway Administration Time-Domain Reflectometry Probe	9
2.2 Waveform signal produced by Time-Domain Reflectometry Probe	10
2.3 Measurement Research Corporation Thermistor Assembly	14
2.4 CRREL Resistivity Probe	15
2.5 UT-3 Weather Station	20
4.1 Onsite and Mobile Units for Data Collection	26
4.2 Typical SMPCheck Display of Daily Average Thermistor Temperatures	32
4.3 Typical SMPCheck Display of TDR and Resistivity Data	34
4.4 Typical AWSCheck Display of Daily Humidity, Radiation, and Precipitation Data	38
4.5 Typical AWSCheck Display of Daily Wind Information	39
4.6 Typical AWSCheck Display of Hourly Radiation and Precipitation Data	40
5.1 Moisture-Density Relations for BS02 Subgrade Soil	43
5.2 Moisture-Density Relations for BE15 Embankment Soil	44
5.3 Resilient Modulus Bi-Linear Model	47
5.4 Typical Displacement Pattern for Resilient Modulus Testing	48
5.5 Resilient Modulus Test Sample Preparation	49
5.6 Resilient Modulus Testing Machine	51
5.7 BS02 Resilient Modulus Test Results at 95% Saturation	53
5.8 Sample BS02 Non-Typical Er Test Results	54
5.9 Resilient Modulus vs. Degree of Saturation for BS02 Soil	54
5.10 Resilient Modulus vs. Degree of Saturation for BE15 Soil	55
5.11 Resilient Modulus vs. Temperature for Asphalt Concrete Surface Layer	60
5.12 Resilient Modulus vs. Temperature for Asphalt Concrete Intermediate Layer	60

6.1	SPS9-ODOT Cross Section Used for ILLIPAVE Analysis	64
6.2	Asphalt Concrete Temperature Variations for September 1, 1996	66
6.3	Asphalt Concrete Temperature Variations for January 11, 1997	67
7.1	Thermistor Correlations for SPS9-ODOT	74
7.2	Thermistor Correlations for SPS1-J2	75
A1.	ILLIPAVE Vertical Displacement, 9/1/96 at 8:00 a.m.	86
A2.	ILLIPAVE Vertical Stress, 9/1/96 at 8:00 a.m.	87
A3.	ILLIPAVE Asphalt Concrete Radial Strain, 9/1/96 at 8:00 a.m.	88
A4.	ILLIPAVE Vertical Displacement, 9/1/96 at 3:00 p.m.	89
A5.	ILLIPAVE Vertical Stress, 9/1/96 at 3:00 p.m.	90
A6.	ILLIPAVE Asphalt Concrete Radial Strain, 9/1/96 at 3:00 p.m.	91
A7.	ILLIPAVE Vertical Displacement, 1/11/97 at 8:00 a.m.	92
A8.	ILLIPAVE Vertical Stress, 1/11/97 at 8:00 a.m.	93
A9.	ILLIPAVE Asphalt Concrete Radial Strain, 1/11/97 at 8:00 a.m.	94
A10.	ILLIPAVE Vertical Displacement, 1/11/97 at 4:00 p.m.	95
A11.	ILLIPAVE Vertical Stress, 1/11/97 at 4:00 p.m.	96
A12.	ILLIPAVE Asphalt Concrete Radial Strain, 1/11/97 at 4:00 p.m.	97
B1.	SPS1-J2 Soil Moisture Content and Rainfall Correlation	99
B2.	SPS2-J3 Soil Moisture Content and Rainfall Correlation	100
B3.	SPS2-J5 Soil Moisture Content and Rainfall Correlation	101
B4.	SPS2-J12 Soil Moisture Content and Rainfall Correlation	102
B5.	SPS9-J1 Soil Moisture Content and Rainfall Correlation	103
C1.	AC Temperature vs. Air Temperature: SPS9-ODOT, Thermistor 1	105
C2.	AC Temperature vs. Air Temperature: SPS9-ODOT, Thermistor 2	106
C3.	AC Temperature vs. Air Temperature: SPS9-ODOT, Thermistor 3	107
C4.	Average AC Temperature vs. Air Temperature: SPS9-ODOT	108
C5.	AC Temperature vs. Air Temperature: SPS1-J2, Thermistor 1	109
C6.	AC Temperature vs. Air Temperature: SPS1-J2, Thermistor 2	110
C7.	AC Temperature vs. Air Temperature: SPS1-J2, Thermistor 3	111
D1.	Pavement Temperature, SPS1-J2, August 1 and September 1, 1996	113

D2.	Pavement Temperature, SPS2-J3, August 1 and September 1, 1996	114
D3.	Pavement Temperature, SPS2-J3, October 1 and November 1, 1996	115
D4.	Pavement Temperature, SPS2-J3, December 1, '96 and January 1, '97	116
D5.	Pavement Temperature, SPS2-J5, August 1 and September 1, 1996	117
D6.	Pavement Temperature, SPS2-J5, October 1 and November 1, 1996	118
D7.	Pavement Temperature, SPS2-J5, December 1, '96 and January 1, '97	119
D8.	Pavement Temperature, SPS2-J12, August 1 and September 1, 1996	120
D9.	Pavement Temperature, SPS2-J12, October 1 and November 1, 1996	121
D10.	Pavement Temperature, SPS2-J12, December 1, '96 and January 1, '97	122
D11.	Pavement Temperature, SPS9-ODOT, August 1 and September 1, 1996	123
D12.	Pavement Temperature, SPS9-ODOT, October 1 and November 1, 1996	124
D13.	Pavement Temperature, SPS9-ODOT, Dec. 1, '96 and Jan. 1, '97	125

List of Tables

	<u>Page</u>
1.1 Asphalt Concrete Studies	6
1.2 Portland Cement Concrete Studies	7
4.1 SHRP Section Identification	29
5.1 Specific Gravity of Subgrade and Embankment Soil	42
5.2 Optimum Moisture Content and Maximum Dry Unit Weight	44
5.3 Atterberg Limits	45
5.4 Shelby Tube Dry Unit Weight and Moisture Content	45
5.5 Resilient Modulus Test Results for BS02 at 95% Saturation	52
5.6 Resilient Modulus vs. Degree of Saturation for BS02 and BE15 Soils	56
5.7 Poisson's Ratio for Asphalt Concrete	58
5.8 Resilient Moduli for ASTM Recommended Temperatures	59
5.9 Indirect Tensile Strength	62
6.1 AC Resilient Moduli and Poisson's Ratio for ILLIPAVE Analyses	67
6.2 ILLIPAVE Results for Conditions on September 1, 1996 at 8:00 a.m.	69
6.3 ILLIPAVE Results for Conditions on September 1, 1996 at 3:00 p.m.	69
6.4 ILLIPAVE Results for Conditions on January 11, 1997 at 8:00 a.m.	69
6.5 ILLIPAVE Results for Conditions on January 11, 1997 at 4:00 p.m.	70
7.1 Regression Constants for Air and Asphalt Concrete Temperature Correlations	73
7.2 Maximum Temperature Differentials for Portland Cement Concrete Pavement	77

CHAPTER 1. INTRODUCTION

As part of the Federal Highway Administration's Strategic Highway Research Program (SHRP), a test road was recently constructed by the Ohio Department of Transportation (ODOT) on U.S. 23 just north of Delaware, Ohio. This road includes four different sets of sections that abide by the guidelines for SHRP's Specific Pavement Studies (SPS) which are designed to study various factors affecting pavement performance. Unlike previous test roads, the DEL-23 project encompasses sensors and gauges to monitor the majority of parameters that affect pavement life. These include both seasonal and structural response instrumentation with the capabilities to monitor subgrade soil and pavement temperatures, soil moisture content, frost depth, soil suction, water table elevation, pavement deflection and strain, and soil deflection and stress. In addition, an on-site weather station monitors daily temperature variations, rainfall, solar radiation, relative humidity, wind speed, and wind direction.

As with the AASHO Road Test (American Association of State Highway Officials) from which current pavement design procedures were derived (Sargand 1994, 1), it is intended that data from the DEL-23 study will lead to the development of a mechanistic design procedure. Current empirical design methods do not account for the variations in subgrade soil and pavement properties that greatly affect pavement life and performance. Rather, emphasis is placed on the number and type of loadings that lead to structural failure as characterized by the AASHO Road Test. The need for better design procedures is apparent on many roads today and is required due to the increased volume of traffic, the ability to transport heavier loads, multiple wheel configurations, and the emergence of new construction materials. With the DEL-23 project, researchers will now have the ability to understand the effects of most parameters on pavement life and design. Possible uses of the data may include:

- validation/modification of the AASHTO equation and other design methods
- prediction of pavement performance
- evaluation and improvement of pavement rehabilitation methods
- material characterization and evaluation
- life-cycle cost analysis
- short-term research such as curling and warping of slabs
- development of a mechanistic design procedure (Morse 1996).

To facilitate ease of construction and to optimize benefits, U.S. 23 near Delaware, Ohio was chosen as the site for the test road. Located 25 miles North of Columbus, the three-mile long site provides a uniform subgrade soil together with a flat, straight pathway. With the extra-wide median between the existing north and southbound lanes of U.S. 23, it was possible to construct both lanes of the test road between the existing lanes. This allowed traffic to be maintained during construction and also allows researchers to divert traffic to the old lanes when testing and rehabilitation is necessary.

In abiding by SHRP's guidelines for the Specific Pavement Studies, the Ohio Test Road was designed to include four different SPS sections:

- SPS-1: Strategic Study of Structural Factors for Flexible Pavement
- SPS-2: Strategic Study of Structural Factors for Rigid Pavement
- SPS-8: Study of Environmental Effects in the Absence of Heavy Traffic
- SPS-9: Asphalt Program Field Verification Studies.

SPS-1 encompasses the majority of the three mile Southbound lane with SPS-9 being a small portion at the Southernmost end. To accommodate the control section, SPS-8, an on-ramp to U.S. 23 South was constructed that had access from Norton, a small town with light traffic levels located at the northern end of the project. SPS-2 consists of the entire lane of U.S. 23 North. In all, 38 individual test sections were included in the test road with 18

instrumented to monitor seasonal and structural response, 15 to monitor structural response only, and 5 that contain no instrumentation (Figure 1.1). Five sections were allotted to Case Western Reserve University that include one SPS-1 section, three SPS-2 sections, and one SPS-9 section in addition to responsibility for the monitoring of the weather station. To obtain maximum benefit from the test road, different pavement designs were used between sections with the intention that some would fail sooner than others. Tables 1.1 and 1.2 are a complete list of all variations between the sections.

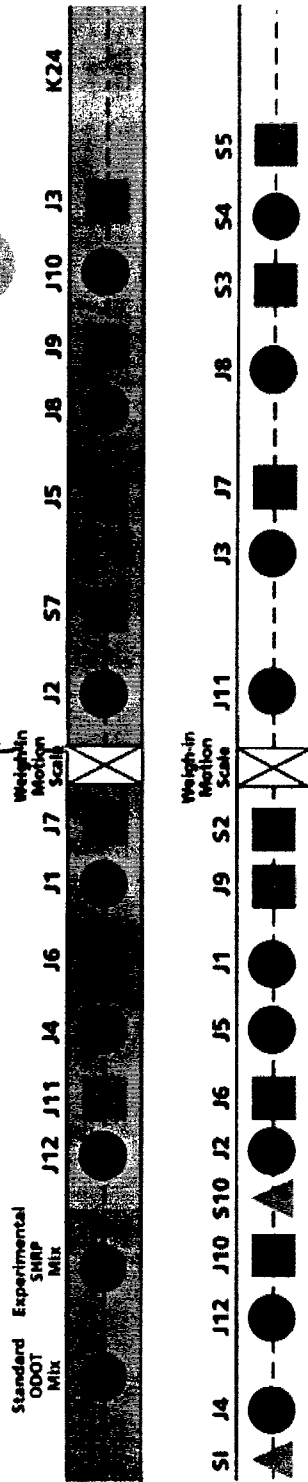
Due to the scope of the DEL-23 project, ODOT enlisted the resources of six Ohio universities to aid in the construction, installation, and monitoring of the test road sensors and equipment. The present study at Case Western Reserve University only involves topics related to seasonal sensor installation and monitoring, thus structural instrumentation and testing will not be addressed in this report. Instead, this discussion will focus on the instrumentation used to monitor soil and pavement temperatures, frost depth, and subgrade moisture content as well as weather station equipment and procedures. Areas that will be addressed include installation, monitoring, data acquisition and analysis, and subgrade soil and asphalt concrete material characterization. A summary of contents of subsequent chapters follows.

Chapter two is a description of the sensors and monitoring equipment used in this study. Included is subgrade soil and pavement sensors, weather station sensors, and onsite and mobile monitoring equipment.

Chapter three describes the installation procedures for seasonal sensors and monitoring equipment.

Chapter four describes data collection and analysis procedures including instructions on the use of the computer programs involved.

SHRP Test Pavement DEL-23-17.48



S.B. RAMP



- Seasonal-Pavement Response
- Pavement Response
- ▲ No Instrumentation

- SPS-1
- SPS-2
- SPS-8
- SPS-9

Chapter five contains the material testing and characterization performed on the subgrade and embankment soils as well as on the asphalt concrete pavement.

Chapter six presents the results of flexible pavement layer finite element analyses that compare the affect of three various modeling techniques for the asphalt concrete resilient modulus. This was performed using ILLIPAVE, a finite element analysis program for pavements.

Chapter seven contains preliminary results and conclusions from initial seasonal instrumentation data.

Chapter eight presents a summary of results with conclusions and recommendations for further research.

Appendix A contains graphs of the ILLIPAVE analyses results from each of the three models at each of the four testing periods. These include plots of vertical deflection, vertical stress, and radial strain as a function of depth from the pavement surface.

Appendix B provides plots of monthly soil volumetric moisture content readings together with daily total precipitation to aid in establishing correlations. Graphs are available for all five CWRU sections between the months of June and December, 1996.

Appendix C contains the graphs and corresponding correlations between asphalt concrete temperature and ambient air temperature based on data obtained from sections SPS1-J2 and SPS9-ODOT. Time spans included run from June 9 to September 4, 1996, and June 13 to November 27, 1996, respectively.

Finally, Appendix D contains graphs of daily pavement temperature variations for the first day of each month between August, 1996 and January, 1997. Data from all CWRU sections was included in the study.

Table 1.1 Asphalt Concrete Studies (Courtesy Sargand, 1994)

SPS-1			
Section	AC Thickness (in)	Base Type and Thickness	Drain
J1	7	8" DGAB	NO
*J2	4	12" DGAB	NO
J3	4	8" ATB	NO
J4	7	12" ATB	NO
J5	4	4" ATB/4" DGAB	NO
J6	7	8" ATB/4" DGAB	NO
J7	4	4" PATB/4" DGAB	YES
J8	7	4" PATB/8" DGAB	YES
J9	7	4" PATB/12" DGAB	YES
J10	7	4" ATB/4" PATB	YES
J11	4	8" ATB/4" PATB	YES
J12	4	12" ATB/4" PATB	YES
S7	7	8" DGAB	NO
K24	7	12" ATB/4" PCTB/6" DGAB	YES
SPS-8			
K13	4	8" DGAB	NO
K14	7	12" DGAB	NO
SPS-9			
SHRP	4	12" ATB/4" PATB/6" DGAB	YES
*ODOT	4	12" ATB/4" PATB/6" DGAB	YES

* Indicates sections assigned to Case Western Reserve University

Table 1.2 Portland Cement Concrete Studies (Courtesy Sargand, 1994)

SPS-2				
Section	PCC LAYER		Base Type and Thickness	Drain
	Strength (psi)	Thickness (in)		
J1	550	8	6" DGAB	NO
J2	900	8	6" DGAB	NO
*J3	550	11	6" DGAB	NO
J4	900	11	6" DGAB	NO
*J5	550	8	6" LCB	NO
J6	900	8	6" LCB	NO
J7	550	11	6" LCB	NO
J8	900	11	6" LCB	NO
J9	550	8	4" PATB/4" DGAB	YES
J10	900	8	4" PATB/4" DGAB	YES
J11	550	11	4" PATB/4" DGAB	YES
*J12	900	11	4" PATB/4" DGAB	YES
S1	900	11	6" DGAB	YES
S2	ODOT	11	4" PCTB/4" DGAB	YES
S3	ODOT	11	4" PCTB/4" DGAB	YES
S4	ODOT	11	6" DGAB	YES
S5	ODOT	11	6" DGAB	YES
S10	ODOT	11	4" PATB/4" DGAB	YES
SPS-8				
J1	550	8	6" DGAB	NO
K15	550	11	6" DGAB	NO

* Indicates sections assigned to Case Western Reserve University

CHAPTER 2. INSTRUMENTATION

2.1 OVERVIEW

The seasonal program within the DEL-23 project involved monitoring of the weather station as well as handling the installation and testing of five seasonal sections for the Seasonal Monitoring Program (SMP). Within these five sections, only soil and asphalt temperature, subgrade moisture content, and frost depth were included in the seasonal instrumentation. This chapter focuses on these three sensors as well as the instruments that comprise the weather station.

2.2 SENSORS

2.2.1 Moisture Content

The moisture content of a soil is required for many important design considerations such as settlement, resilient modulus, and freeze-thaw capacity. Based on similar road tests conducted throughout the U.S., time-domain reflectometry probes (TDR) were chosen as the best instruments available to monitor volumetric water content (Figure 2.1). Installed every six to twelve inches down to depths of six feet, TDR probes consist of a coaxial cable with a three-pronged probe at one end. When an electromagnetic wave is carried to the probe, the time for the pulse to travel from one end of the probe to the other is recorded. The pulse is displayed graphically by the cable tester where the first inflection point represents the wave entering the probe, and a second inflection point is produced when the signal reflects at the end of the probe (Figure 2.2). The time of travel between these two points is a function of the dielectric constant of the soil. Equation 2.1 gives the relationship for finding the dielectric constant of the material:

$$\varepsilon = \left[\frac{(L_a)}{(L)(V_p)} \right]^2 \quad (2.1)$$

FHWA Moisture Probe

Specifications for the FHWA Moisture Probe:

The center rod of the FHWA probe is connected to the signal lead of the coax cable. The other rods are connected to the shield of the coax cable. The probe connect directly to a 50 ohm RG58 coax cable. The end view shows the circuit board used to connect the 0.2 m (8-in) stainless steel rods to the coax cable.

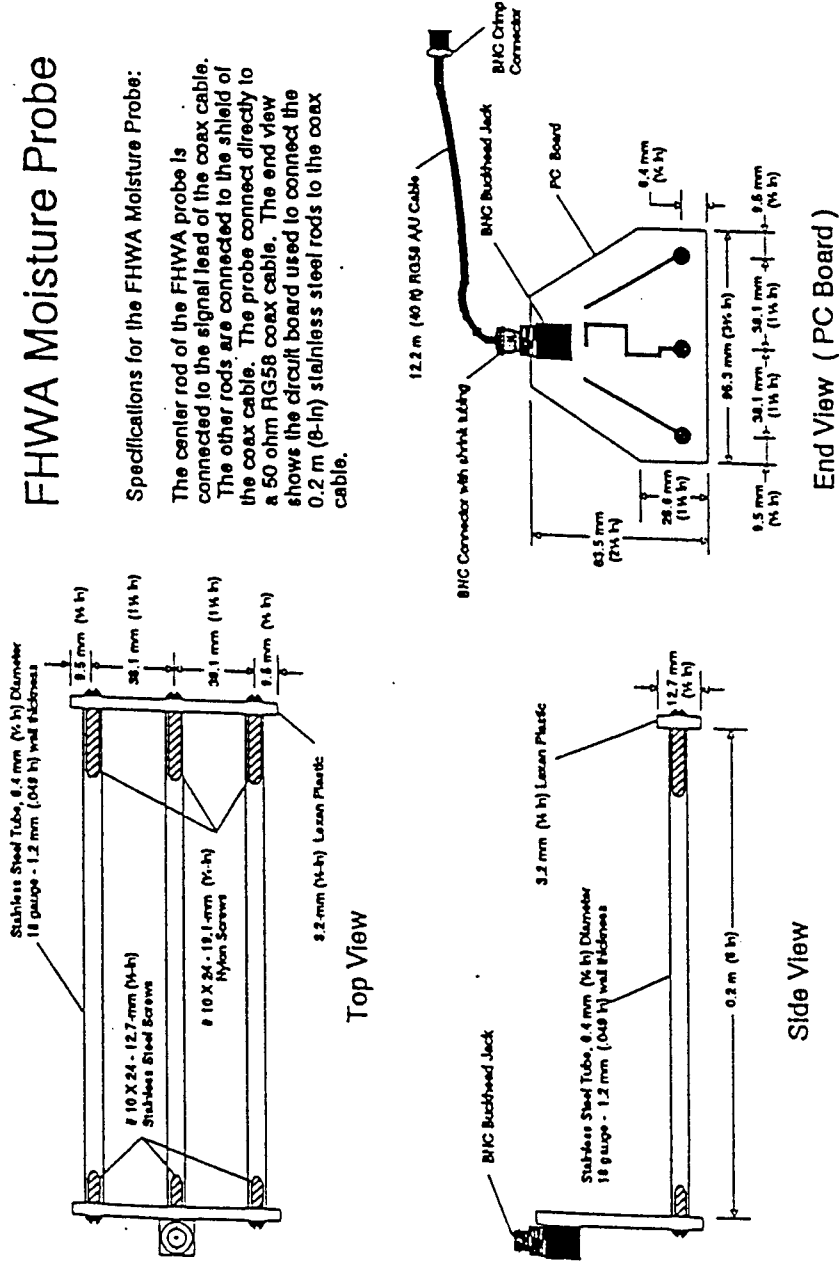


Figure 2.1 Federal Highway Administration Time-Domain Reflectometry Probe (Rada et al., SMP Guidelines, Version 2.1 (1994)).

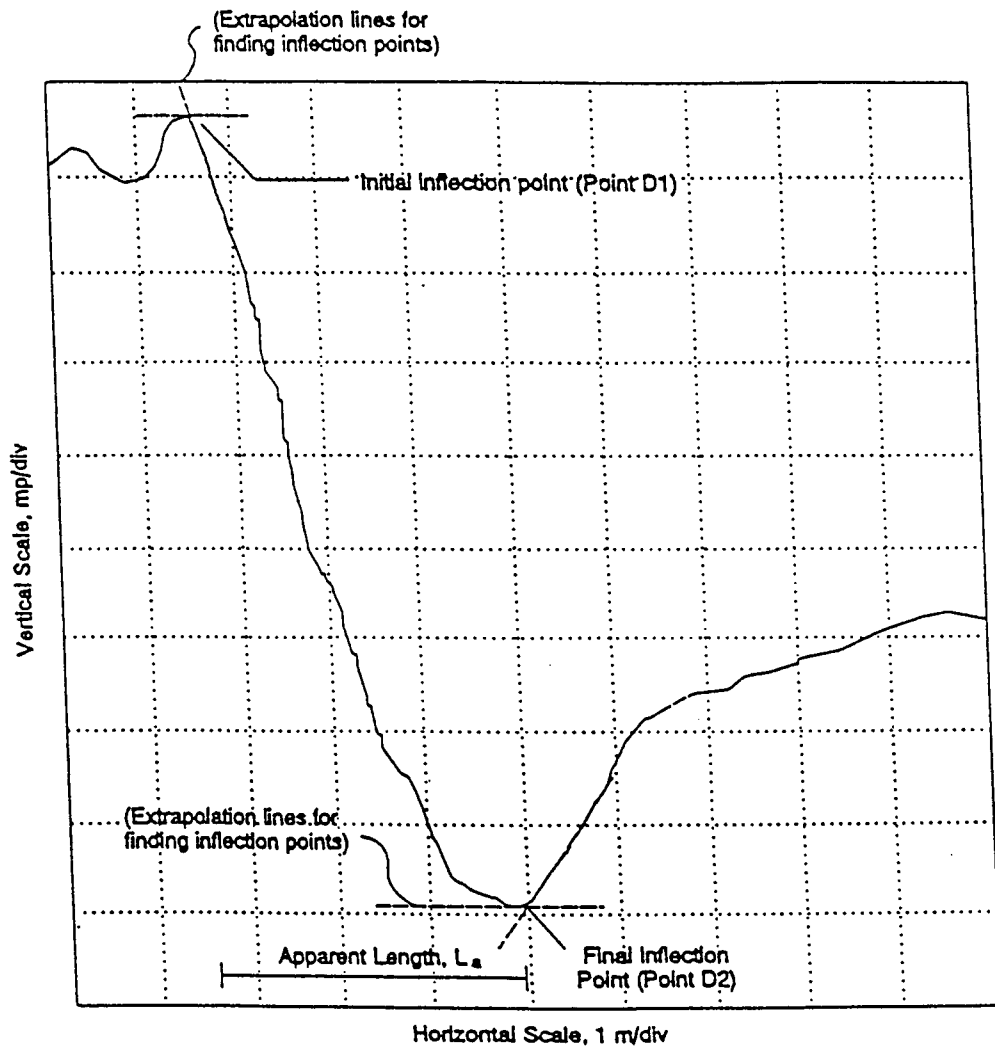


Figure 2.2. Waveform signal produced by TDR probe (Rada et al, SMP Guidelines 1994)

where ϵ = dielectric constant
 L_a = apparent length of probe (horizontal distance between inflection points on trace)
 L = actual length of probes (0.203m for FHWA probe)
 V_p = phase velocity setting on TDR cable tester (usually 0.99); this is the ratio of the actual propagation velocity to the speed of light (Rada et al, 1994, II-3).

The dielectric constant of the soil is in turn calibrated with the soil's volumetric moisture content. For preliminary use, this relationship is given in Equation 2.2 (Topp's Equation), and is based on a previously developed regression equation.

$$\theta = (-0.053 + 0.0293\epsilon - 0.00055\epsilon^2 + 0.0000043\epsilon^3) * 100 \quad (2.2)$$

where θ = volumetric water content, in percent.

Laboratory analysis of soil moisture content for site samples will be used to determine the accuracy of this relationship. Using Equation 2.3, this value is then easily converted to a weight-based moisture content that is used in most design calculations. The end result is the ability to determine the change in the degree of saturation of soils throughout the year from which resilient properties of soils may be inferred.

$$w = \theta \left(\frac{\rho_w}{\rho_d} \right) \quad (2.3)$$

where	w	=	gravimetric water content, in percent.
	θ	=	volumetric water content, in percent.
	ρ_w	=	density of water, gm/cm ³ (= 1.0 gm/cm ³).
	ρ_d	=	dry density of soil, gm/cm ³ .

2.2.2 Temperature

As important as moisture content determination is for subgrade soils, similar is the importance of temperature determination for the majority of pavement layers above the subgrade. Temperature plays a major role in fatigue life and deflection determination as it directly affects resilient modulus and ultimate tensile strength values for asphalt concrete pavements. For Portland cement concrete pavements, the variation of temperature throughout the slab creates curling of the slab which will accentuate the effect of load stresses during certain times of the day. In addition, it will also lead to expansion and contraction in long slabs that is of interest in determining joint performance.

Temperature variations on the test road will be monitored by thermistors, or temperature-sensitive resistors. Slight temperature changes create major variations in resistance values of the thermistors. To find the resistance, a known voltage is applied and the output voltage is read between the thermistors leads. Knowing the change in resistance, Equation 2.4 is used to determine temperature.

$$\frac{1}{T} = C_1 + C_2 \ln R + C_3 (\ln R)^3 \quad (2.4)$$

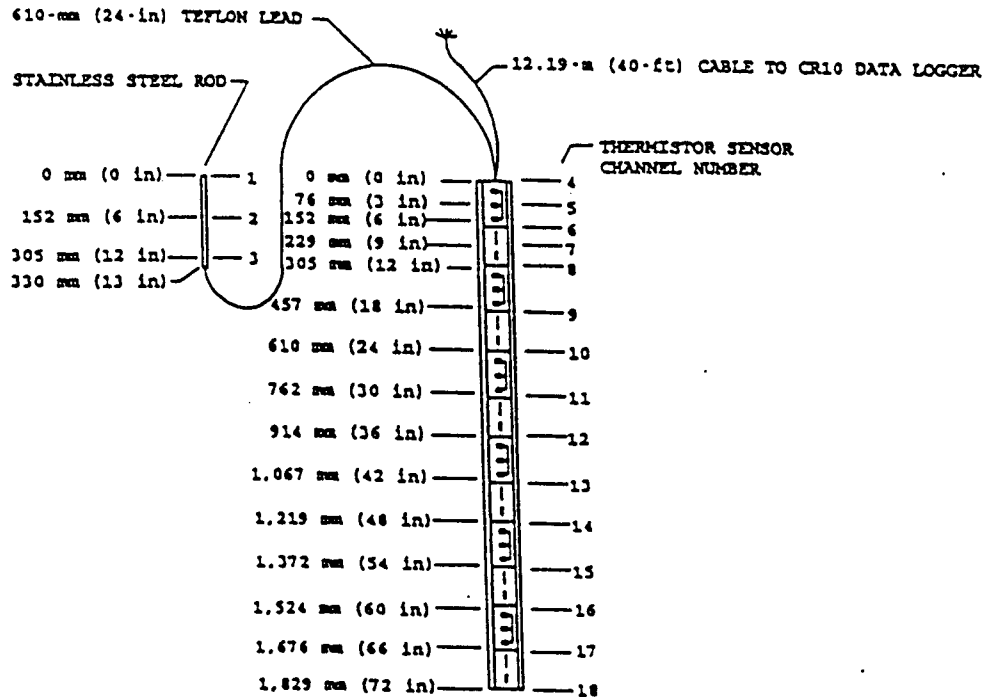
where	T	=	absolute temperature, Kelvin.
	R	=	resistance, ohms.
	C_1, C_2, C_3	=	constants for individual thermistor.

These constants are 9.3441×10^{-4} , 2.2124×10^{-4} , and 1.2665×10^{-7} , respectively for the type of probe used in the DEL-23 project (Rada et al, SMP 1994, II-6). The Measurement Research Corporation (MRC) TP101 thermistor probe (Figure 2.3) was chosen to obtain pavement and soil temperature measurements. This device consists of individual but interconnected probes for both pavement and soil temperature measurements. A variable length metal rod (depending on the pavement thickness) containing up to four thermistors was used for the pavement layer temperature measurements followed by a six foot, clear PVC pipe that housed 15 thermistors for the subgrade soil temperature measurements.

2.2.3 Frost Depth

Since the DEL-23 project is located in a geographic area that experiences multiple freeze/thaw cycles during the year, it is necessary to measure the depth of frost penetration in the subgrade soil as well as the number of freeze/thaw cycles during the winter. This depth is important in determining the thickness of base layers that will limit or prevent frost heave in the soil and pavement. Also, since the stiffness of soils tends to decrease after each freeze/thaw cycle, mechanistic design procedures and overlay design will require this information to lead to a more durable pavement cross section.

After studying the methods available for monitoring frost depth, the Federal Highway Administration (FHWA) considered electrical resistance and resistivity methods to be the most reliable for the DEL-23 project. A probe developed by the U.S. Army Corps of Engineers' Cold Regions Research and Engineering Laboratory (CRREL) was chosen for the program (Figure 2.4). This probe consists of a 73 inch solid PVC pipe upon which 36 metal wire electrodes are mounted and spaced every two inches (Rada et al, SMP 1994, II-8). When a function generator creates an AC

**NOTES:****Dimensions:**

Probe: 1,829 mm x 25 mm (72 in x 1 in) OD
 External Sensors: 330 mm x 6 mm (13 in x 1/4 in) OD

Model TP101

Manufactured by Measurement Research Corporation
 Total of 18 Thermistors
 Degree of accuracy ± 0.1 degree C
 External 330 mm (13 in) Lead attached by 610 mm (24 in)
 of Teflon Wire
 76 mm (3 in) spacing from 0.0 mm (0 in) to 305 mm (12 in)
 and 152 mm (6 in) spacing from 305 mm (12 in) to 1,829 mm
 (72 in) and for the External Lead

Figure 2.3. Measurement Research Corporation Thermistor Assembly
 (Rada et al, SMP Guidelines, Version 2.1 (1994))

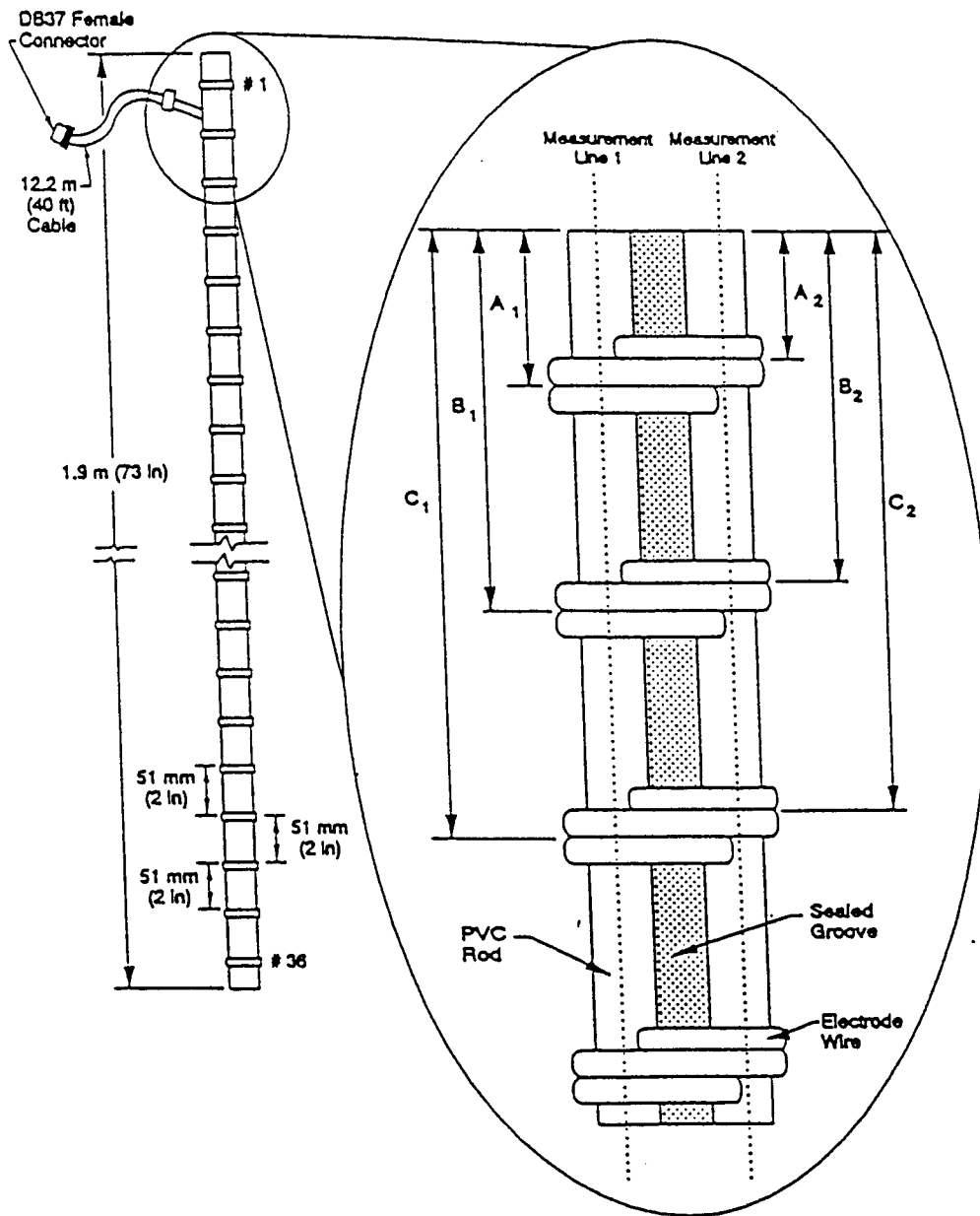


Figure 2.4. CRREL Resistivity Probe (Rada et al, SMP Version 2.1 (1994))

current in two outer electrodes, voltage drop and resistance are measured and compared across the two inside electrodes.

Bulk, or apparent, resistivity can be computed from Equation 2.5:

$$\rho = G \times R = G \times \frac{V}{I} \quad (2.5)$$

where

ρ	=	bulk electrical resistivity, ohm-meter.
G	=	geometric factor for the electrode array, meters.
	=	$4\pi a$, for CRREL sensor
		(a = uniform spacing between electrodes, meters).
R	=	Electrical resistance, ohms.
V	=	Voltage, volts
I	=	Current, amps

Since ice has a much greater electrical resistivity than water, areas of high resistivity will correspond to frozen layers in the subgrade soil.

2.2.4 Ground Water Table Depth

The use of a 14.5 foot long, slotted PVC observation piezometer enables water table depth measurements. Made of two individual 1 inch diameter pipes coupled together, the piezometer is threaded to a metal floor flange or anchor on the bottom of the bore hole. If necessary, this pipe can also serve as a swell-free benchmark for surface level measurements. A total of nine piezometers were installed at various locations throughout the project.

2.3 SENSOR PREPARATION

Prior to installation, all sensors were thoroughly checked for correct operation. Using a walk-in freezer, the thermistors were checked at three different known temperatures after allowing enough time for acclimation. For the resistivity probe, it was only necessary to make sure that continuity existed between the connector pins and the electrodes. This was performed using an Ohmmeter. Finally, the output traces from the TDR probes were checked in several environments. The first trace was taken after shorting the TDR probe with a metal rod placed across the center electrode and one outer electrode. Following this, a trace was taken with the short removed and the probe suspended in air by its main cable. Lastly, a trace was taken with the probe suspended in distilled water of a known temperature. With the above equations, the dielectric constants for air and water could be calculated and compared to known values. If the constants were within an acceptable range, the TDR probe was deemed to be functioning properly.

2.4 MONITORING EQUIPMENT

2.4.1 Onsite Equipment

Because moisture content and frost levels are not expected to vary much throughout the day, these readings are only taken once a month during the monitoring program. Temperature, however, is recorded on an hourly basis. To be able to do this economically, an onsite equipment cabinet is required at each seasonal section. This cabinet houses a CR10 datalogger and the necessary electrical components required for automatic data storage. Due to data storage restrictions, it is necessary to download the stored temperature data to a personal computer once a month. This is performed with the ONSITE program described later. In order to shield the equipment cabinet from possibly harmful weather-related affects, it was mounted to the inside of a concrete pull box installed at each section between the existing road

and the new test road. Each box contains an electrical outlet and houses cables from all sensors installed in the adjacent pavement section.

2.4.2 Mobile Equipment

Unlike the temperature readings, moisture content and frost depth measurements are not stored at the site. Using the mobile equipment, the user must connect all necessary cables once a month in order to monitor and download the data to the personal computer. This equipment consists of two separate cabinets: the first contains a Tektronix 1502B Cable Tester and a CR10 datalogger/controller; the second contains two SDMX50 Multiplexers plus an automated multiplexer for resistivity measurements. The ten TDR cables corresponding to the soil and base moisture sensors are connected to the multiplexers, and the corresponding traces are displayed on the cable tester's screen. The CR10 communicates with the cable tester and multiplexers to monitor and record data. Data can then be downloaded to the microcomputer from the mobile unit using the GraphTerm (GT) program described later.

2.5 WEATHER STATION COMPONENTS

2.5.1 Overview

To monitor climate changes that will enable a possible correlation between surface conditions and soil and pavement conditions, a weather station was installed near the North end of the test road just East of the Northbound lane. This station has the capacity to monitor solar radiation, air temperature, wind speed, wind direction, relative humidity, and rainfall amount.

With hourly air temperature data, a correlation can be established between the average asphalt concrete temperature and the ambient air temperature at various times

of the day. This would then allow for the resilient properties of the asphalt concrete to be directly inferred from the air temperature.

With rainfall data, a correlation can be developed with the subgrade soil moisture content based on TDR readings. As a result, the time lag that exists from the date of rainfall to the period of change in moisture content and soil stiffness could be observed.

For the Portland cement concrete pavement, the relative humidity data may allow for a better understanding of warping in the slabs. In addition, solar radiation data will provide information on drying potential and aging in asphalt concrete. General observations can be made with the wind direction data that will illustrate current prevailing weather patterns. For example, southerly winds usually result in warmer temperatures whereas winds out of the northwest bring colder conditions.

2.5.2 Air Temperature and Relative Humidity

As with the ground temperature measurements, a thermistor is used to measure air temperature variations. This thermistor, manufactured by BetaTHERM, is coupled with a capacitive relative humidity sensor manufactured by Vaisala into one probe (Model HMP35C). Its cable is connected to an additional CR10 mounted in an equipment cabinet on the pole that will monitor and store all weather-related measurements. Working ranges are -36° to 49° C for the thermistor and 0 to 100% relative humidity for the Vaisala sensor. Figure 2.5 is an illustration of the entire weather station.

2.5.3 Rainfall

To monitor rainfall amounts, a tipping bucket rain gauge was installed a few feet away from the weather station pole. When the level of water reaches a calibrated

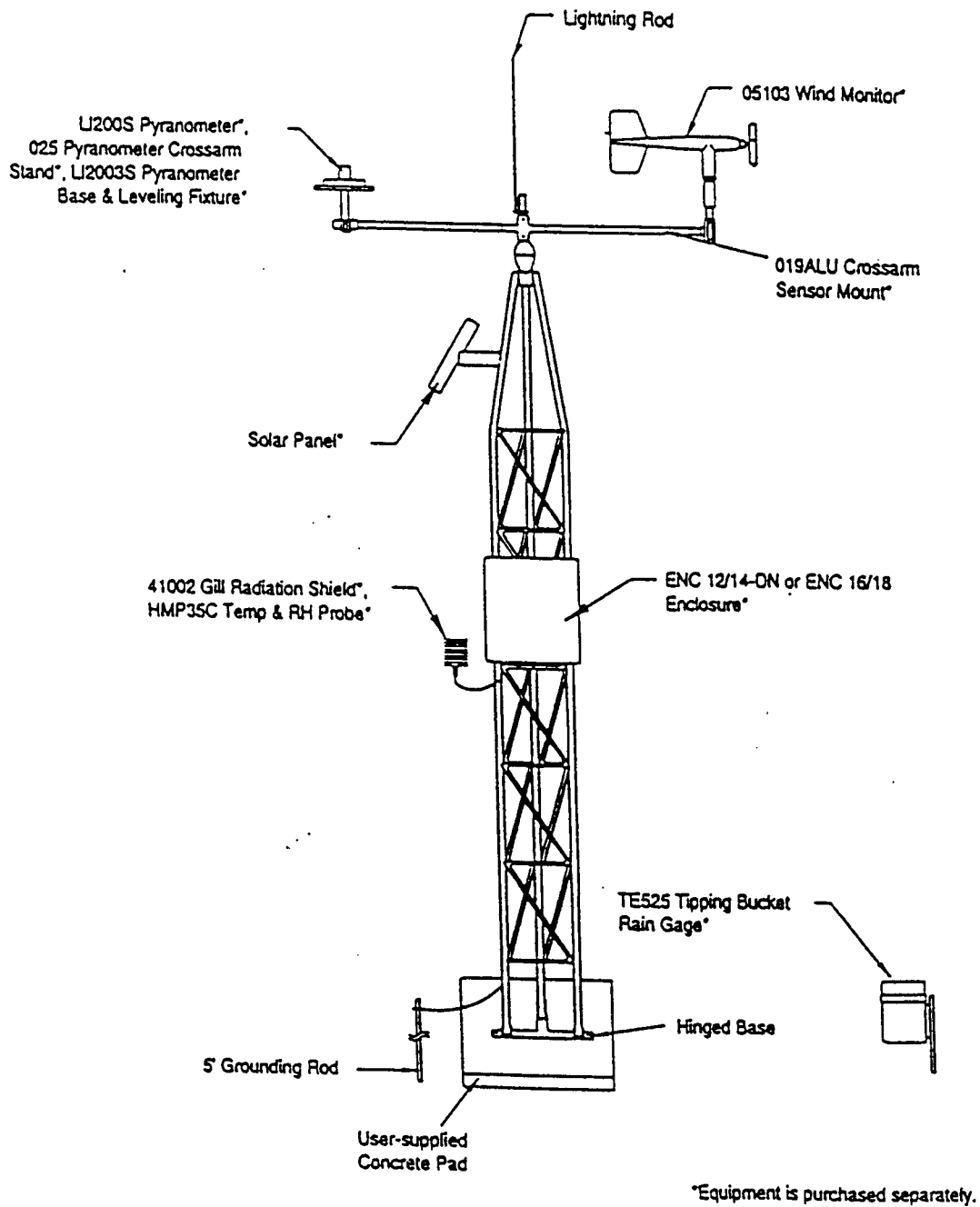


Figure 2.5. UT-3 Weather Station (Courtesy Campbell Scientific, Inc.)

Note: Del-23 weather station does not use the solar panel shown above

depth, the bucket tips and sends a pulse to the CR10 datalogger. The water drains after each tip and then returns to its upright position. The total number of pulses recorded by the CR10 can then be used to calculate the total rainfall amounts. In addition, the bucket is equipped with a heating device that melts accumulated snowfall. The corresponding water level can then be recorded as well.

2.5.4 Wind Speed and Direction

To measure wind speed and direction, a wind monitor manufactured by R.M. Young (Model 05305) was installed on the weather station pole. As the propeller rotates, sine wave signals are produced with a frequency proportional to wind speed. Wind direction is determined by the azimuth angle of the vane. As the vane rotates, a potentiometer produces an output voltage proportional to the angle (Campbell Scientific, 1993). The weather station's CR10 records and stores these values.

2.5.5 Solar Radiation

A pyranometer manufactured by LI-COR (model LI200SZ) was installed on the weather station to monitor incoming solar radiation in terms of energy per surface area. This is performed by a silicon photovoltaic detector that produces an output current based on levels of radiation. A resistor in the cable then converts this current to a voltage that is recorded by the weather station's CR10 Datalogger. A cosine correction on the sensor allows for accurate readings of radiation having incident angles with the surface (Campbell Scientific, 1994). For low radiation levels at nighttime, negative readings are common due to system noise and may be set to zero if desired.

CHAPTER 3.

SENSOR INSTALLATION

3.1 OVERVIEW

The installation procedure followed for TDR, Thermistor, and Resistivity probes is based on the LTPP Seasonal Monitoring Program Guidelines, Version 2.1. Slight modifications were made during installation and are discussed in this chapter.

3.2 SUB-SURFACE SENSOR INSTALLATION

3.2.1 Borings

To begin installation, it was first necessary to drill a 12 inch diameter hole at the desired location, usually near the outer wheel path of the truck lane. This was done after placement and compaction of the required base layers. Using a sheet of plywood with a hole cut in the center, the drill rig would bore through the hole and into the soil for six to twelve inches at a time. When the drill was removed, the recovered soil was scraped off of the auger and plywood and placed in numbered buckets. This would allow for the soil to be replaced in its original position by backfilling in reverse order. This process was repeated until the required depth of 74 to 76 inches was reached.

3.2.2 Probe Installation

With the hole backfilled slightly to the required depth for the sensor, the first TDR probe (# 10) was lowered to rest horizontally on the bottom surface. With this centered in the hole, the resistivity rod and thermistor rod were placed vertically on opposing sides of the hole so that they rested on the bottom, but did not touch the TDR probe. The cables for all sensors were grouped together at the surface to be buried later in a trench.

With these sensors correctly positioned, the hole was backfilled beginning with soil from the last bucket. Two samples were collected from this bucket to be used later for moisture content determinations since accurate estimates of these values are required for use in the TDR equation. A long tamper with a flat round end was used to compact the soil. This

tamper had a small half-moon removed on one side to fit around the thermistor and resistivity probes to allow for full compaction. To protect the resistivity elements, however, a section of PVC pipe split longitudinally was used to cover the entire probe, and was raised gradually as the hole was backfilled. When the proper depth was reached, usually every six inches, the next TDR probe was installed on the bottom and two more soil samples were taken from the current bucket. This process was repeated until the final TDR probe (#1) was placed. Since this probe was close to the surface, it was necessary to invert it so that the cable exited the probe downward. With this complete, the hole was entirely backfilled.

To protect the thermistor probe that was to be installed in the pavement layer, it was necessary to temporarily bury it inside of a small rubber hose until paving proceeded or was completed. The probe would later be vertically pulled to its proper elevation by boring through the pavement layer (in asphalt concrete) at the surveyed probe location and hooking it up with a wire. To achieve this, the precise location of the probe in its temporary position had to be recorded for later reference. This was accomplished by introducing four permanent markers on the existing road (two on each side of the sensor), whose diagonals intersected at the point of sensor installation. Once the Portland cement concrete paving was near the sensor location, the markers were used to locate it so that it could be raised to the surface immediately after the paver passed by. For the asphalt concrete, however, it was necessary to return to the site and bore a hole at the sensor location after the asphalt concrete had hardened. Once the thermistor was positioned correctly, the borehole containing the probe was tamped full with fresh asphalt concrete.

3.2.3 Cable Installation

With the sensor hole completely backfilled prior to paving, it was necessary to excavate a trench roughly twelve inches deep within the base material. This trench ran from the hole to the edge of the test road. All sensor cables were tied and placed in the trench which was then backfilled and compacted lightly. A final compaction would take place before paving.

Once the paving was completed, the trench was extended from the edge of the road to the concrete housing box where the cable ends would be accessible. Since final grading had not been performed beyond the right shoulder, this trench was excavated to depths of two to three feet using a trenching machine. The cables were again tied and buried in the trench. To protect the exposed cable ends from moisture and debris, they were enclosed in a short PVC pipe section having one end capped.

3.3 Onsite Monitoring Equipment Installation

With the sensors and cables installed, the onsite monitoring equipment could be permanently mounted inside the concrete housing box. After connecting the thermistor cable to the CR10 unit appropriately, the equipment cabinet was secured to one of the concrete walls using anchors and screws. Startup and operating procedures will be described later.

CHAPTER 4.

SENSOR MONITORING PROCEDURES AND DATA ANALYSIS

4.1 OVERVIEW

To facilitate ease of data collection, and to maintain uniformity and consistency between data collection agencies, the guidelines developed by SHRP have been adhered to during site monitoring procedures. These guidelines describe in detail the process for CR10 program setup, sensor monitoring, and data collection.

4.2 CR10 DATALOGGER SETUP

Before the CR10 Dataloggers can be used to monitor and store data, a computer program has to be uploaded to each unit. This program will instruct the datalogger to collect, store, and delete data at required intervals. This is necessary for both onsite and mobile units and is performed using the GraphTerm (GT) software package. This program is the main source of communication between the datalogger and the personal computer. After starting the program, the source code that will control either the onsite or mobile unit is uploaded to the CR10 following specific instructions shown on the screen. Next, the datalogger clock is set to the personal computer's time, and the system is then ready to monitor the sensors at the preset time intervals. This process must be performed each time data is taken with the mobile units since power is cut to the unit after each use. For the onsite datalogger, however, this process is performed only at initial startup since the datalogger will be monitoring and storing soil temperatures continuously. Should a power failure occur, a battery backup is present to allow uninterrupted monitoring of temperatures.

4.3 DATA RETRIEVAL

4.3.1 Onsite Unit

As mentioned above, the onsite unit for monitoring temperatures operates continuously. Once a month, the data must be downloaded to a personal computer by connecting a serial cable and an interface (for PC protection) to the CR10. Once this is done, the GraphTerm program is initiated, and data is collected from the unit by selecting 'U' from

the menu. Using a station file (*.stn) from the current directory, the CR10 is instructed of the date and time of data collection. The station file is then updated automatically for its use during the following month's data collection schedule.

After downloading is complete, the user can view the current thermistor temperatures by selecting 'M'. The thermistor numbers and their corresponding temperatures are displayed on the screen which allows the user to verify if everything is working properly. To check that the data has been downloaded properly, the program ONSFIELD can be executed. This program allows the user to graphically view the temperature data. If everything looks satisfactory, the program is exited and the cable and interface are unplugged from the onsite unit. At this point, the user must remember to avoid turning off the CR10 so that the source code is not lost. Figure 4.1 illustrates the onsite unit (mounted to wall of pull box) with the mobile units and portable computer present.

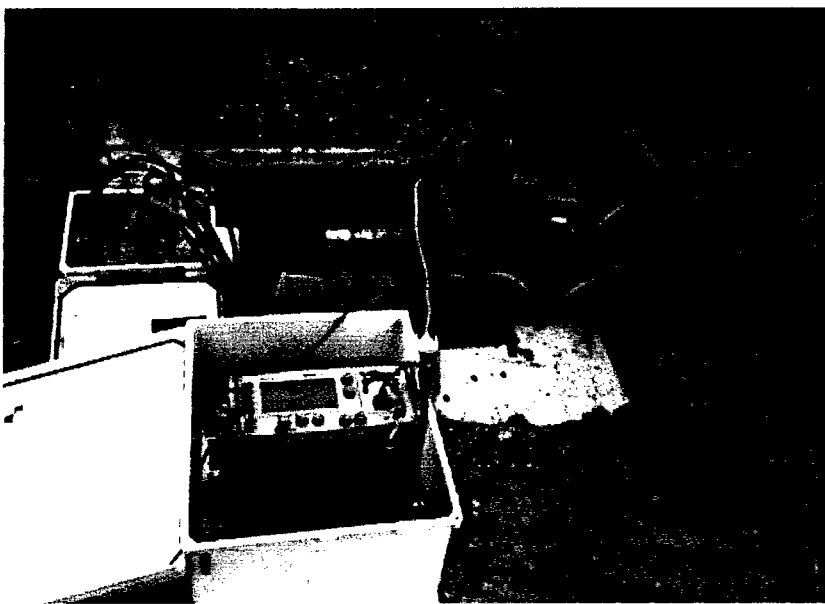


Figure 4.1 Onsite and Mobile Units for Data Collection

4.3.2 Mobile Units

To begin data acquisition with the mobile units, the resistivity and TDR probe cables must first be connected to the multiplexer following the numbered ports. Next, the cable

tester is connected to the multiplexer board and the CR10 is linked with the serial cable and interface to the portable computer. The GraphTerm program is executed, source code and time are uploaded to the CR10 as before, and the system is ready to monitor. 'M' on the menu initiates this, whereupon the various probe numbers will appear on the screen. If successful, the resistivity values will begin to appear followed by an initialization of the cable tester. At this point, the TDR traces will appear on the screen as the multiplexer switches through all ten probes. With this complete, the data is collected by pressing 'U', and the setup can be dismantled.

As with temperature, resistivity and TDR data can be checked in the field using the MOBFIELD program. All ten TDR traces are displayed as well as a graph of the resistivity values throughout the subgrade. Should problems be immediately visible in the graphs, the user can repeat the monitoring process.

The first time that the TDR probes were monitored for each site using the mobile units, however, one additional step was necessary to obtain usable readings. The source code provided for upload to the CR10 for each site contains information relating to TDR probe length and cable length. This information was obtained from manually monitoring the TDR probes after their installation in the subgrade. The first time that data is collected with the mobile unit, however, the screen-displayed traces may need to be shifted left or right so that the first peak is centered on the vertical axis. This is performed using the EDLOG editor in order to manually adjust the probe lengths in the source code. The amount of adjustment is determined from the trace display, and the corresponding probe length is increased or decreased accordingly. This process is repeated until every TDR trace is aligned correctly on the cable tester's screen.

4.4 DATA ANALYSIS

Once data has been downloaded from the CR10's at both the seasonal sites and the weather station, it has to be checked and edited for quality. If the data meets quality assurance checks, it is then sent to the FHWA's storage facility, which for this project is

located in Champaign, Illinois. From this point, the data can be accessed by any organization wishing to examine and analyze the results.

To facilitate the process of data analysis, a computer program was written to allow all participants to analyze and edit the data in a consistent format. A separate program was created for both seasonal road data and weather station data. The former is known as SMPCheck (Seasonal Monitoring Program Check), while the latter is known as AWSCheck (Automated Weather Station Check). Both provide a menu-driven front-end that allows for easy use on a DOS platform.

4.4.1 SMPCheck Program

The SMPCheck Program requires the user to specify a site and to enter relevant installation data such as sensor depth and soil properties specific to that site. The user can then monitor the onsite and mobile data using graphs prepared by the program. In order to meet SHRP specifications, the data must pass a Level D check before that data can be sent to the collection site. This check is performed by the program which then alerts the user to the current status. If the data passed all checks, an upload file can be created whereas data that failed must be edited for content. All can be done within the program.

4.4.2 Procedure

Once the SMPCheck program is installed and executed, the user is immediately prompted for a specific site identification number that includes state code, site letter designation, and the SHRP number. For Ohio, the SPS1-J2 section, for example, would be entered as 39P0102. Table 4.1 lists the required name designations for the sites involved in this study.

Once the Escape key is pressed, the program creates a subdirectory, in this case 39P, which in itself contains five subdirectories: CHKFILE, IMSDATA, ONSDATA, MOBDATA, and PROINFO. The user must then copy the individual onsite and mobile data

Table 4.1 SHRP Section Identification

Section	SPS1-J2	SPS2-J3	SPS2-J5	SPS2-J12	SPS9-ODOT
SHRP #	390102	390203	390205	390212	390901
Designation	P	H	E	C	K

files downloaded from the CR10s into the ONSDATA and MOBDATA directories, respectively. This can be done through the “DOS Shell” menu choice, or by exiting the program. It is important that these files be previously renamed according to SHRP guidelines, as illustrated below:

ssS#yyab.cde

where ss is the state code (39 for Ohio),

S is actually ‘S’ for every data file,

is the designation letter as seen in Table 4.1 above,

yy is the year that the data was collected,

a is the identification for each sequential visit; A=1st, B=2nd... ,

b is the month of data collection; A=Jan, B=Feb...,

cde is the file extension; ons for onsite data, mob for mobile data.

Once this has been done, the user can return to the program by exiting the DOS shell, and then re-enter the site identification section if necessary.

With each site directory created, the DATA PROCESS menu is selected that allows the user to enter project data, or to process onsite and mobile data. If the “Project Data” option is selected, the user has the option to enter one of five types of site data. This includes information that was collected during sensor installation at each site and was recorded on the corresponding data sheets provided by SHRP. The identification number of each data sheet corresponds to the number following the available options on the menu, and include:

- 1) Instrument Location and TDR Depth (IO2),
- 2) Thermistor Probe Depth (CO2),
- 3) Resistivity Probe Depth (CO3),
- 4) Field Gravimetric Moisture Content (IO5), and
- 5) Field Measured Dry Density (IO7).

Once all available data is entered, the computer automatically stores the information in the PROINFO subdirectory where it must now be checked for quality. This is done by choosing the OFFICE QC option on the main menu, and then selecting the "C and D Level" option. The program will then check the data for allowable content based on SHRP's guidelines, and a file named SC##.qc (where SC is the two-digit state code, # is the site ID, and * is either 'MANUL, ONSIT, MOBLE, or PRJCT' depending on the type of data being processed) will be created in the CHKFILE subdirectory (SMPCheck 1996, 27). Using any editor, the user can view this file to determine if the data has passed Level D status. If it hasn't, the user must find and correct any mistakes made on the data entry screens and execute the quality check again.

With project data entered, the user can proceed to process the onsite, mobile, or manual data that has been collected. Manual data consists of any preliminary readings collected with equipment other than the onsite and mobile dataloggers. If required, all sensors can be monitored with the exception of air temperature probes and rain gauge devices (Rada et al, 1994, II-21). Equipment for manual data collection is described in the Seasonal Monitoring Program Guidelines and will not be discussed here.

At this time, the user can process onsite or mobile data. If the "Onsite Data" option is selected, the program displays all data files available in the site directory for processing. One or all of the files may be selected, whereupon a screen is displayed listing all chosen files and their start and end dates for data collection. Typically, these files will have overlapping dates which the computer will adjust automatically. If two or more files start on the same day, it is

only necessary to select the one file that has the latest end date. If necessary, the user may make time corrections for Daylight Saving Time by adding or subtracting up to two hours from specific days.

With this complete, the program checks the data files, adjusts for overlap and time corrections, and then prepares six graphs that include the following:

- 1) daily average, min, max air temperature and rainfall data,
- 2) daily average air, rainfall, and first 5 MRC sensors temperature data,
- 3) daily all 18 MRC sensors average temperatures,
- 4) daily all 18 MRC sensors maximum temperatures,
- 5) daily all 18 MRC sensors minimum temperatures, and
- 6) hourly air temperature, rainfall, and first 5 MRC sensors temperature data.

Since this program was developed with other data collection sites in mind, the air temperature and rainfall data will be absent from these graphs in all Ohio Test Road monitoring sites. Typically, each instrumentation site will have its own air temperature and rainfall gauges, whereas the DEL-23 project obtains this data through the use of one weather station for the entire site. This data is viewed and edited with the AWSCheck Program described later. Figure 4.2 provides an example of selection 4) above which illustrates daily average temperatures for all eighteen thermistors. Although the sensor number is not visible in the graph, it is seen that temperatures near the surface fluctuate intensely while temperatures deep in the subgrade undergo little change.

With the graphs displayed, the user must scan for possible data points that are clearly inaccurate and that may reveal an equipment malfunction. If any are found, the editing keys listed on the screen are used to remove the points. With this complete, as with the project data, the onsite data must pass a level D quality check. To do this, the OFFICE QC option is again selected on the main menu, followed by the “C and D Level” option. Once “Onsite

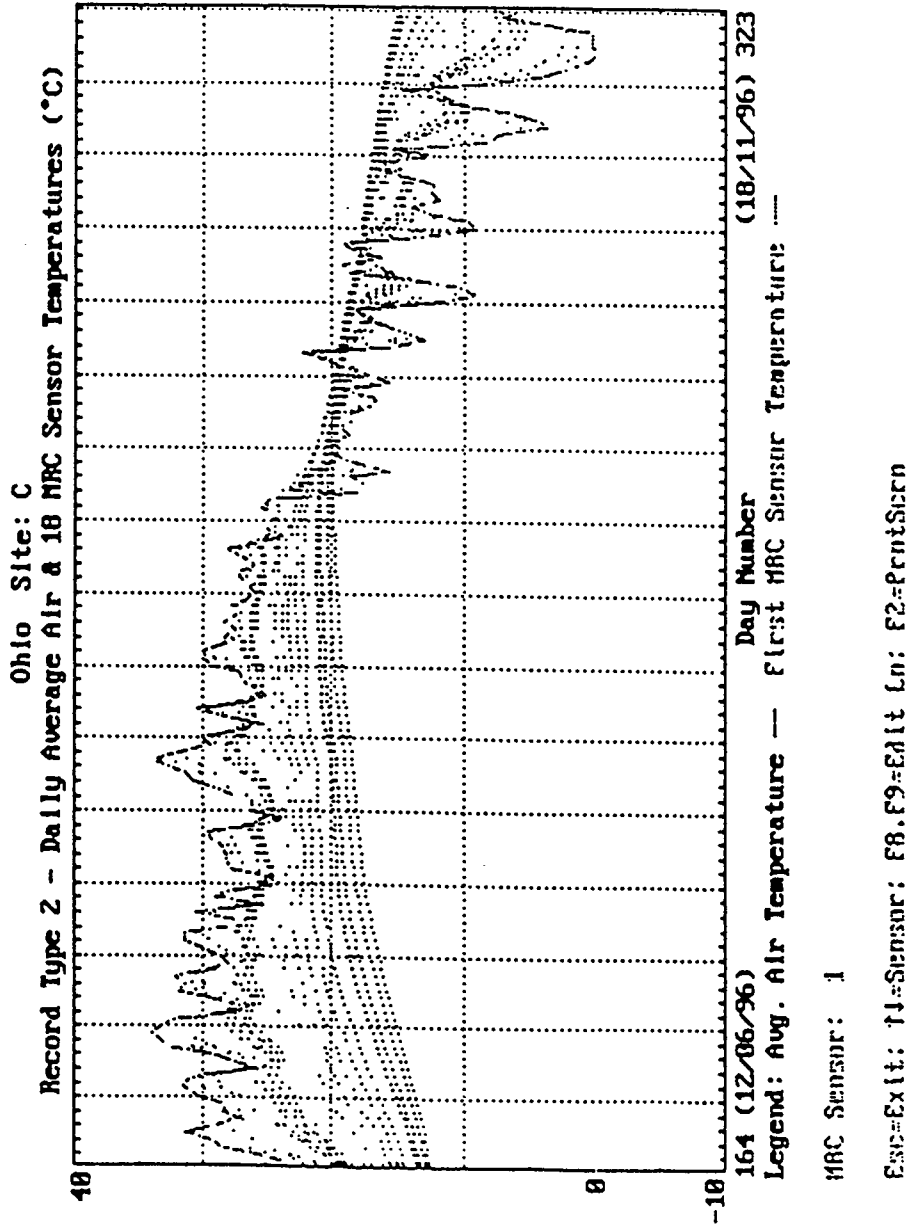
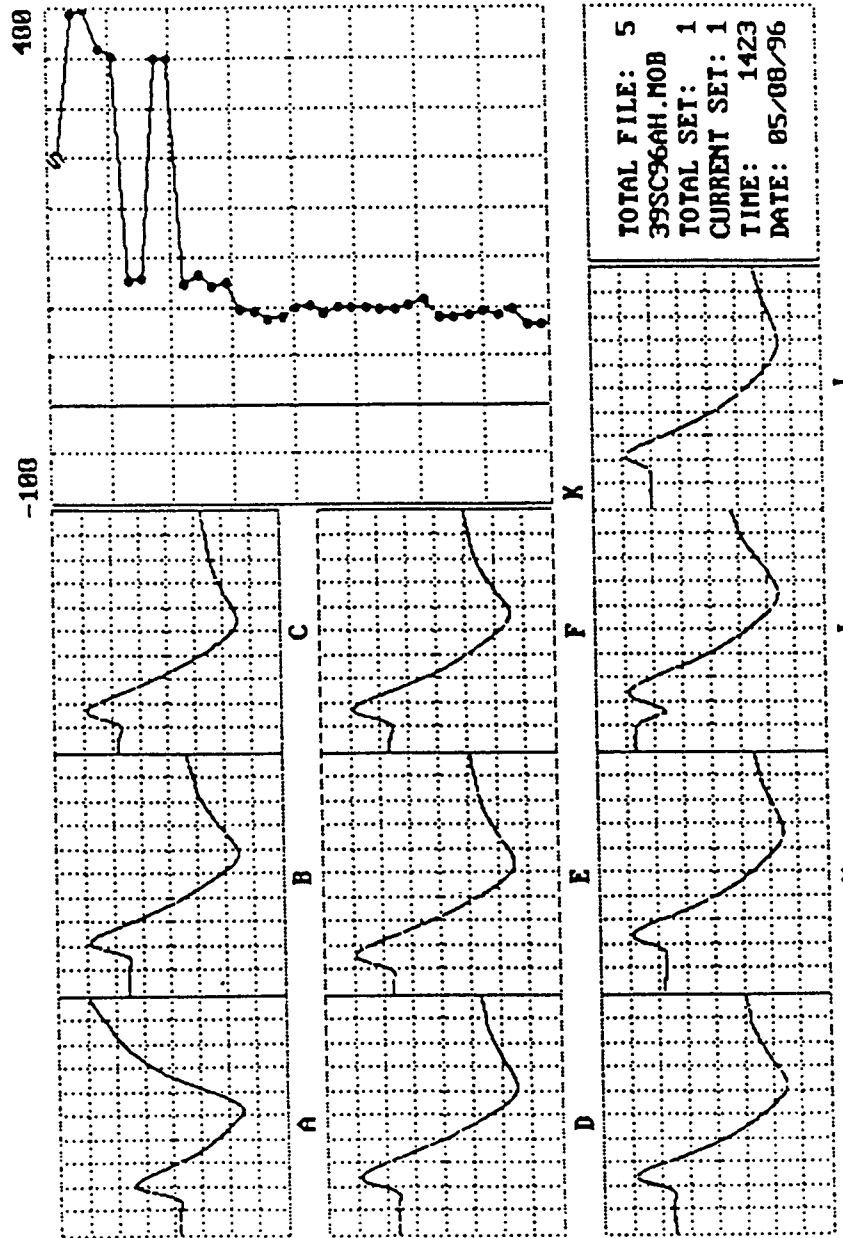


Figure 4.2 Typical SMPCheck Display of Daily Average Thermistor Temperatures

Data” is chosen, the computer performs a quality check similar to that performed by the user. The results of this check are written to two files, SC#onsit.msg and SC#onsit.qcr (using the same notation described above), that are placed in the CHKFILE subdirectory. When viewed, the *.qcr file lists the status of each type of data field checked by the program. For onsite data and mobile data, the description of every field is listed in Appendix B of the Seasonal Monitoring Program Guidelines. If a field did not pass level D status, as required by SHRP, a description or list of the bad data points is provided so that the user can return to the graphs and remove the faulty data. Appendix A of the SMPCheck Manual provides sample graphs of acceptable and unacceptable data to help the user identify bad data points. The quality check must be performed each time the data is edited until every field passes Level D. Should the user attempt to create an upload file, any data not passing Level D will not be included.

Similarly, the mobile data analysis is conducted in the same manner. Once selected, plots of the TDR traces and resistivity values are displayed, as shown in Figure 4.3 below. For mobile data, however, it is only necessary to choose those plots which are valid by typing the corresponding number under the graph. Appendix B of the SMPCheck manual provides samples of acceptable and unacceptable data. The computer will include these plots for processing and quality control when the OFFICE QC option is selected. Again, a SC#moble.msg and a SC#moble.qc file are created displaying selected data and quality control status, respectively. If a file does not pass Level D, the mobile data must be re-evaluated to find the problem.

With all of the project, manual, onsite, and mobile data passing level D, it is then necessary to create the upload file to be sent to the data storage facility. This is performed by selecting the IMS OUTPUT option on the main menu followed by the “Create Upload File” option. A screen appears displaying all of the data available for upload (which has passed Level D), and the user is prompted to select which data to include in the upload file. Any or all of the data can be selected whereupon the computer creates a file in the IMSDATA subdirectory following the format below:



Alt+Letter: Instant UMC; Ctrl+T: change time; Ctrl+D: change date; Ctrl+C: comment
ESC=Exit; Letter select(=): PgUp/PgD=PrInr/Next Set; Ctrl+PgUp/PgD=PrInr/NextFile

Figure 4.3 Typical SMPCheck Display of TDR and Resistivity Data

ssmMddy.UPL

where ss is the LTPP two digit state code in which the test section is located,
m is the SMP multiple site agency code; A= 1st SMP section in state, B=2nd.,
M is the letter designation for month that upload file is created; A-Jan, B-Feb.,
dd is the day the upload file was created,
yy are the last two digits of the year the upload file was created, and
UPL is the file name extension used for all upload files (SMPCheck '96, D-1).

With the creation of the upload file, the analysis is complete, and the user can begin the process on any remaining instrumentation sites.

4.4.3 Problems

In all, the SMPCheck program is straightforward and easy to use. However, a few problems were encountered that did not allow the program to complete execution and prepare the data correctly.

The first of these problems involved a time overlap within one of the onsite files for SPS2-J12. Although the program was developed to eliminate the overlaps between separate data files, it can not remove an overlap within one file. Therefore, it was necessary to manually edit the file and delete the repeated data. In addition, many data files began with fields that had been cut in half during data collection because of the ring memory type of storage in the CR10, and as a result did not specify a field number. Again, these lines were manually deleted.

Once the program was able to execute properly, several problems were found in the onsite data for every site. These were noticeable while viewing the daily maximum and daily minimum soil temperature graphs. At several days throughout the year, large, unexplained spikes appeared in all of the sensor readings. While this may not be uncommon for sensors in the pavement, sensors in the deeper subgrade soil typically maintain constant temperatures

with little or slow variation. It was noticed, however, that these spikes only occurred on days that data was downloaded from the onsite units. It is believed that these spikes were created as a result of deleting the station file prior to downloading the data. Because of this, when the datalogger prepared the daily report for this date, it only had several hours of data available to determine highs, lows, and averages.

4.4.4 AWSCheck Program

The AWSCheck Program used to monitor weather station data follows the same format and procedure for the SMPCheck Program previously described. Again, the data is displayed graphically whereupon the user removes corrupt data points, and an upload file is created providing the data passes the level D check.

4.4.5 Procedure

Like the SMPCheck Program, the user is immediately prompted for the site identification for the weather station that includes the state code, site code, and SHRP section ID. For Ohio, the state code is 39 and the site code is 'A'. Site code is determined from the number of weather station sites in the state using 'A' for the first, 'B' for the second, and so on. As for the SHRP section ID, it was assumed that this would be the number for the site closest to the weather station since it was not actually installed at a particular test site. For the Ohio Test Road, the closest section was SPS2-J3, or 0203. Once this has been entered, the computer creates subdirectories much like those described above. The user must then copy the collected data files to the newly created AWSDATA directory, and then proceed to process the project data and weather station data. Project data consists of information relating to weather station positioning at the site such as elevation, latitude, and longitude, and is only entered once for each station.

After selecting the "AWS Data" option under the "Data Processing" menu, the user must select which data files to be processed. Data files that begin at the same date, but end with different end dates will be combined by the program unless the user specifies which file

to use. Again, a correction for Daylight Saving Time is available that allows up to two hours to be added or subtracted from within desired time spans.

With this complete, the “View selected data” option is chosen, and the program displays several options for viewing:

- 1) daily average, min, max air temperature and precipitation data,
- 2) daily relative humidity, solar radiation, and precipitation data,
- 3) daily wind information
- 4) hourly temperature and precipitation data,
- 5) hourly relative humidity and precipitation data,
- 6) hourly solar radiation and precipitation data, and
- 7) hourly wind information.

Figures 4.4 to 4.6 provide samples of selections 2), 3), and 6) respectively. As with the Onsite data, the weather station data must be checked for quality and consistency. Options 1 through 3 above only permit viewing of the data, while options 4 through 7 permit the user to edit the data manually. Obvious ‘bad’ data, such as extremely high or low temperatures for a season, is removed by selecting a start date and end date, and then deleting the points in between. After all of the data has been checked and edited if necessary, the “Office QC” option is selected from the main menu, followed by the “C&D Level” option. The computer then checks the data for allowable ranges and writes the status level to a file in the “CHKFILE” directory. If the status has passed Level D, an upload file may be created as done with the onsite data. If necessary, the user must re-edit the data until the status passes Level D.

4.4.6 Problems

Unlike the SMPCheck program, processing ran smoothly for the weather station data, and an upload file was created with very little editing required. The only problem involved the weather station itself in which during the first activation of the station, the selected option

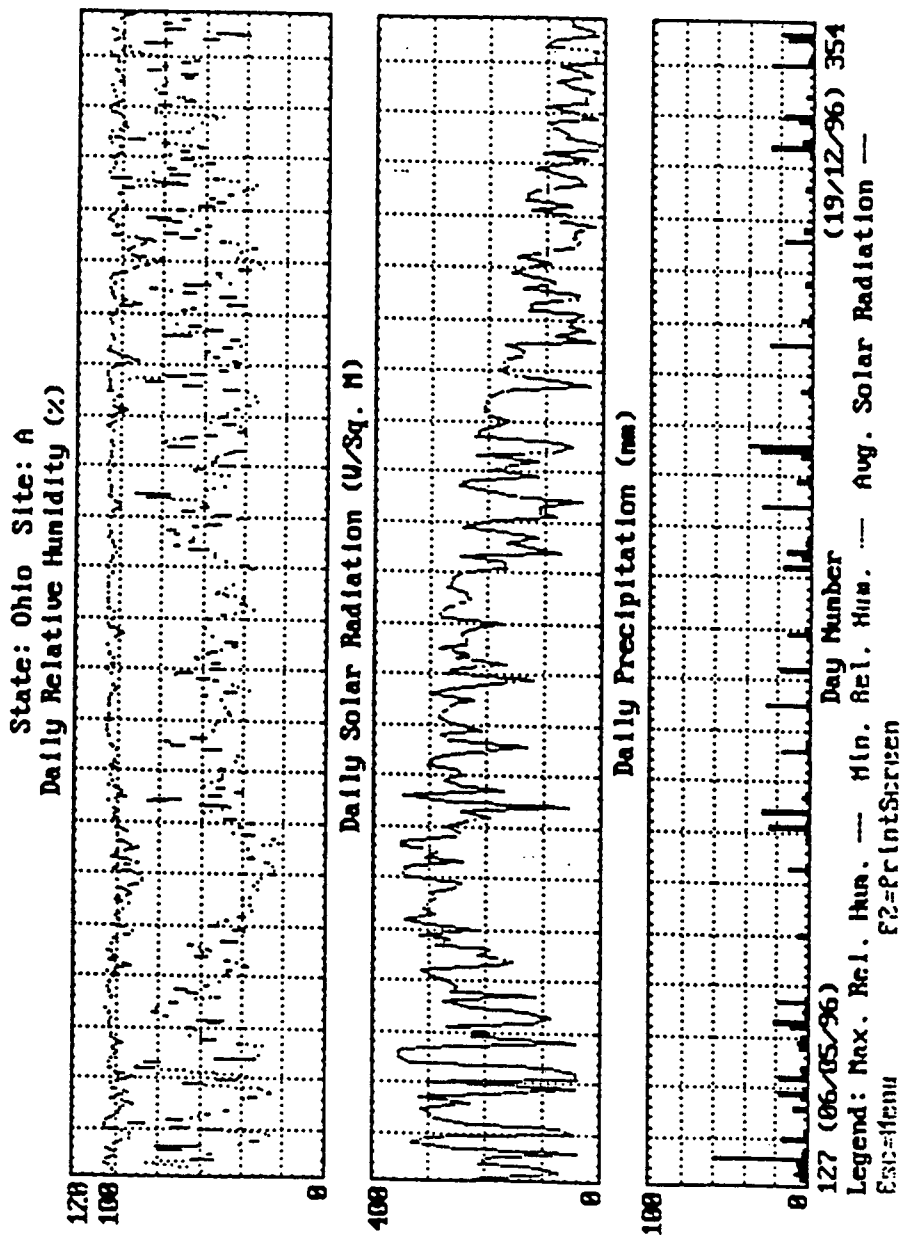


Figure 4.4 Typical AWSCheck Display of Daily Humidity, Radiation, and Precipitation Data

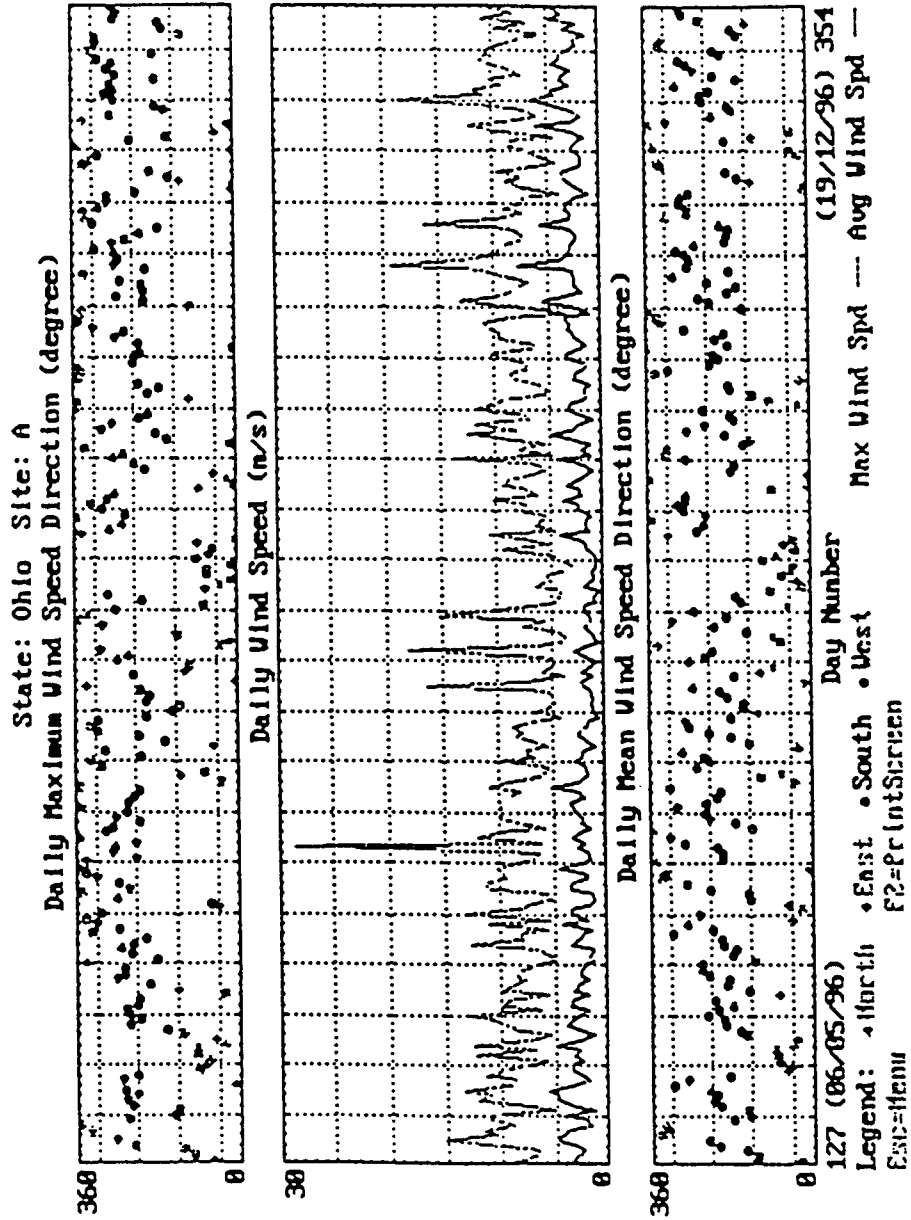
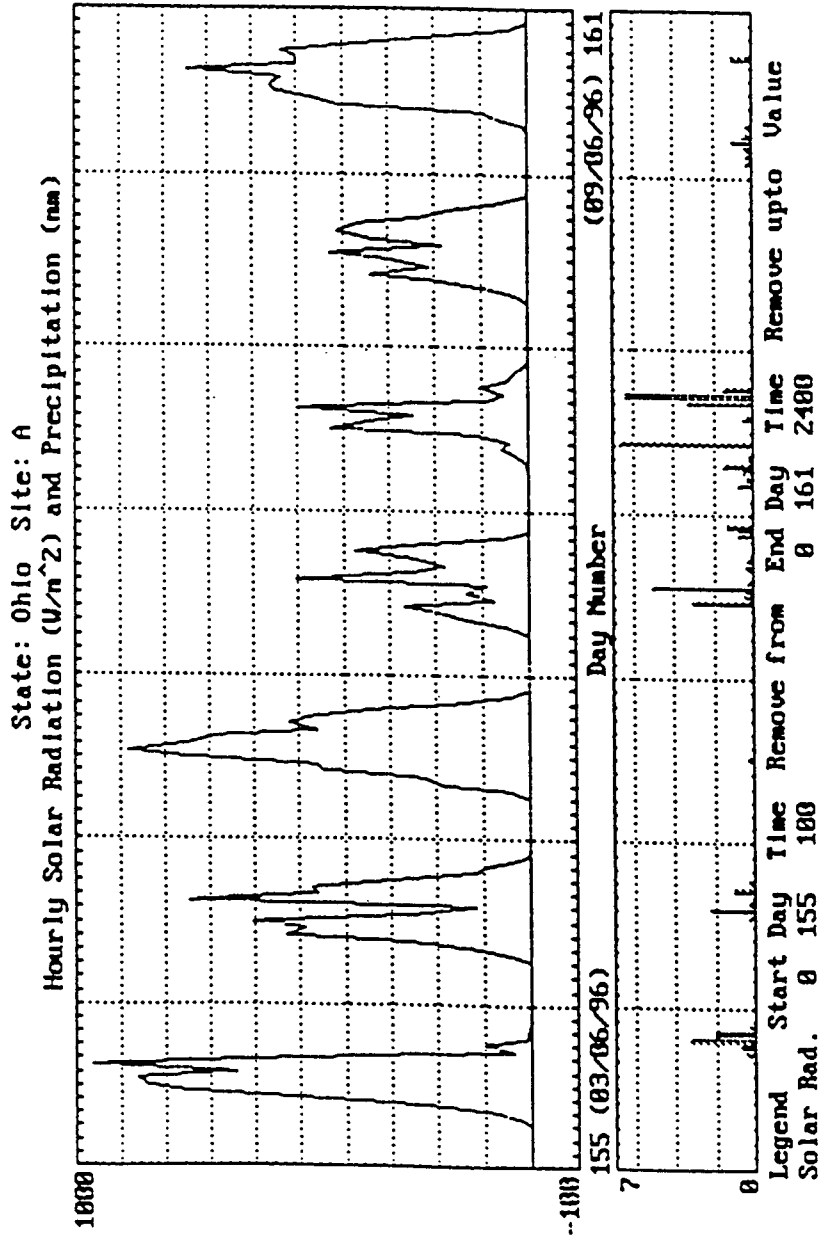


Figure 4.5 Typical AWSCheck Display of Daily Wind Information



Esc=Menu; PgUp, PgDn=Print; Next Week: F8, F9=Exit; Ctrl+F10=Remove; F2=PrintScreen

Figure 4.6 Typical AWSCheck Display of Hourly Radiation and Precipitation Data

in the uploaded program to the CR10 indicated that the unit would stop collecting data after all memory had been used, rather than selecting the ring memory option where the oldest data is deleted to provide space for new data. As a result, several weeks of data are missing and appear as a blank area on the graphs. Fortunately, however, this does not affect the data that was obtained. Subsequent operation of the weather station has been performed with the ring memory option which allows for up to approximately six months of data storage without any losses between collection periods.

CHAPTER 5.
SUBGRADE SOIL AND ASPHALT CONCRETE TESTING AND
CHARACTERIZATION

5.1 OVERVIEW

To achieve the goals set for the Ohio Test Road, it is necessary to have a strong knowledge of the properties of the materials used in the construction of the road. Therefore, material monitoring and testing was a high priority during all phases of construction. This included sampling of subgrade and embankment soils, sampling of each of the numerous types of base materials, and sampling of both asphalt concrete and Portland cement concrete pavements. In addition, specific sampling was also conducted at individual instrumentation sites. With the extensive amount of testing that could be performed on each material, the participating universities were enlisted to facilitate the process.

This chapter will focus on the soil and asphalt concrete testing performed during this study. For the subgrade and embankment soils, types BS02 and BE15 soils respectively, the types of tests included specific gravity determination, moisture-density relations, Atterberg Limits determination, and resilient modulus testing. For the asphalt concrete, the types of tests included resilient modulus and indirect tensile strength determination.

5.2 SUBGRADE AND EMBANKMENT SOIL CHARACTERIZATION

5.2.1 Specific Gravity

In order to perform resilient modulus testing on the soil, it was first necessary to determine its basic properties. Table 5.1 provides the ranges and averages found for the specific gravity of both subgrade and embankment soils.

Table 5.1 Specific Gravity of Subgrade and Embankment Soil

	Test 1	Test 2	Test 3	Test 4	Average
BS02	2.700	2.691	2.685	2.696	2.693
BE15	2.726	2.721	2.712	2.684	2.711

This testing was performed according to ASTM D 854 and AASHTO T 100 specifications. Both values fell within the expected ranges for a silty clay.

5.2.2 Moisture-Density Relationships

To develop moisture-density curves for each soil, both standard and modified Proctor compaction tests were performed. These tests were conducted in accordance with ASTM D 698-78 and AASHTO T 99-90 and T 180-90 specifications. Figures 5.1 and 5.2 show the relationships for each soil and include the modified curve, the standard curve, and the zero air-voids curve. Table 5.2 lists the optimum moisture contents and maximum dry unit weights for each soil as determined from the graphs.

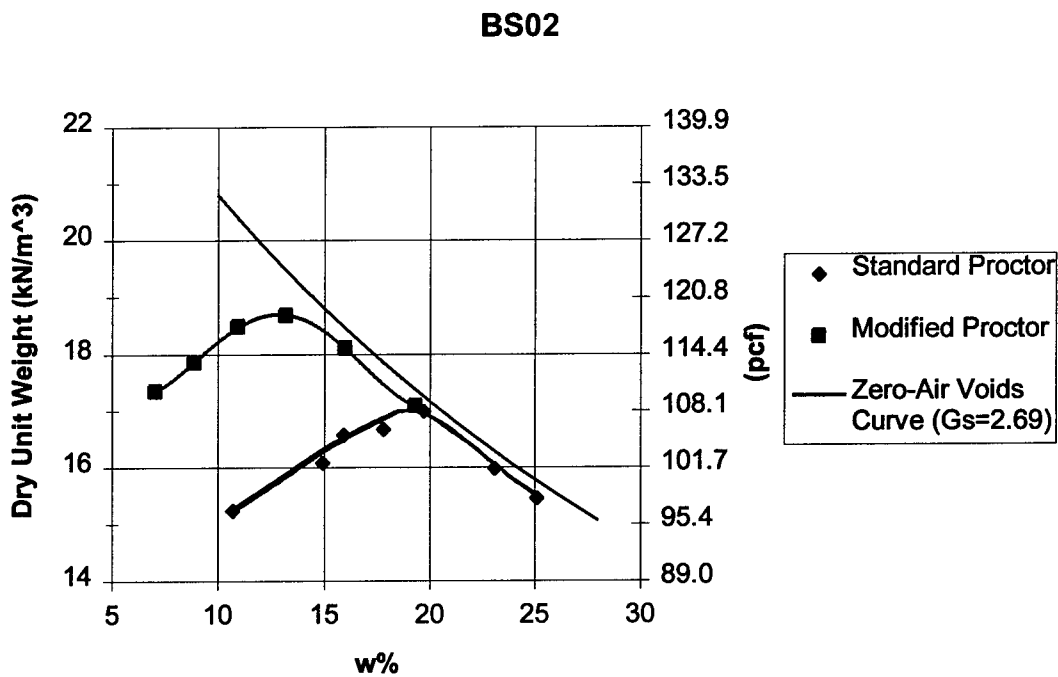


Figure 5.1 Moisture-Density relations for BS02 subgrade soil.

BE15

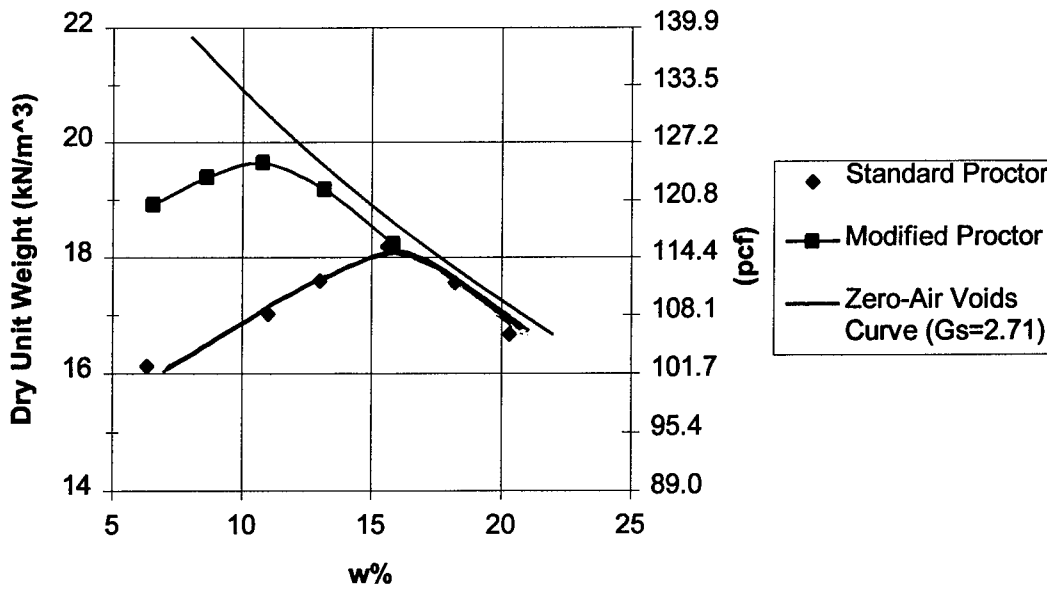


Figure 5.2 Moisture-Density relations for BE15 embankment soil.

Table 5.2 Optimum moisture content and maximum dry unit weight

	Standard Proctor			Modified Proctor		
	Optimum Moisture (%)	Max Dry Unit Weight (pcf)	Max Dry Unit Weight (KN/m³)	Optimum Moisture (%)	Max Dry Unit Weight (pcf)	Max Dry Unit Weight (KN/m³)
BS02	19.0	108.7	17.1	12.2	118.9	18.7
BE15	16.0	115.7	18.2	10.25	124.7	19.6

5.2.3 Atterberg Limits

The liquid and plastic limits were determined for each soil following ASTM D 4318 and AASHTO T 89 and T 90. Table 5.3 presents the test results.

Table 5.3 Atterberg Limits

	Liquid Limit	Plastic Limit
BS02	33.6%	20.45%
BE15	34.3%	21.1%

Based on these limits, and knowing that they are mostly fine-grained, both soils are classified as an A6 soil by the AASHTO Soil Classification System or CL by the Unified Soil Classification System.

5.2.4. Shelby Tube Sampling

To obtain a representative sample of actual field conditions, one Shelby Tube sample was taken from the center of section J4 on SPS8. Table 5.4 lists the dry unit weight and moisture content found at various depths from the subgrade surface for each Shelby Tube section.

Table 5.4 Shelby Tube Dry Unit Weights and Moisture Content

Shelby Tube Section	5A-1	5A-2	5A-3	5B-1	5B-2	5C-1	5C-2	5C-3
Depth (in)	7.5	14.5	22.0	37.5	47.0	59.0	66.5	74.0
γ_d (pcf)	103.5	106.0	109.8	102.5	117.6	118.1	120.6	121.5
w%	20.1	20.0	18.8	22.9	15.5	14.4	14.0	14.3

Due to voids present in the extracted samples, dry unit weights may be off slightly. This is most likely the cause for the decrease in γ_d for section 5B-1 in combination with the high moisture content at this elevation. In comparison with the compaction test results, the Shelby Tube dry unit weights compare well with maximum γ_d values resulting from the BS02 and BE15 Modified Proctor tests. Starting at depths of four feet, the Shelby Tube dry unit weight levels off between approximately 95% and 97% of the modified maximum γ_d for the BE15 soil. Again, depending on the variation in results due to voids in the Shelby Tubes, these dry unit weight values are also roughly 100% of the modified maximum γ_d for the BS02 soil. The latter case is more likely since at these depths the material is expected to be the subgrade soil. At shallower depths, where the material is expected to be embankment soil,

the dry unit weight values range between 90% and 95% of the standard maximum γ_d for the BE15 soil.

5.2.5 SUBGRADE SOIL RESILIENT MODULUS

5.2.5.1. Overview

For mechanistic pavement design procedures, it is necessary to know the resilient modulus of both the subgrade soil and the asphalt concrete. A subgrade soil experiences a static normal stress from the overburden pressure as well as a dynamic, repeated stress from cyclic wheel loading (Jin, et.al. 1994, 606). The resilient modulus, E_r , is a measure of the soil's ability to withstand this repeated loading, and represents a cyclic Young's modulus.

The most accepted representation of a fine-grained soil's E_r characteristics is the Thompson-Robnett bilinear model (Figuroa, et.al. 1994, 32) shown in Figure 5.3 below. With this model, as the normal (deviator) stress is increased on the test specimen, the resilient modulus drops linearly, and changes slope at a breakpoint. The slope of the line before the breakpoint is K_1 and that after the breakpoint is designated as K_2 . The equations for these lines are determined from a linear regression analysis, and the intersection point is found. E_{ri} is the resilient modulus at this intersection corresponding to a deviator stress designated as σ_{di} .

To calculate E_r , the deviator stress applied to the soil specimen, σ_d , is divided by the resilient (recoverable) strain, ϵ_r . Without confining pressures, σ_d is equal to the applied normal pressure, σ_1 . During testing, the sample experiences a permanent deformation in addition to a recoverable deformation. The strain is then found by dividing this recoverable displacement by the original length of the specimen, L_o .

Figure 5.4 is an example of the displacement pattern resulting from the resilient modulus test. Shown are the results from four different applied pressures with ten repetitions each. Recoverable deformation, marked by peak to valley distances, and permanent deformation, marked by the increasing baseline, add to give the total deformation.

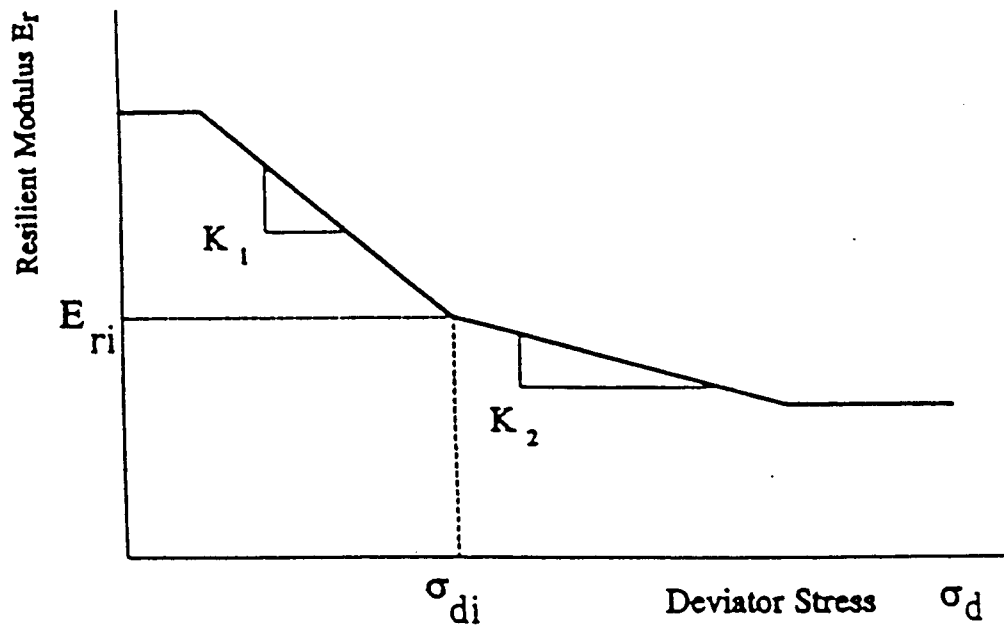


Figure 5.3 Bi-linear Model for Resilient Modulus Test Results (Figuroa, 1994)

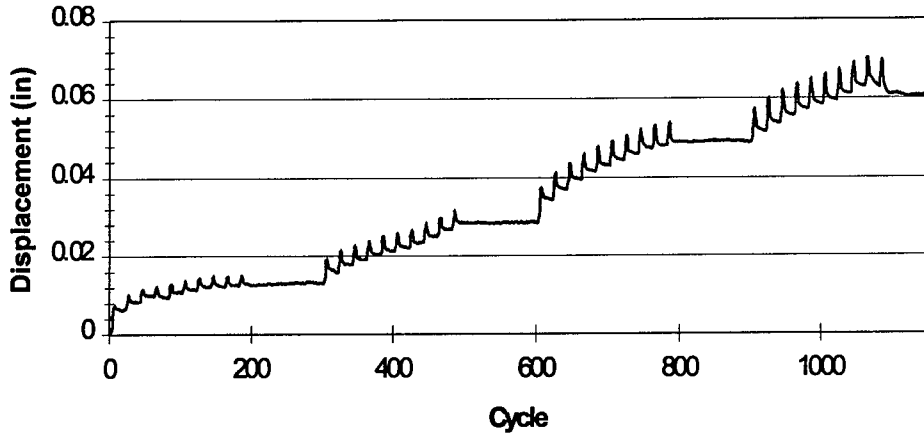


Figure 5.4 Typical displacement pattern for E_r testing.

5.2.5.2. Sample Preparation

Following the AASHTO T 292 Standard Method of Test for Resilient Modulus of Subgrade Soils, cylindrical samples of soil were prepared having a diameter of 2.8 inches and a length of twice the diameter, or 5.6 inches. Samples of both BS02 and BE15 subgrade and embankment soils were used in the testing. Based on Shelby Tube dry unit weights and the Standard Proctor test results, 108 pcf was chosen as the dry unit weight for all sample preparation. Since the resilient modulus is expected to be a function of degree of saturation, three samples were prepared at nominal degrees of saturation of 65, 70, 75, 80, 85, 90 and 95 for the BS02 soil and of 65, 70, 75, 85, 90 and 95 for the BE15 soil for a total of 39 specimens. Knowing the dry unit weight and the desired degree of saturation, Equation 5.1 was used to determine the moisture content needed to prepare the sample.

$$\gamma_d = \frac{G\gamma_w}{1 + \left(\frac{wG}{S}\right)} \quad (5.1)$$

where γ_d = dry unit weight of soil, pounds per cubic foot
 G = specific gravity of soil solids

γ_w = unit weight of water, pounds per cubic foot

w = moisture content of soil, (percent)

S = degree of saturation, (percent).

Once the volume of the mold and the initial moisture content of the soil was determined, the mass of the soil and the additional water needed was calculated. This soil was then placed in a blender where the water was added gradually. Once thoroughly mixed, the soil was at the desired moisture content and it was only necessary to measure the desired mass to add to the mold for compaction.

The mold used consisted of a hollow steel cylinder with an inside diameter of 2.8 inches and an inside length of 5.6 inches. An aluminum ring, also with an inner diameter of 2.8 inches, was placed on top of the cylinder. This ring helped contain the uncompacted soil while guiding a solid aluminum loading platen, driven by a compression machine, to compact the soil specimen. Figure 5.5 illustrates the compaction process with the mold in the compression machine.

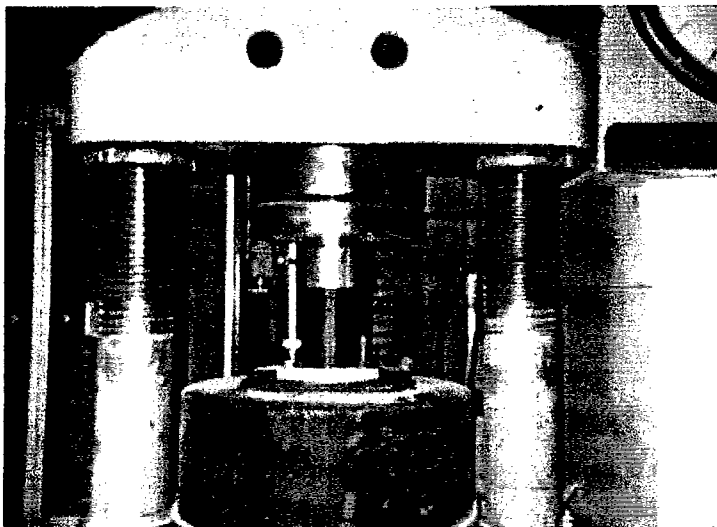


Figure 5.5 Resilient Modulus Test Sample Preparation.

Once the loading platen was flush with the top ring, the load was held temporarily to allow the specimen to adjust and to eliminate any expansion that might occur once the load was removed. To extrude the test sample, a hand-operated hydraulic jack was used to push the loading platen through the mold and drive out the sample. The specimen was then weighed, sealed with plastic food wrap, and placed in a constant humidity chamber for at least one week. This was done with the intention of preventing “thixotropic” strength gain in the soil (Thompson and Robnett 1979, 75).

5.2.5.3. Testing Procedure

Although the AASHTO specifications call for triaxial testing procedures, a uniaxial test was used instead. It is generally accepted that for a fine-grained soil with cohesion, confining pressures are unnecessary and do not affect the results. In fact, both unconfined and triaxial resilient modulus testing was initially performed on these soils and no appreciable differences were noted in the results. Thus, due to its expedience, the unconfined resilient modulus testing was adopted subsequently. This was the method employed by Thompson and Robnett as well, who cite that finite element and elastic layer analyses show that the upper regions of the subgrade soil experience less than 5 psi confining pressure under a typical pavement. In addition, previous testing at the University of Illinois has shown that resilient modulus testing with lateral confining pressures up to 5 psi reveal no significant changes in results compared to uniaxial testing (Thompson and Robnett 1979, 75).

To perform the test, the specimen is subjected to a repeated normal pressure while the corresponding vertical displacement is recorded. Figure 5.6 illustrates the resilient modulus testing machine with the specimen in place. The cyclic load was produced using air pressure and a Bellofram cylinder, controlled by an electrically-operated servo valve. The cyclic axial load was measured with a load cell connected in series with the Bellofram cylinder and the loading shaft. Deformation was measured with a linear variable differential transformer (LVDT) also connected in series with the loading shaft. Outputs from both the load cell and LVDT were monitored with a high-speed strip chart recorder to graphically record the output voltages.

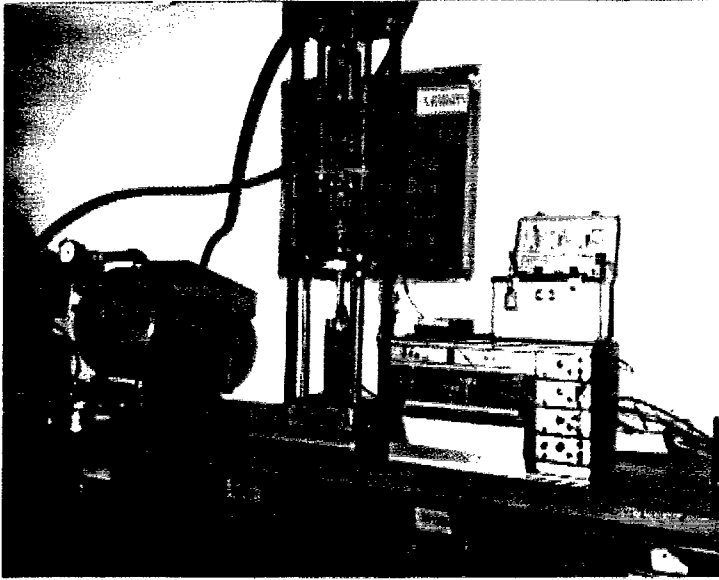


Figure 5.6 Resilient Modulus Testing Machine

Before starting the actual test, a conditioning load was applied for at least 50 repetitions in order to reduce errors that may have been caused by imperfect contact between the sample and the loading platen. This was performed at a reference point of 5 psi on the dial gauge. Due to losses, however, this did not correspond to the exact pressure applied to the specimen. To find the actual applied pressures, the voltage output from the load cell was converted to pounds which was then divided by the area of the soil specimen. Following the conditioning, testing began at the same pressure by recording ten consecutive cycles and repeating the process every 5 psi until 80 psi was reached on the dial gauge. For samples with higher degrees of saturation, it was often necessary to halt the test at lower pressures if extreme permanent deformations occurred in the specimen.

With testing complete, the actual applied pressure and resilient deformation were calculated using one representative cycle from each set. A graph could then be constructed with resilient modulus versus applied normal stress.

5.2.5.4. Results

Results from the majority of resilient modulus tests were not as expected. Rather than exhibiting the typical bi-linear properties associated with fine-grained soils, both BS02 and BE15 soils tended to have a constant modulus regardless of applied stress and degree of saturation. Such was the case for all specimens except for the BS02 samples prepared at a nominal 95% degree of saturation. Figure 5.7 provides graphs for these specimens with Table 5.5 summarizing the results. Figure 5.8 illustrates one of the non-typical test results.

Table 5.5 Resilient Modulus Test Results for BS02 at 95% Saturation

Specimen	γ_{dry} (pcf)	w%	E_{ri} (psi)	σ_{di} (psi)	K_1 (psi/psi)	K_2 (psi/psi)
1	107.1	20.1	1952.5	8.97	-615.1	-8.63
2	107.0	20.1	2270.0	7.62	-448.5	-157.3
3	106.7	20.2	1810.0	7.77	-838.16	-12.34

These results for the BS02 soil at 95% saturation prove acceptable when compared with previous testing performed on Ohio A6 subgrade soils, except for the K_2 values (Figuroa, et.al. 1994, 56).

To try to account for the unexplained behavior in all other specimens, the third test within each BE15 sample was conducted at a confining pressure of 4 psi. This did not affect the outcome, however, which supports the choice for uniaxial testing as mentioned above. The only important conclusion that can be drawn from these results is that the resilient modulus decreases with increasing degrees of saturation. This was expected, however, and has been illustrated in previous subgrade testing (Figuroa, et.al. 1994, 47). Figures 5.9 and 5.10 illustrate this trend for the BS02 and BE15 soils, respectively. These were prepared using an average resilient modulus value or at the break point (within the scatter) from each test. A summary of these results is also shown in Table 5.6.

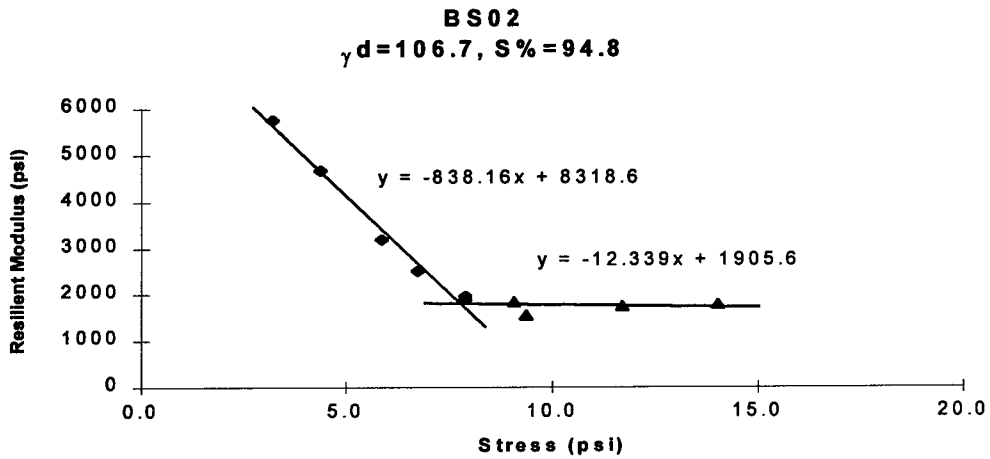
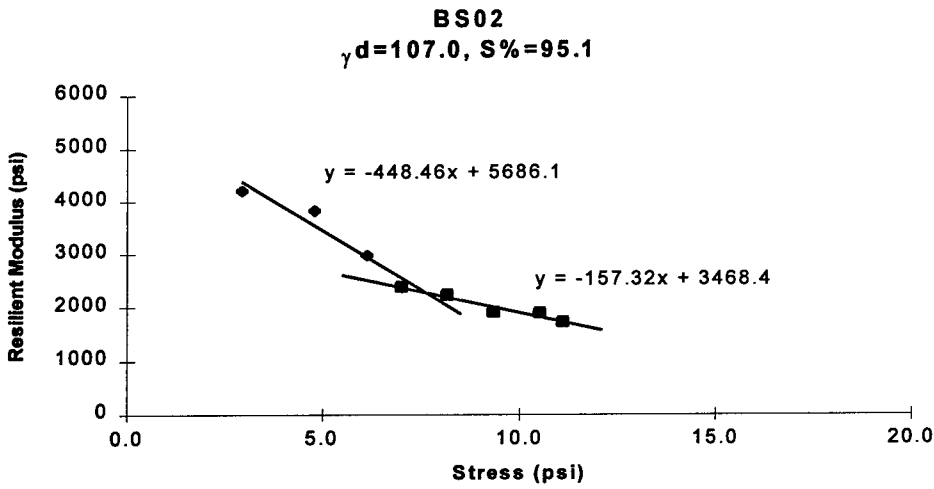
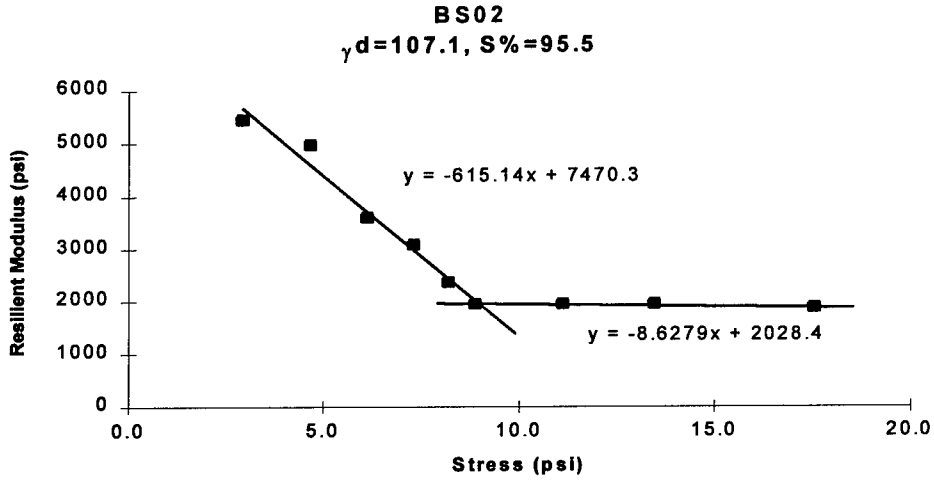


Figure 5.7 BS02 Er Tests at 95% Saturation

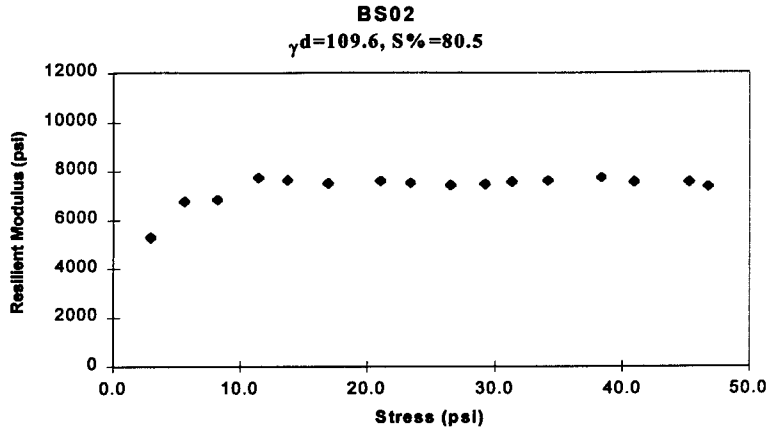


Figure 5.8 Sample BS02 Non-typical Er test results

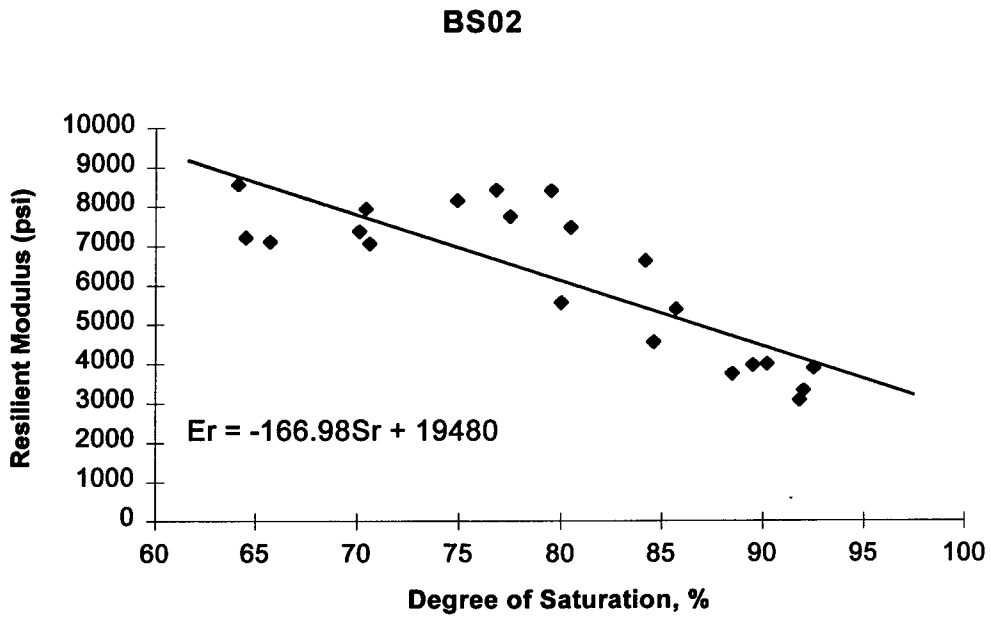


Figure 5.9 Resilient Modulus vs. Degree of Saturation for BS02 soil.

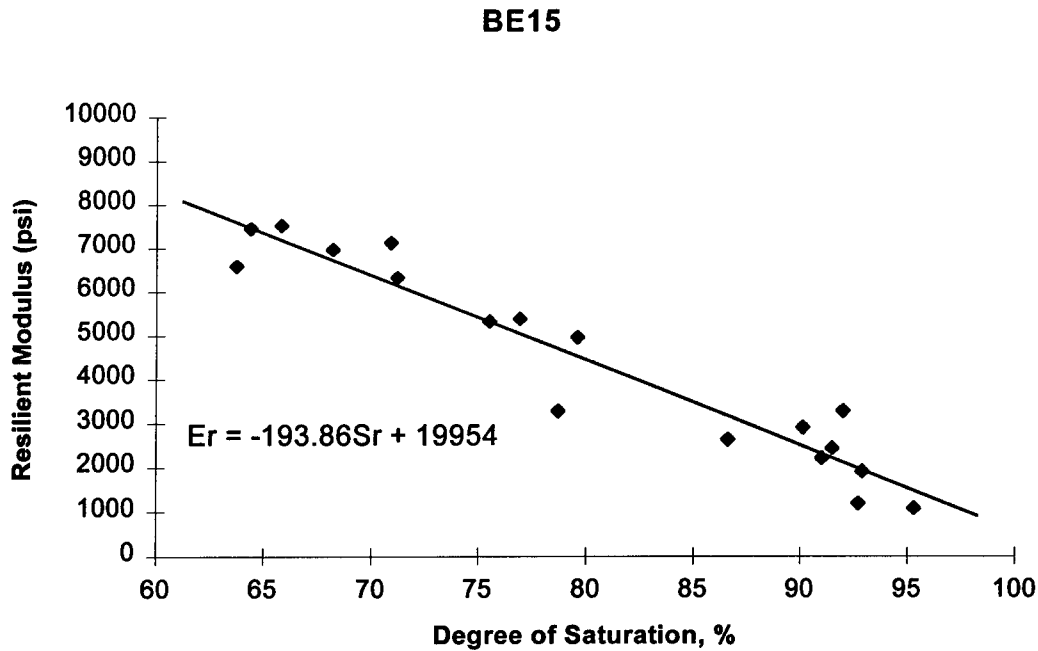


Figure 5.10 Resilient Modulus vs. Degree of Saturation for BE15 soil.

5.3 ASPHALT CONCRETE TESTING AND CHARACTERIZATION

5.3.1 Overview

For material characterization and analysis purposes, it was also necessary to conduct resilient modulus and indirect tensile strength tests on the asphalt concrete (AC) used for the SPS1 and SPS9 pavement studies. Pavement sections typically included both a surface course composed of fine aggregate and an intermediate course with larger aggregate. Having the resilient modulus-temperature relationships, it is then possible to conduct further flexible pavement analyses with a finite element program, as will be shown in Chapter 6. Indirect tensile strength results may be used on future studies relating to the fatigue characteristics of asphalt concrete.

A total of thirty, 4 inch diameter asphalt concrete cores were taken at various sections along SPS1 to be used in this and further studies. Descriptions of the types of tests conducted on these cores are presented next.

Table 5.6 Resilient Modulus vs. Degree of Saturation for BS02 and BE15 Soils

BS02 Soil		BE15 Soil	
Sr (%)	Er (psi)	Sr (%)	Er (psi)
64.1	8567	63.7	6590
64.5	7219	64.3	7451
65.7	7113	65.8	7528
70.1	7382	68.2	6984
70.4	7934	70.9	7137
70.6	7061	71.2	6330
74.9	8155	75.5	5318
76.8	8427	76.9	5382
77.5	7754	78.7	3280
79.5	8399	79.6	4956
80.0	5562	86.6	2648
80.5	7463	90.1	2913
84.2	6627	91.0	2216
84.6	4560	91.5	2448
85.7	5390	92.0	3272
88.5	3751	92.7	1197
89.5	3968	92.9	1918
90.2	3998	95.3	1090
92.0	3329		
91.8	3072		
92.5	3890		

5.3.2 RESILIENT MODULUS

5.3.2.1 Overview

Unlike the resilient modulus for fine-grained soils, the resilient characteristics of asphalt concrete are temperature dependent. However, they can also be considered stress independent. At low temperatures, the AC becomes more rigid as the modulus increases sharply, while at high temperatures, the AC is softer and flexible. The resilient modulus of the AC is one of the most important parameters required in the mechanistic design of flexible pavements in order to determine adequate layer thicknesses to carry the projected traffic.

Several procedures exist for the determination of asphalt concrete resilient modulus, but the indirect tension test method has been recognized as the most repeatable (Brown and

Foo 1991, 2). The guidelines for this method are found under ASTM D 4123-82: Standard Test Method for Indirect Tension Test for Resilient Modulus of Bituminous Mixtures.

In accordance with these guidelines, three cylindrical specimens taken from actual pavement cores were tested at various temperatures. To begin, it was necessary to separate the surface, intermediate, and base courses from the cores using a masonry saw. Construction documents for each test section were used to identify boundaries in the core to permit easy separation. Based on this, surface layer slices were typically 1.75 inches thick with intermediate and base slices ranging up to four inches.

Because the test is nondestructive, the same three specimens were used at each temperature. ASTM recommends testing at 41, 77, and 104 °F, but testing was performed at 45, 55, 65, 75, and 85 °F in order to develop a better curve-fit. Equation 5.2 is normally used to determine the resilient modulus from the results of this test.

$$E_R = \frac{P(\nu + 0.27)}{t\Delta H} \quad (5.2)$$

where

E_R	=	resilient modulus of elasticity, psi
P	=	repeated load, lbf
ν	=	Poisson's ratio
t	=	thickness of specimen, inches
ΔH	=	total recoverable horizontal deformation.

As with the fine grained soil resilient modulus testing, the asphalt concrete cylinder is subjected to a repeated load provided by an air-operated Bellofram cylinder controlled by a servovalve to simulate cyclic traffic loading. In this instance, however, the load is applied vertically through the specimen's vertical diametrical plane and horizontal deformations 90 degrees from the load are measured rather than the vertical deformations. If the Poisson's ratio is unknown, an equation to solve for it is provided in the ASTM specifications requiring

the vertical deformation as an input. For the calculation of the resilient modulus in this project, however, Poisson's ratio was estimated from the results of previous studies on its relationship to the asphalt concrete temperature, and therefore the vertical deformation was not needed. Table 5.7 indicates values of Poisson's ratio used in the calculations.

Table 5.7 Poisson's ratio for Asphalt Concrete

Temp, °F	45°	55°	65°	75°	85°
ν	0.3	0.35	0.38	0.4	0.44

5.3.2.2 Testing Procedure

To begin the resilient modulus test, the AC slice is secured in an apparatus that supports two spring-loaded linear variable differential transformers (LVDTs), horizontally opposed to each other along the central axis. This permits the core to deform vertically and to expand horizontally under the load. The LVDTs may move up or down following the vertical deformation, but still measuring the horizontal expansion. The frame supporting these LVDTs is clamped to the center of the core using a set of thumb screws. To accommodate the temperature requirements, the entire test system is housed in a temperature-controlled room. Before testing, the specimens were allowed to reach the test temperature for at least 24 hours. With LVDTs in place, the core is then placed on a half-inch wide loading strip having a radius of curvature equal to the radius of the specimen. An identical strip is placed on top of the slice to receive and distribute the load generated by the air cylinder across the specimen.

To represent traffic loading, the air pressure was monitored to load the specimen with a frequency of 0.5 Hz. Based on trial structural testing on the test road, it was found that load durations were approximately 0.3 seconds for a vehicle traveling at 45 mph. Therefore, testing was conducted with loading durations of 0.3 seconds and a rest period of 1.7 seconds. Again, high-speed strip chart recorders were used to monitor the voltage outputs from the load cell and both LVDTs. The specimen was subjected to at least fifty conditioning cycles at

the test load in order to adjust the specimen and LVDTs if necessary. Following this, 10 additional cycles were recorded, and a representative cycle was chosen for calculations. This process was repeated on the same three specimens at each temperature for both asphalt courses. Asphalt treated bases were not tested at this time.

5.3.2.3 Results

Figures 5.11 and 5.12 illustrate the resilient modulus-temperature relationship for the surface and intermediate courses, respectively, with both polynomial and exponential best-fit lines displayed. With the exception of the low temperature test points, there was little variability in the results for the three specimens. At the low temperatures, however, any error induced during the test procedure affecting displacement readings becomes a much larger factor due to the minute displacements recorded. At higher temperatures, and therefore larger displacements, the same disturbances are less significant. Table 5.8 provides the expected resilient modulus values for 41, 77, and 104 °F based on the best-fit lines defined in the graphs below.

Table 5.8 Resilient Moduli for ASTM Recommended Temperatures, psi

Pavement Layer	41 °F		77 °F		104 °F	
	Expo.	Poly.	Expo.	Poly.	Expo.	Poly.
Surface	1512500	1261800	258240	278890	68593	13122
Intermediate	1763600	1515100	247030	253990	56561	169460

As seen in these results, the polynomial curve-fit is not representative of actual conditions at high temperatures. Similarly, for very low temperatures, the exponential curve-fit produces extremely high moduli values uncommon for asphalt concrete. Therefore, it is recommended that the polynomial and exponential functions be used for the low and high temperatures, respectively, outside of the actual tested range. Within tested ranges, either regression may be applied.

AC Surface Layer

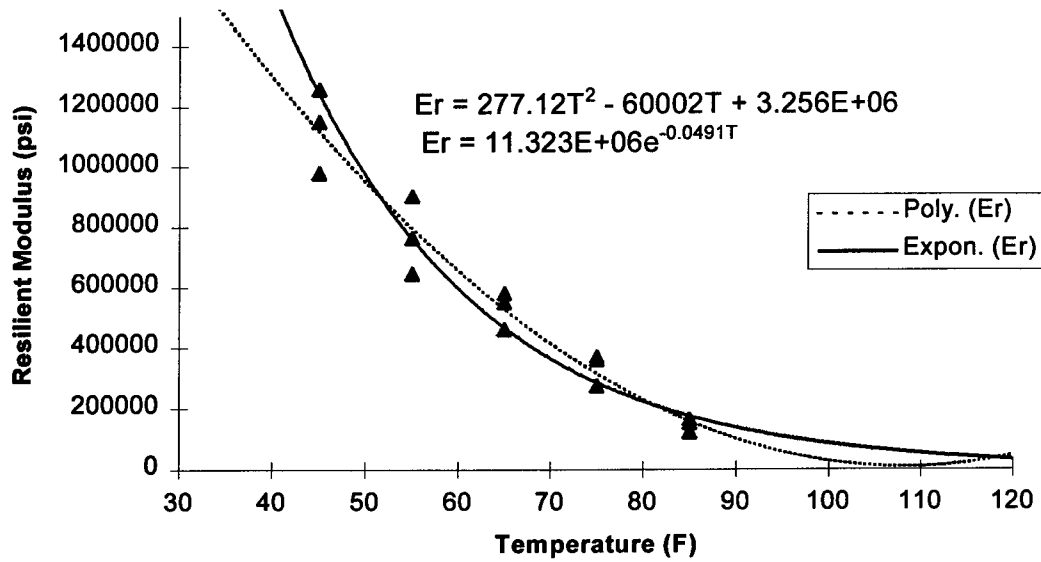


Figure 5.11 Er vs Temperature for Asphalt Surface Layer

AC Intermediate Layer

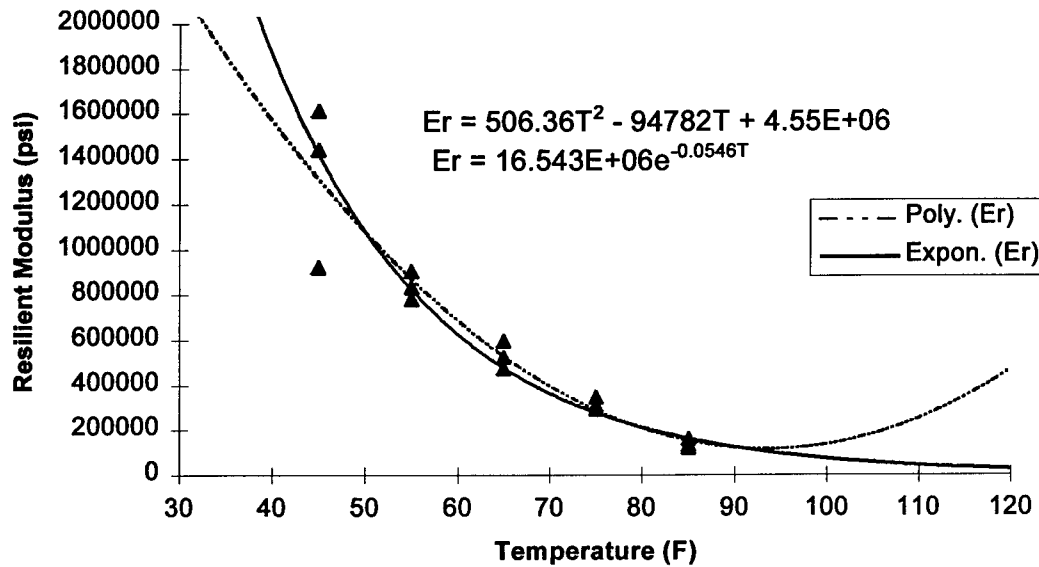


Figure 5.12 Er vs Temperature for AC Intermediate Layer

5.3.3 INDIRECT TENSILE STRENGTH

5.3.3.1 Overview

For flexible pavement design, another important parameter that needs to be characterized is the fatigue life of the asphalt concrete. Under repeated loading, a typical failure pattern begins with the initiation of cracks at the bottom of the asphalt layer. These cracks are the result of excessive tensile strains similar to those experienced in a beam element. To determine the asphalt's tensile strength, the indirect tensile strength test was employed.

Although essentially a compression test, the procedure produces a fairly uniform 'indirect' tensile stress along the loaded diametrical plane of the specimens. This follows a process similar to the resilient modulus test described above, however this time the load is increased in order to maintain a constant vertical displacement rate. Equations to predict the stresses were developed by Frocht using Timoshenko's theory for a circular disk loaded in this manner (Maupin and Freeman 1976, 31). The end result is Equation 5.3 to calculate the indirect tensile strength.

$$S_t = \frac{2P}{\pi t D} \quad (5.3)$$

where

S_t	=	indirect tensile strength, psi
P	=	maximum load, lbf
t	=	specimen height, inches
D	=	specimen diameter, inches.

5.3.3.2 Procedure

Since an ASTM standard was not available at the time of testing, a proposed standard under review by ASTM was used as a guideline. Following this, asphalt slices like those used

in the resilient modulus test were tested at various temperatures. With this being a destructive test, however, specimens could not be reused.

To begin, a specimen was taken from the temperature-controlled room and placed in a compression machine capable of applying loads at the recommended displacement rate of 2 inches/minute. The same curved loading strips were positioned on the slice 180° from each other along the vertical diametrical plane. Since thickness and diameter were previously measured and maximum load was the only variable required, the machine was started and allowed to load until failure. This occurred when the load began to decrease as a failure crack developed along the loaded plane. The maximum load was recorded, and Equation 5.3 was used to calculate the indirect tensile strength. This process was repeated at least two times for each asphalt layer at each temperature.

5.3.3.3 Results

Table 5.9 contains a summary of the results. Unfortunately, the maximum load for sample 1 at 41°F was not obtainable as it surpassed the compression machine's loading capacity. For 77 °F, however, a third sample was not tested due to the limited number of specimens available. Regardless, the results appear satisfactory based on precision studies conducted for this test procedure with nineteen participating laboratories. Within the same laboratory for the same operator, a standard deviation of 8 psi in the tensile strength for identical samples was the average value with a standard deviation of 23 psi deemed the maximum acceptable. Between laboratories, the maximum acceptable standard deviation is 67 psi. All tests fell well below the 23 psi standard deviation, and only the intermediate course at 41 °F was above the typical 8 psi standard deviation.

Table 5.9 Indirect Tensile Strength, psi

Temp °F	Surface Layer			Intermediate Layer		
	Sample 1	Sample 2	Sample 3	Sample 1	Sample 2	Sample 3
41°	-----	139.1	139.6	132.9	112.4	136.3
77°	44.7	46.4	-----	40.9	47.8	-----

CHAPTER 6.

FLEXIBLE PAVEMENT ANALYSIS WITH ILLIPAVE

6.1 Overview

With emphasis being placed on mechanistic design methods, finite element analysis (FEA) programs allow designers to study the effects of material properties on pavement and subgrade deflections, stresses, and strains. Previously, this had to be done by inputting 'expected' values that might be encountered in the field, and results were not always verifiable. With the implementation of the Ohio Test Road, however, the exact field conditions with respect to pavement and subgrade temperature variations, moisture content, and frost depth can now be used with the FEA programs to predict the results. In addition, structural testing will allow comparison of FEA results with actual displacements, stresses, and strains generated by a known axle load to validate computer codes which eventually may be used to develop rational and mechanistic pavement design procedures.

As structural testing results are not yet available from the test road, this study investigates the affect of the asphalt concrete's resilient modulus variation throughout the pavement layer. To do so, actual pavement temperatures from section J1 (ODOT) on SPS9 were used in conjunction with results from the resilient modulus testing of both AC pavement layers and subgrade soils. The objective was to determine if deflections, stresses, and strains calculated by the FEA program vary significantly when the pavement's E_r parameters are entered in three different manners:

- 1). E_r is calculated from the readings by each thermistor depth using actual temperatures. The AC layer was considered to be divided into a number of sublayers corresponding to the number of thermistors.
- 2). E_r is entered as one value for the entire AC pavement depth by averaging actual values obtained in 1),
- 3). E_r is calculated using the average pavement temperature and is entered as one value for the entire pavement depth.

The program used for this study was ILLIPAVE, a finite element analysis package developed at the University of Illinois. In order to efficiently model a wheel load and its corresponding effect throughout the pavement and subgrade, ILLIPAVE generates a two-dimensional element grid representing a vertical slice from the axisymmetric influence region beneath the wheel load (ILLIPAVE Manual 1979, 5). The user inputs material properties and layer thicknesses, and ILLIPAVE generates a representative finite element mesh. After execution, calculated deflections at each node and stresses for each element are written to an output file for viewing.

6.2 Procedure

To execute ILLIPAVE, the user must first create a free-format input file containing all necessary information as described by the manual. With the exception of asphalt concrete resilient modulus values, material properties were left unchanged throughout the testing. Figure 6.1 is a cross-section of SPS9-ODOT used in the analysis.

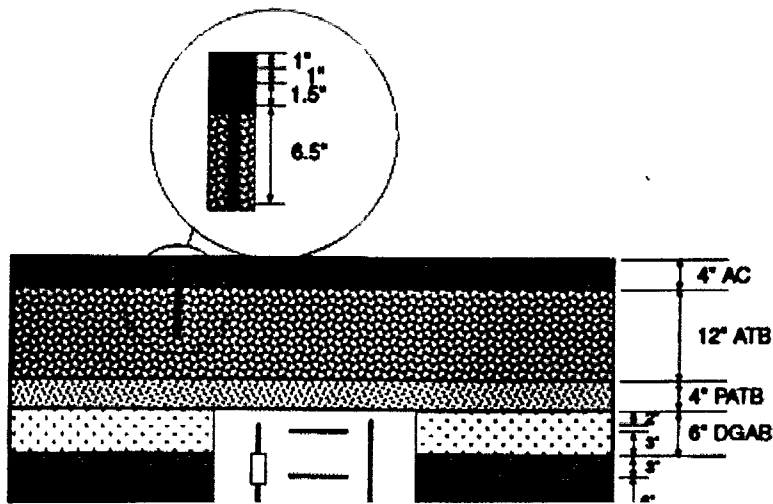


Figure 6.1 SPS9-ODOT: Cross-Section used for ILLIPAVE Analysis.

For this study, the 12" of asphalt treated base (ATB) was modeled as asphalt concrete since it housed the fourth thermistors. The 4" of permeable asphalt treated base (PATB) with very low tensile resistance and the 6" of dense graded aggregate base (DGAB) were modeled

as typical gravels, exhibiting also a stress dependent behavior. The remaining subgrade soil layer was modeled to a depth of 300 inches, beyond which displacements and stresses are negligible.

Material properties and input parameters common to each trial include axle load, tire radius, surface contact pressure, and gravel and soil properties. Using a 9 kip axle load with a six inch loading radius, the surface contact pressure equates to 79.6 psi. Asphalt concrete density was maintained at 137 pcf and was determined from cores extracted from the test road. Gravel density was inputted at 130 pcf, a typical value, and subgrade soil density was determined to be 119 pcf based on averages found from post-construction sampling and testing. Poisson's ratio for both gravel and subgrade soil was input as 0.45.

Because modulus functions vary between materials, ILLIPAVE allows for the input of such differences. Asphalt concrete layers were modeled using a constant modulus function whereas gravel has a modulus that is a function of the stress invariant. Subgrade soil was modeled as a cohesive material having a modulus as a function of the applied deviator stress, as seen in Chapter 5. For this type of material, ILLIPAVE requires the boundaries and key values from the bi-linear relationship previously discussed. Because of limited results from the subgrade testing described in Chapter 5, these values were obtained from previous testing on Ohio subgrades (Figuroa 1994). For an A6 soil classification, these values include the breakpoint stress of 7.0 psi, a K_1 value of -350 psi/psi, a K_2 value of -100 psi/psi, a breakpoint resilient modulus of 5200 psi, and 4 psi and 14 psi as lower and upper applied stress limits, respectively.

Analyses were conducted for two different days using two periods from each day. September 1, 1996 was chosen randomly for its typical high summer temperature whereas January 11, 1997 was chosen for its low values. Temperatures were obtained from the 8:00 a.m. and 3:00 p.m. readings for September 1st, and from the 8:00 a.m. and 4:00 p.m. readings for January 11 as these were times of lows and highs for both days. In addition, they are times when the temperature distribution is either reversed or non-linear. For September, the

top layer is the warmest and the bottom layer is the coldest at 3:00 p.m., yet the reverse is true for 8:00 a.m. In either case, the temperature fluctuates almost linearly between the top and bottom of the asphalt concrete. For January 11th, however, this does not hold true. At both times of the day, the top and bottom layers are about the same temperature, but the two middle locations are much colder. Figures 6.2 and 6.3 illustrate these temperature variations. Using both scenarios will help validate the accuracy of the finite element analysis. Table 6.1 displays the values input for AC resilient modulus (obtained from the polynomial curve at low temperatures and the exponential curve at high temperatures) and Poisson's ratio for each trial.

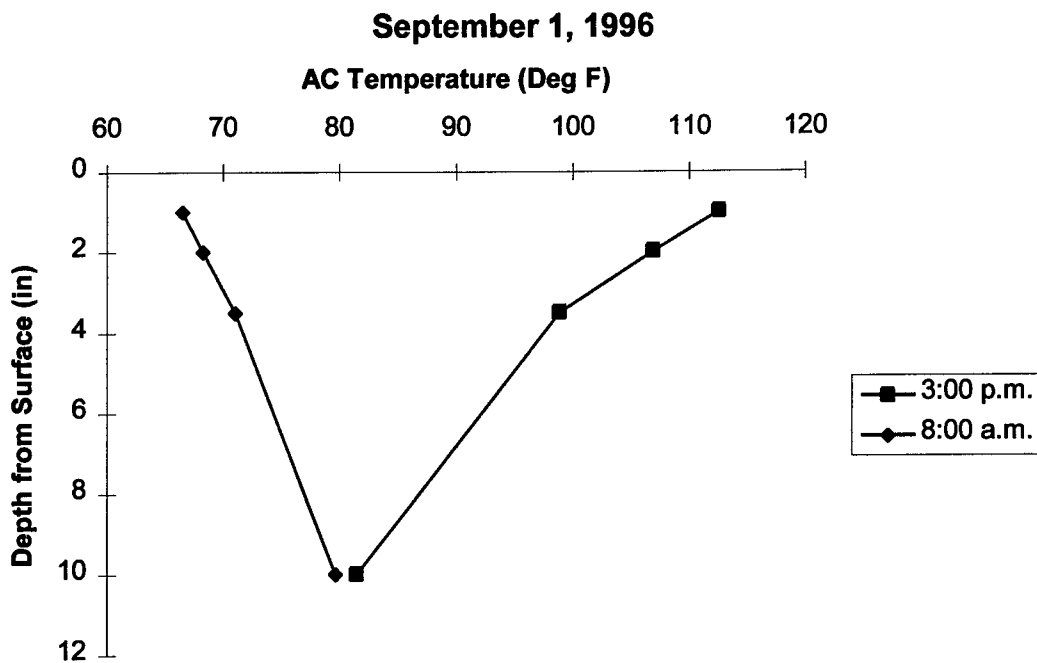


Figure 6.2 AC Temperature Variations for September 1, 1996

6.3 Results

The most important parameters influencing asphalt concrete pavement design include deflections at both the pavement surface and subgrade soil, the vertical stress at the top of the subgrade soil, and the radial strain at the bottom of the asphalt concrete layer.

Tables 6.2 to 6.5 highlight these values that were generated by ILLIPAVE for each resilient modulus input condition.

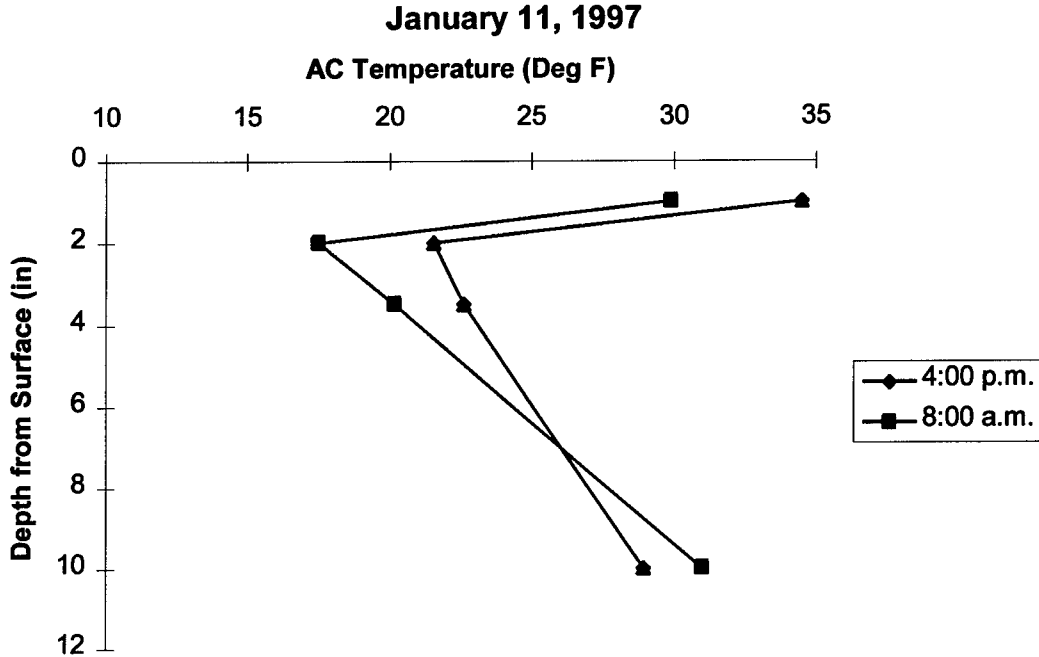


Figure 6.3 AC Temperature Variations for January 11, 1997

Table 6.1 AC Modulus and Poisson's Ratio for ILLIPAVE Analyses

	9/1/96 8:00a.m.		9/1/96 3:00p.m.		1/11/97 8:00a.m.		1/11/97 4:00p.m.	
	Er (psi)	v	Er (psi)	v	Er (psi)	v	Er (psi)	v
Layer 1	443190	0.38	46312	0.47	1705300	0.21	1536300	0.24
Layer 2	403800	0.39	48015	0.46	3085000	0.1	2709900	0.14
Layer 3	324580	0.4	70367	0.44	2856900	0.13	2602260	0.15
Layer 4	209710	0.42	198570	0.42	2035500	0.22	2293090	0.18
Ave Er	345320	0.4	90815	0.45	2420700	0.17	2285388	0.18
Ave T	333560	0.39	70367	0.45	2514300	0.16	2366800	0.17

Values in parentheses indicate the percent difference between results generated using one AC layer and those generated using four AC layers. The latter values are expected to be the most accurate since they are more representative of actual field conditions. Appendix A contains graphs that illustrate the total variation of these parameters with respect to depth from the pavement surface.

After viewing the tabulated results and their percent differences, it is apparent that using one resilient modulus value for the entire pavement provides accurate results at cold temperatures. With the exception of the radial strain values, all results are within roughly five percent from those generated by separating the asphalt concrete into four distinct layers. All radial strain values are within ten percent which may be considered acceptable considering any safety factors that are included in the design process. In addition, the values displayed below are taken from slightly different elevations due to the method that ILLIPAVE uses to assign element thicknesses, and therefore there is a small initial difference in strain values.

The results obtained at warmer temperatures are less satisfactory, however. Radial strain values with a percent difference in excess of 65 percent are unacceptable although the majority of other parameters were within ten percent. In general, the model that uses a resilient modulus based on the average value for the entire pavement generated the closest results in all trials. Nevertheless, the summer months with higher temperatures are the worst-case scenario for asphalt concrete since the resilient modulus is at its lowest. This results in larger subgrade stresses, and therefore larger deflections in the subgrade and at the surface. Although the expected values obtained for September 1st at 3:00 p.m. are higher than the actual values (and therefore safer for design), the inconsistency between the two trials for this day show that it is unacceptable to model the pavement using either an average resilient modulus or a resilient modulus determined from the average pavement temperature.

Table 6.2 ILLIPAVE Results for Conditions on 9/1/96 at 8:00 a.m.

Input Conditions	δ_{surface} (in)	δ_{subgrade} (in)	σ_{subgrade} (psi)	$\epsilon_{\text{radial for AC}}$ (in/in)
4 AC layers, 4 Er values	1.19E-02	8.85E-03	1.16	9.81E-05
1 AC layer, Er Average	1.09E-02 (-8.40 %)	8.52E-03 (-3.73 %)	1.09 (-6.0 %)	8.46E-05 (-13.8 %)
1 AC layer, Er from Ave Temp	1.11E-02 (-6.72 %)	8.60E-03 (-2.82 %)	1.10 (-5.17 %)	8.62E-05 (-12.1 %)

Table 6.3 ILLIPAVE Results for Conditions on 9/1/96 at 3:00 p.m.

Input Conditions	δ_{surface} (in)	δ_{subgrade} (in)	σ_{subgrade} (psi)	$\epsilon_{\text{radial for AC}}$ (in/in)
4 AC layers, 4 Er values	1.78E-02	1.08E-02	1.65	1.26E-04
1 AC layer, Er Average	1.88E-02 (5.62 %)	1.14E-02 (5.56 %)	1.87 (13.3 %)	1.95E-04 (54.8 %)
1 AC layer, Er from Ave Temp	2.14E-02 (20.2 %)	1.22E-02 (13.0 %)	2.09 (26.7 %)	2.09E-04 (65.9 %)

Table 6.4 ILLIPAVE Results for Conditions on 1/11/97 at 8:00 a.m.

Input Conditions	δ_{surface} (in)	δ_{subgrade} (in)	σ_{subgrade} (psi)	$\epsilon_{\text{radial for AC}}$ (in/in)
4 AC layers, 4 Er values	7.37E-03	6.85E-03	6.63E-01	1.27E-05
1 AC layer, Er Average	7.32E-03 (0.68%)	6.83E-03 (-0.29 %)	6.60E-01 (-0.45 %)	1.25E-05 (-1.57 %)
1 AC layer, Er from Ave Temp	7.29E-03 (-1.1 %)	6.81E-03 (-0.58 %)	6.56E-01 (-1.06 %)	1.20E-05 (-5.51 %)

Table 6.5 ILLIPAVE Results for Conditions on 1/11/97 at 4:00 p.m.

Input Conditions	δ_{surface} (in)	δ_{subgrade} (in)	σ_{subgrade} (psi)	$\epsilon_{\text{radial for AC}}$ (in/in)
4 AC layers, 4 Er values	7.36E-03	6.85E-03	8.47E-01	1.20E-05
1 AC layer, Er Average	7.36E-03 (0.0 %)	6.85E-03 (0.0 %)	8.96E-01 (5.79 %)	1.33E-05 (10.8 %)
1 AC layer, Er from Ave Temp	7.33E-03 (-0.41 %)	6.84E-03 (-0.15 %)	8.86E-01 (4.60 %)	1.27E-05 (5.83 %)

CHAPTER 7.

PRELIMINARY SEASONAL FINDINGS

7.1 OVERVIEW

Data collected between the months of August 1996 and January 1997 has been studied to visualize any preliminary conclusions and to help identify problem areas. This has been limited to temperature and moisture data from each test section as well as temperature and precipitation data from the weather station. Relationships between air and asphalt concrete temperatures, soil moisture content and rainfall, and pavement temperature variations are discussed.

7.2 SOIL MOISTURE CONTENT AND RAINFALL CORRELATIONS

Appendix A contains graphs of daily variation in soil volumetric moisture content together with daily total precipitation data for each test site. This was done with the intent of establishing any relationships that may exist between the two parameters as well as studying the affect of drains in the section. For ease of preparation, graphs were plotted with respect to the Julian calendar which numbers days sequentially beginning with January 1. This is the system employed by the dataloggers when assigning data to a particular day of the year. Since the first TDR moisture readings were obtained in July of 1996 and once a month thereafter, precipitation data was used from 183 (July 1) to 355 (December 20) when the last data was obtained.

All moisture sensors were used in this study with the exception of sensor 1. In all test sites except for SPS2-J5, this sensor was installed in a layer of base material rather than the subgrade soil. As a result, moisture readings from these sensors were substantially lower than those obtained from the remaining nine sensors.

The absence of data for SPS1-J2 is due to damage of the sensors as a result of the structural failure in the asphalt concrete and subsequent replacement of the section. After roughly one month of traffic loading, the four inch asphalt concrete layer developed rutting.

During removal of the pavement and base layers in preparation for replacement, however, the seasonal sensors were damaged beyond repair.

7.2.1 Results and Conclusions

Based on a visual comparison of the graphs, it appears that no correlation exists between subgrade soil moisture content and total precipitation. It was expected that any relationship would not be seen until several hours or days after a heavy rainfall depending on the permeability of the soil and surface runoff amounts. During this time, however, roughly one half of the sensors reported an increase in moisture content while the other half showed a decline. This is true for sections with or without drains installed in the subgrade. One important consideration, however, is the length of time between TDR readings. Since moisture data is not stored throughout the month, the monthly readings are only an indication of conditions at the time of the reading. For lack of information, data points on the graphs are connected with a straight line although in actuality the moisture content may vary significantly.

In general, all sites show a declining trend in moisture content from the initial reading in July to December. Other than this, no information is derivable even concerning the effect of drains in the subgrade. It is recommended that, if feasible, the TDR sensors be monitored several times a month during a wet season in order to eliminate the uncertainty that exists between the once a month readings. If nothing is gained after at least a two month trial period, then it would be reasonable to resume the initial practice of monthly monitoring.

7.3 AIR AND ASPHALT CONCRETE TEMPERATURE CORRELATIONS

As seen in the ILLIPAVE analysis in Chapter 6, it is necessary to have a knowledge of asphalt concrete pavement temperature so that its resilient modulus may be inferred for design purposes. In support of this, pavement and air temperatures were studied in order to develop a reliable correlation that would allow asphalt concrete pavement temperatures to be inferred from air temperature readings.

This study was conducted using weather station data together with onsite data from sections SPS9-ODOT and SPS1-J2 before reconstruction.

7.3.1 Results and Conclusions

Appendix C contains the graphs of asphalt concrete temperature plotted as a function of air temperature for each thermistor installed in the pavement. Hourly averages for both pavement and air temperature were used beginning with data collected in June throughout November of '96. Specifically, data spans June 9 to September 4 for SPS1-J2 and June 13 through November 27 for SPS9-ODOT. A regression analysis to produce the best-fit line in each case resulted in a second-order polynomial following the form in Equation 7.1:

$$T = C_1 + C_2A + C_3A^2 \quad (7.1)$$

where T = Asphalt Concrete Temperature (Deg C)
 C₁, C₂, C₃ = Regression Constants
 A = Hourly average air temperature (Deg C)

Table 7.1 lists the regression constants obtained for each thermistor at both test sites as well as the values for average asphalt concrete pavement temperature.

Table 7.1 Regression Constants for Air and AC Temperature Correlations

	SPS9-ODOT			SPS1-J2		
	C ₁	C ₂	C ₃	C ₁	C ₂	C ₃
Sensor 1	8.8149	0.3334	0.0312	15.535	-0.1076	0.037
Sensor 2	3.7632	0.8504	0.0164	-----	-----	-----
Sensor 3	4.4528	0.9708	0.0083	23.773	-0.2477	0.0257
Average	5.677	0.7182	0.0186	-----	-----	-----

Figures 7.1 and 7.2 compare the correlations between individual thermistors for SPS9-ODOT and SPS1-J2, respectively. As expected for these months of the year, Thermistor 1 near the surface of the pavement maintains the highest temperature correlation with

Thermistor 3 having the lowest. Interestingly, the graphs begin to merge near an air temperature of 15 °C. This is somewhat expected, however, as surface conditions will become colder than the lower pavement layers as the air temperature decreases. Because year-round data is not yet available, this effect does not appear on the graph. At lower temperatures, the curves should flip with Thermistor 3 being the highest and Thermistor 1 becoming the lowest.

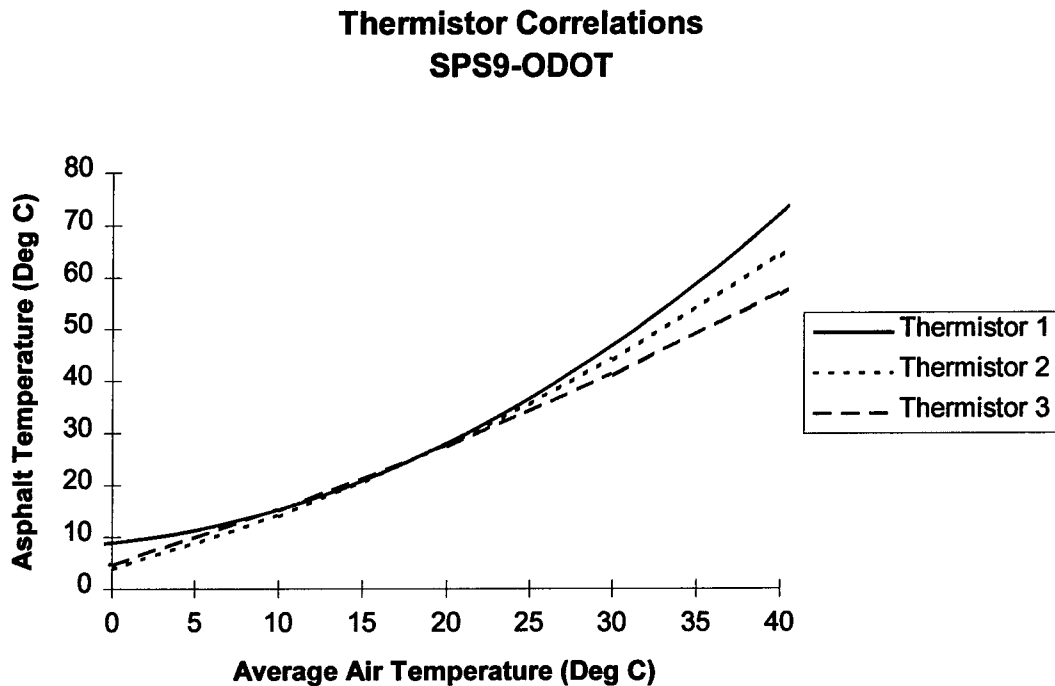


Figure 7.1 Thermistor Correlations for SPS9-ODOT

As seen from the ILLIPAVE analysis discussed in Chapter 6, the results generated when using values for average pavement temperature will not be as accurate as those obtained by breaking the pavement into distinct layers of different temperatures. Unfortunately, Thermistor 2 for SPS1-J2 malfunctioned after several weeks of operation as can be seen in Figure C6. At various times throughout the day, readings would be extremely high (over 200 °F) for unknown reasons. It was noticed, however, that the ‘unacceptable’ readings always began around 1:00 p.m. and lasted until 8:00 p.m. Because of this, it appears that the thermistor operation was affected after the pavement reached a high temperature. At other

Thermistor Correlations SPS1-J2

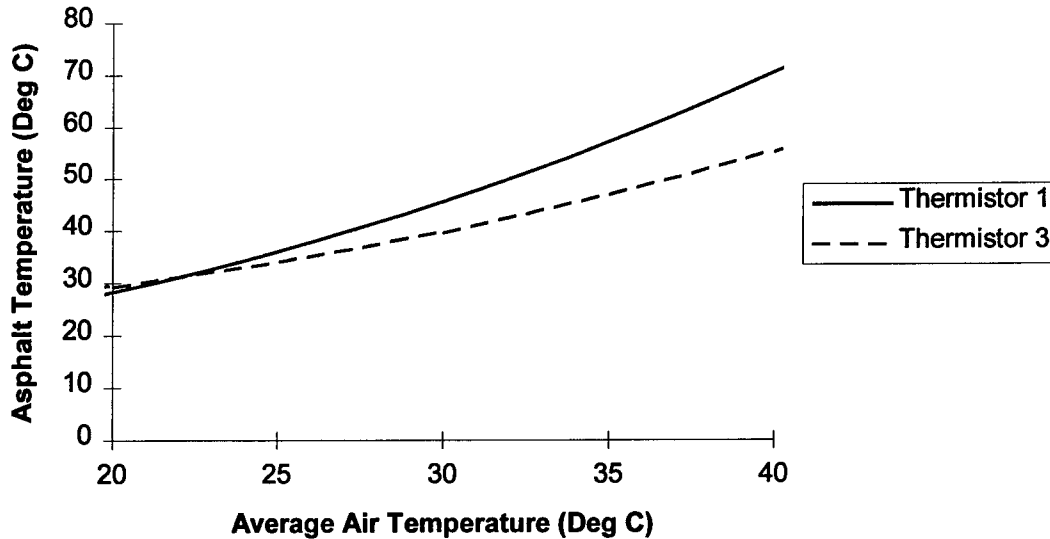


Figure 7.2 Thermistor Correlations for SPS1-J2

times of the day, the sensor provided readings consistent with those obtained from sensors 1 and 3. Even so, it is not advisable to regard this data as being truly accurate.

Because of the different time spans and the malfunctioning thermistor, comparisons can not be made between the two asphalt concrete sections. In comparison with similar research conducted in nearby Knox and Licking counties, however, the average coefficient values for SPS9-ODOT compare rather well considering a full year of data is not yet available. Even so, it is recommended that a similar analysis be conducted on SPS9-ODOT as well as other AC sections for the remaining months of the year to establish proper correlations. Since the worst conditions for asphalt concrete appear in the summer (when the asphalt concrete is the softest), these months should have the highest priority.

7.4 HOURLY PAVEMENT TEMPERATURE VARIATIONS

7.4.1 Portland Cement Concrete Temperature Differentials

As previously mentioned, temperature differentials in concrete pavements create curling stresses in addition to the continually present traffic load stresses. When the surface temperature is greater than that at the lower boundary of the pavement, the concrete slab tends to expand longitudinally on the top and to contract on the bottom. The weight of the slab prevents it from doing so which results in compressive stresses on the surface and tensile stresses at the bottom. Similarly, when the temperature differential is reversed, tensile stresses occur at the surface and compressive stresses occur near the bottom (Huang 1993, 168). In order to calculate these stresses effectively, the temperature differential between the top and bottom of the slab must be determined.

7.4.2 Results

Appendix D contains graphs from the first day of each month that the thermistors have been in operation. These are intended mostly for visual purposes and include plots of pavement temperature as a function of time throughout the day. All sections were used including the AC sections even though the curling stresses are not present in these flexible pavements. Regardless, the plots are useful in determining times of key fluctuations and maximum temperatures.

From the graphs, the two extreme cases of temperature differential for each day are visible. Table 7.2 highlights the maximum differentials for each concrete section for both curling conditions. For the days studied, 11.2 °C (20.2 °F) is the highest temperature differential throughout all of the concrete slabs when the surface temperature is the warmest. For the opposite case when the surface is the coldest, 6.48 °C (11.7 °F) is the largest differential to date. It will be necessary to study the remaining months (and all days of the months) in order to determine the actual maximum temperature differentials for the year. It would be expected that points of maximum ΔT for each section would occur on the same day, however, other factors such as base type and subgrade conditions influence the concrete temperatures as well. This makes it difficult to establish good correlations between concrete

temperatures and the related parameters although maximum temperature differential is probably one of the most important pieces of information to be obtained from the recorded data.

Table 7.2 Maximum Temperature Differentials for PCC Pavement, °C

	PCC Thickness	Surface Temp Highest			Surface Temp Lowest		
		ΔT	Time	Date	ΔT	Time	Date
SPS2-J3	11 "	8.89	5:00 p.m.	Aug. 1	5.418	11:00 p.m.	Nov. 1
SPS2-J5	8 "	9.56	3:00 p.m.	Oct. 1	5.493	11:00 p.m.	Nov. 1
SPS2-J12	11 "	11.23	3:00 p.m.	Sept. 1	6.475	11:00 p.m.	Nov. 1

7.4.3 Other Observations

Although the Portland cement concrete and asphalt concrete pavements are different thicknesses, some observations can be made between the two. As expected, the surface temperature of the AC pavement is greater than that of the PCC pavements. Due to its color, the AC pavements reach a temperature approximately 10 °C greater than the PCC surfaces at warmest times of the day. This holds true throughout both summer and winter months of preliminary testing. For early morning hours, however, both pavements maintain similar temperatures up until the colder months starting with November. At this point, AC surface temperatures start to remain approximately 8 °C above PCC surface temperatures.

During the warmer months throughout October, both pavement types typically experienced two periods of uniform pavement temperature for each day. This occurred in the morning between 10:00 and 11:00 and again in the evening between 9:00 and 10:00. For the colder months, there was only one daily period of uniform temperatures for the Portland cement concrete. The AC pavement, however, did not display this behavior. Instead, the surface remained the warmest layer throughout the entire day. This is the opposite of what would be expected since lower layers are generally warmer during the coldest parts of the

day. These patterns could be the result of a passing weather front for that particular day. Regardless of the explanation, care must be taken when analyzing temperature data obtained during the winter of 1996-97. Since the test road was not in use during this time and safety was not a concern, thick patches of ice and snow were allowed to accumulate. This appeared sporadically throughout all SPS sections in patches that covered both lanes entirely. Hopefully, combined temperature data from all sites will distinguish between areas that were either covered or subjected to normal ambient temperatures.

CHAPTER 8.

CONCLUSIONS AND RECOMMENDATIONS

Five seasonal instrumentation sites have been installed and monitored on the Ohio Test Road near Delaware, Ohio as part of the Long Term Pavement Performance Program's (LTPP) Specific Pavement Studies (SPS). Seasonal instrumentation includes thermistors for pavement and subgrade temperature measurement, time-domain reflectometry (TDR) probes for subgrade soil moisture content determination, and resistivity probes for frost depth measurement. In addition, an onsite weather station has been monitored for daily and hourly wind speed and direction, air temperature, total precipitation, relative humidity, and solar radiation amounts.

In accordance with project guidelines, seasonal data and weather station data have been analyzed for quality using the SMPCheck and AWSCheck programs, respectively. Both are user-friendly and allow the removal of faulty data points prior to the transmittal of the upload files to the SHRP regional coordinator.

In general, the seasonal instrumentation and the weather station are working as expected. Preliminary studies have been conducted using pavement temperature, subgrade soil volumetric moisture content, air temperature, and total precipitation data on a monthly basis between June, 1996 to January, 1997 inclusive.

An attempt was made to establish correlations between subgrade soil moisture content and total precipitation as well as to study the influence of drains in the subgrade. This was not successful, however, using the currently available monthly TDR measurements. Although it is expected that the moisture content will fluctuate minimally on a daily basis, additional monthly measurements are required if a meaningful precipitation-moisture content correlation is to be developed. To determine the effect of precipitation and the benefits of drainage, monitoring periods must be increased for a trial period. In general, the only observation is that moisture contents decrease as a whole from June to December.

Equations were developed for the correlations between asphalt concrete pavement temperature and ambient air temperature for sites SPS1-J2 and SPS9-ODOT. With the lack of data from thermistor 2 on SPS1-J2, however, an average correlation using all three thermistors could only be developed for SPS9-ODOT. A vertical shift between thermistor correlation equations was evident with Thermistor 1 giving the highest temperatures. Although this study includes the warmest months of the year (when AC moduli are the lowest), it will be necessary to conduct the same study for the remaining months using additional SPS1 AC sections. Once the correlations are validated, they can be used in conjunction with AC resilient modulus-temperature correlations to infer the resilient modulus directly from air temperature.

Hourly pavement temperature variations were studied for the first day of each month in the monitoring period. From this, the largest temperature differential from top to bottom of the Portland cement concrete pavements was 11.23 °C which occurred on September 1 at 3:00 p.m. when the surface was the warmest. Results show that this temperature differential is a function of base material properties and not air temperature alone since maximum differentials for other sections did not occur at the same date. Two points of no temperature differential (uniform temperature throughout) were typically seen for each section when surface and bottom pavement temperatures reversed. These occurred between 10 a.m. and 11 a.m. and again between 9 p.m. and 10 p.m. for the warm months ending in October. For the colder months, the pavements typically experienced one daily point of uniform temperature beginning in December. Interestingly, this did not occur for the AC pavement on SPS9-ODOT. Instead, the surface layer remained the warmest throughout the entire day. These patterns could be the result of a passing weather front. Data taken during this time of the year, however, must be analyzed with caution since the test road was not in use throughout the winter. As a result, ice and snow were allowed to accumulate on the surface which could have greatly affected the normal temperature fluctuations. Again, it will be necessary to continue monitoring on a daily basis throughout the year in all sections to develop significant observations.

Characterization tests performed on the subgrade and embankment soil (specific gravity, Atterberg Limits, and compaction tests) classified them as an A6 silty clay (CL for the Unified system). Resilient modulus testing provided non-typical results at low degrees of saturation as the modulus was relatively unaffected by the applied stress. At 95% saturation, however, the soil displayed an expected bi-linear behavior. Correlations were developed between the average resilient modulus and the degree of saturation which illustrated the anticipated decrease in modulus as saturation levels were increased. Breakpoint resilient moduli and deviator stresses at 95% saturation compared well with previous results obtained from Ohio subgrades.

Asphalt concrete characterization included resilient modulus and indirect tensile strength testing for the surface and intermediate AC layers. Exponential and polynomial correlation equations were developed relating the resilient modulus to the AC temperature which can be used in conjunction with the AC temperature-air temperature correlations previously discussed. Because of problems outside of the tested range, however, it is recommended that trends relating the resilient modulus to the inverse or inverse squared of the temperature be studied. Indirect tensile strength testing was performed at 41 and 77 °C for both layers. The lack of available cores prevented testing at 104 °C which will need to be performed eventually for use in asphalt fatigue studies.

The finite element flexible pavement analysis program ILLIPAVE was used to study the effect of using three procedures of inputting the asphalt concrete resilient modulus. These models incorporated actual material properties and pavement temperatures from SPS9-ODOT and varied only by the procedure used to determine the resilient modulus. In the first procedure, the pavement was considered to be composed of a number of layers equal to the number of thermistors. Resilient moduli were calculated for each layer using actual temperatures and results from AC resilient modulus testing. In the second procedure, one average resilient modulus was determined from the values given in the first procedure and was used as input for the entire pavement. Finally, the third procedure used a single resilient

modulus calculated from the average pavement temperature. Testing involved temperatures on two separate days using the two times from each day at which temperature differentials were the largest.

ILLIPAVE outputs of subgrade and pavement deflections, subgrade stresses, and AC radial strains were monitored. Assuming the first procedure is the most representative of actual conditions, the second and third models were compared accordingly. Both yield satisfactory results for stresses and deflections at large depths. However, predicted radial strain values exceeded those from the first procedure by more than 60% and were considered to be unacceptable. In general, the procedure incorporating average resilient modulus values yielded somewhat better results.

In closing, the summary report for the AASHO Road Test in 1962 predicted that any road experiment attempting to monitor all parameters affecting pavement life would be totally infeasible with regards to cost and implementation. In addition, if such a road were constructed that stayed within these limits but still attempted to monitor all parameters, it would most likely yield information of little value. However, considering the advances in technology including monitoring devices, data acquisition and analysis systems, a wealth of knowledge regarding pavement behavior is to be gained with the Ohio Test Road, provided already established strict quality control norms are followed.

Future research should be focused on collecting additional data including weather station parameters, TDR measurements and temperature readings within the pavement and the subgrade to obtain meaningful observations and correlations. Ultimately the variation of the asphalt concrete modulus and the resilient modulus of subgrade soils could be determined on a monthly or seasonal basis, which will contribute to a more realistic design of pavements.

LITERATURE CITED

“The AASHO Road Test, Report 7, Summary Report”. Highway Research Board of the NAS-NRC Division of Engineering and Industrial Research. National Academy of Sciences-National Research Council, Washington, D.C. 1962.

AASHTO Designation T292-01. “Standard Test Method for Resilient Modulus of Subgrade Soils and Untreated Base/Subbase Materials”, Standard Specifications for Transportation Materials and Methods of Sampling and Testing. Sixteenth Edition, 1993: 931-945.

ASTM Designation D 4123-82, “Standard Test Method for Indirect Tension Test for Resilient Modulus of Bituminous Mixtures”, Annual Book of ASTM Standards, Vol 04.03: 501-503.

Brown, E.R. and Kee Y. Foo. “Evaluation of Variability in Resilient Modulus Test Results (ASTM D 4123)” Journal of Testing and Evaluation Vol. 19, No. 1 (1991): 1-13.

Campbell Scientific, Inc. HMP35C Temperature/RH Probe Instruction Manual. Utah, 1994.

Campbell Scientific, Inc. LI200X Pyranometer Instruction Manual. Utah, 1994.

Campbell Scientific Inc. UT-3 Weather Station Instruction Manual. Utah, 1993.

Campbell Scientific, Inc. 05103-5/05305-5 Wind Monitor Instruction Manual. Utah, 1993.

Datalynx Instruments. Tipping Bucket Rain Gauges Instruction Manual. California, 1989.

Department of Civil Engineering, University of Illinois. “The ILLIPAVE Program for Pavement Analysis User’s Manual”, 1979.

Elkins, Gary E., Haiping Zhou, and G.R. Rada. “LTPP Seasonal Monitoring Program: SMPCheck Users Guide Version 2.5”. PCS/Law Engineering. Maryland, 1996.

Figuroa, J.L., E. Angyal, and X. Su. “Characterization of Ohio Subgrade Types”, Case Western Reserve University, Cleveland, Ohio 1994.

Huang, Yang H. Pavement Analysis and Design. New Jersey: Prentice-Hall, Inc., 1993.

Jin, Myung S., and William D. Kovacs. "Seasonal Variation of Resilient Modulus of Subgrade Soils" Journal of Transportation Engineering 120, No. 4 (1994): 603-616.

Maupin, G.W. Jr., and J.R. Freeman, Jr. Simple Procedure for Fatigue Characterization of Bituminous Concrete. Virginia Highway and Transportation Research Council. Virginia, 1976.

Morse, Aric. "Improving Pavement Design Procedures in Ohio". The Ohio SPS Test Road Pavement Instrumentation Workshop. Delaware, Ohio, 1996.

Rada, G.R., et al. "LTPP Seasonal Monitoring Program: Instrumentation Installation and Data Collection Guidelines". PCS/Law Engineering. Maryland, 1995.

Sargand, Shad. "Development of an Instrumentation Plan for the Ohio SPS Test Pavement (DEL-23-17.48)" Ohio University, Athens, Ohio 1994.

Thompson, Marshall R., and Quentin L. Robnett. "Resilient Properties of Subgrade Soils" Transportation Engineering Journal 105, No. TE1 (1979): 71-89.

Zhou, H, G.R. Rada, and G.E. Elkins. "LTPP-SPS Automated Weather Stations: AWSCheck Users Guide Version 1.1." PCS/Law Engineering. Maryland, 1996.

APPENDIX A

ILLIPAVE RESULTS

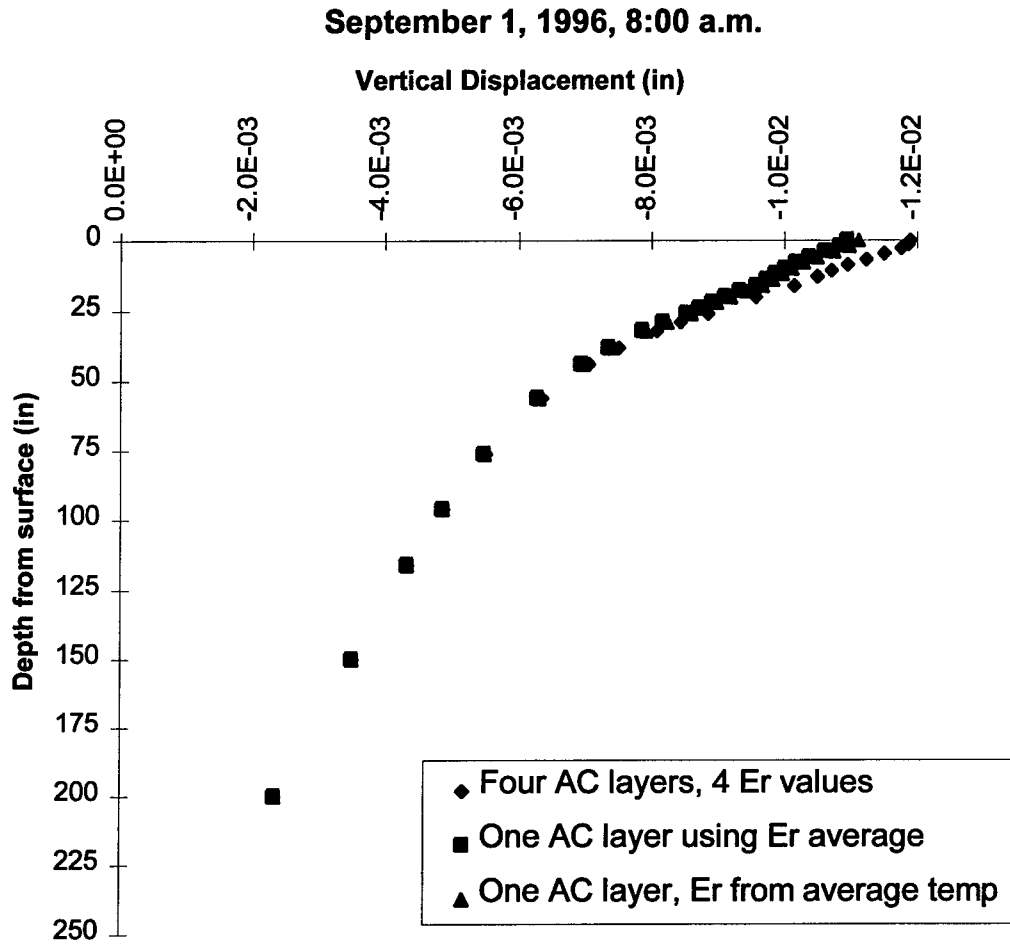


Figure A1. ILLIPAVE Vertical Displacement, 9/1/96 at 8:00 a.m.

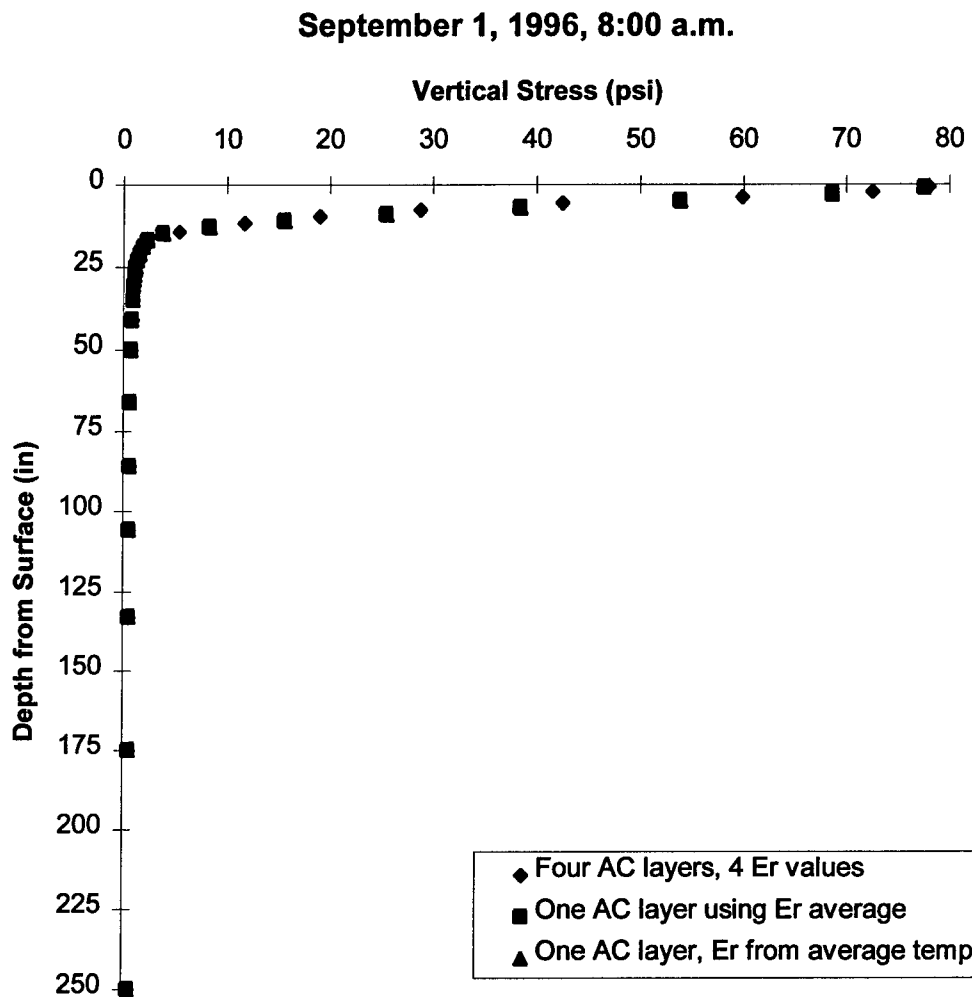


Figure A2. ILLIPAVE Vertical Stress, 9/1/96 at 8:00 a.m.

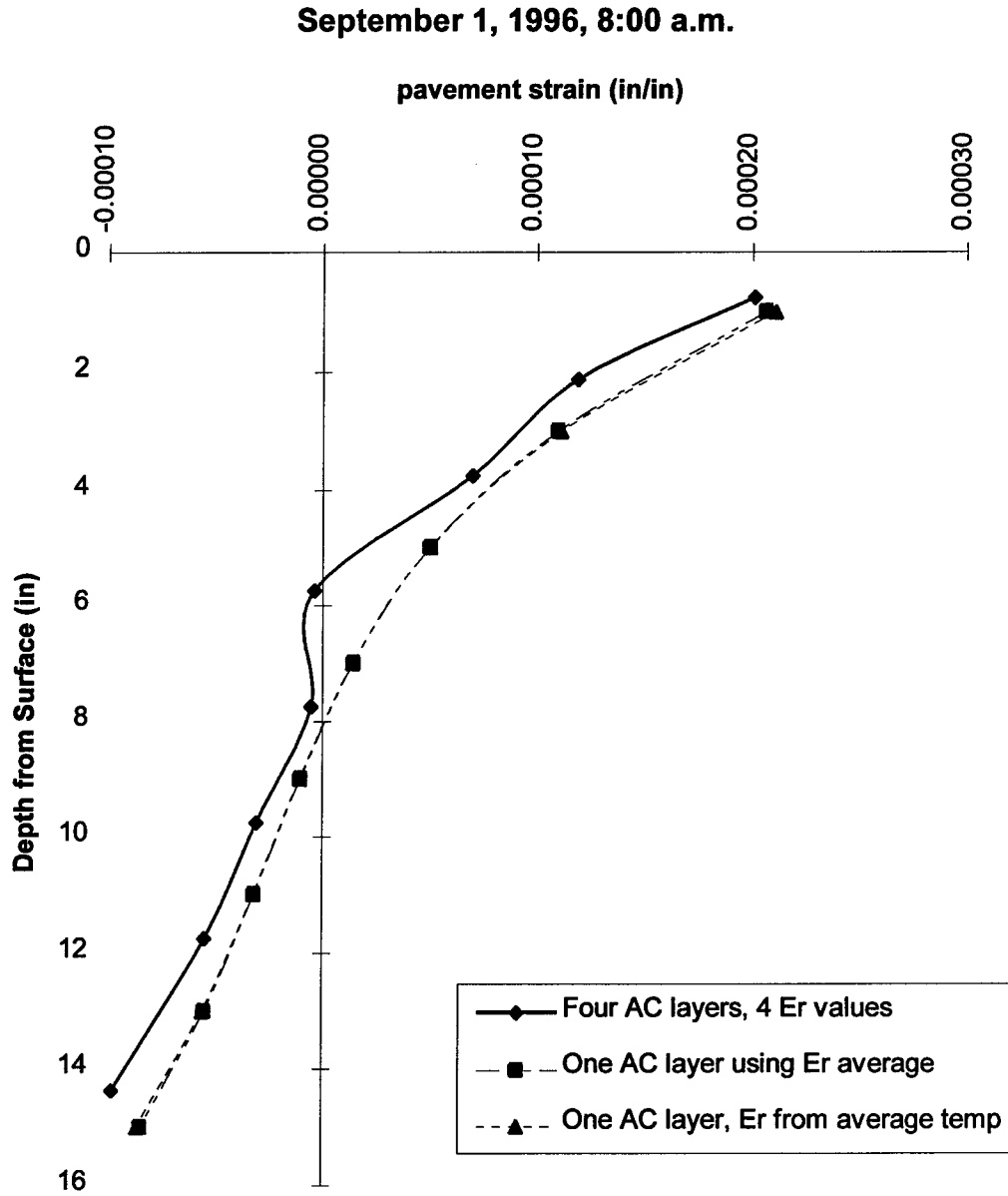


Figure A3. ILLIPAVE AC Radial Strain, 9/1/96 at 8:00 a.m.

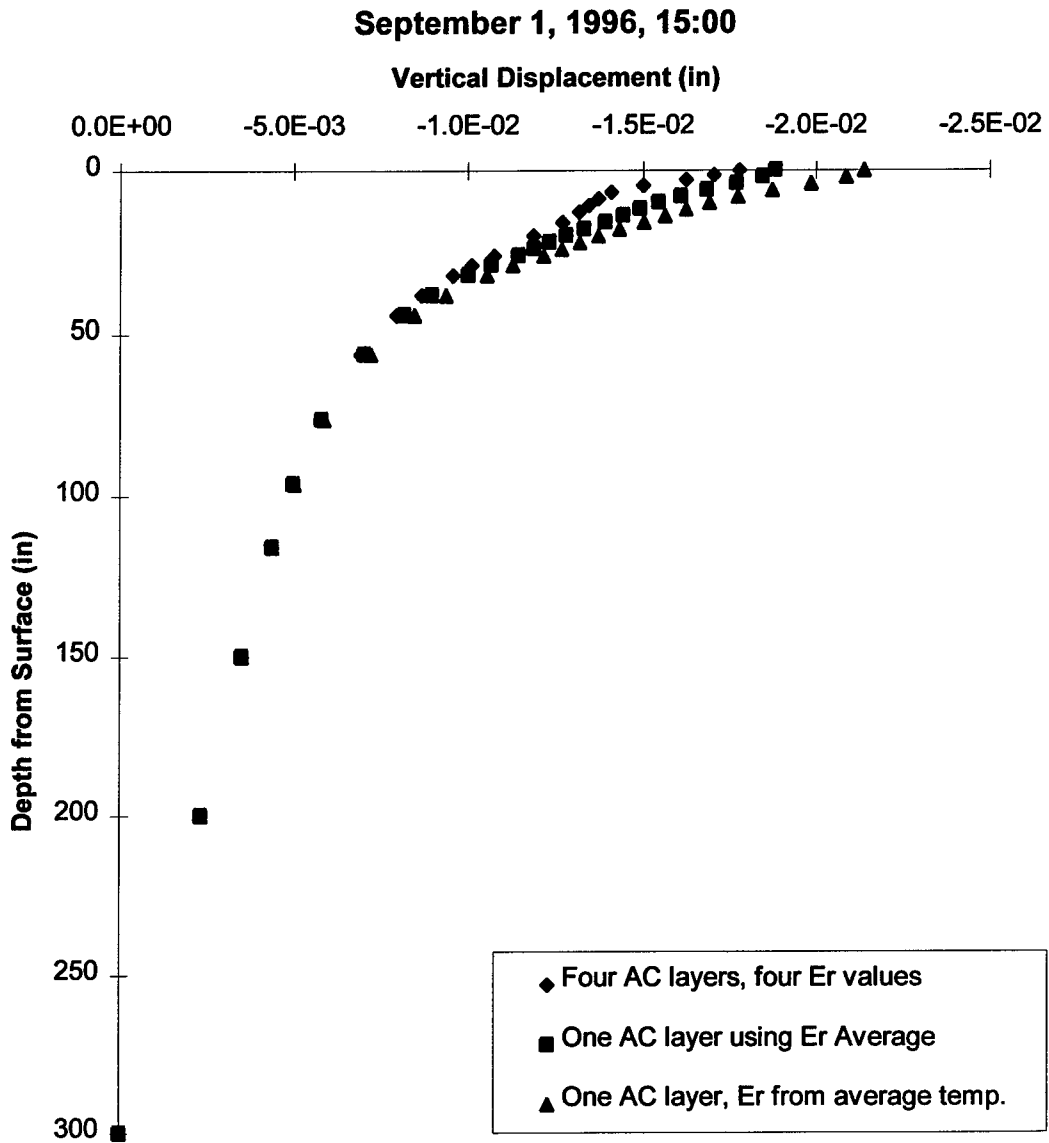


Figure A4. ILLIPAVE Vertical Displacement, 9/1/96 at 3:00 p.m.

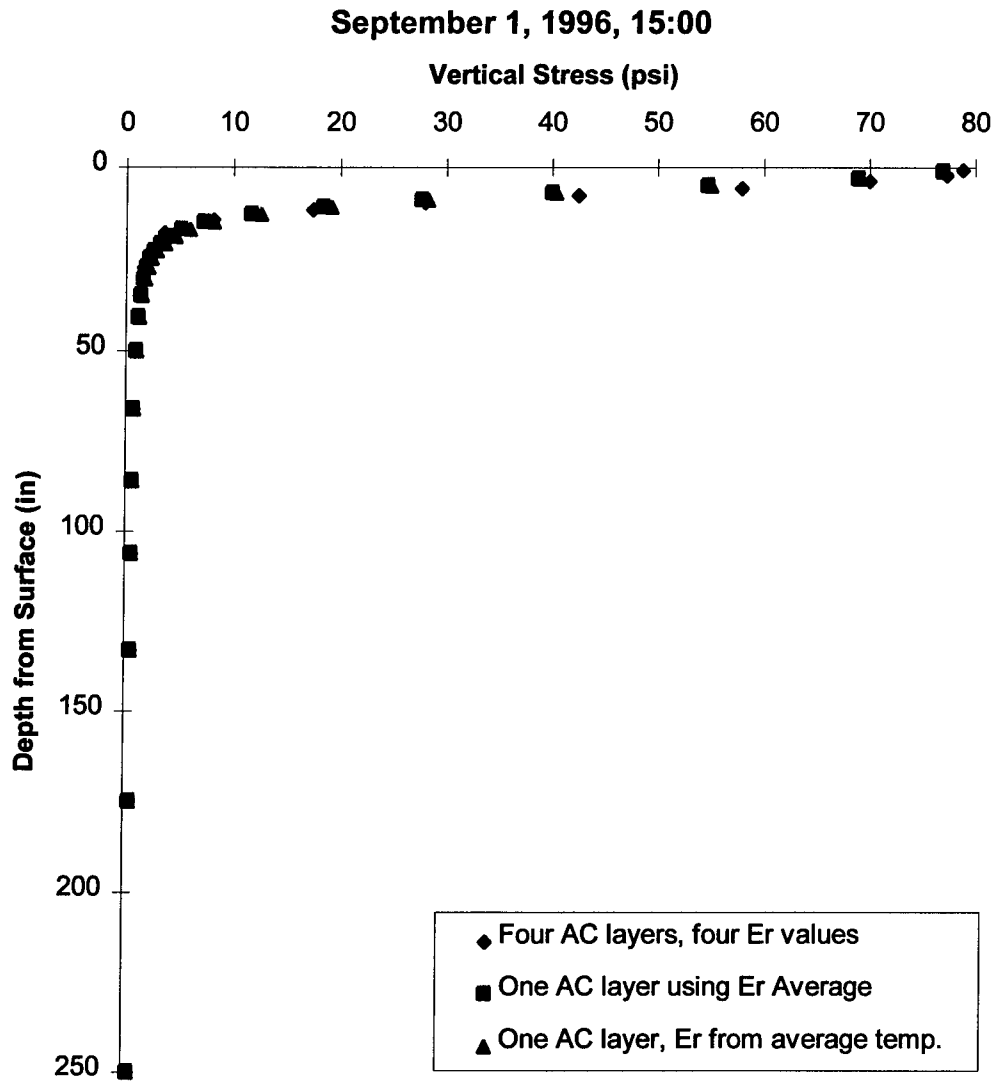


Figure A5. ILLIPAVE Vertical Stress, 9/1/96 at 3:00 p.m.

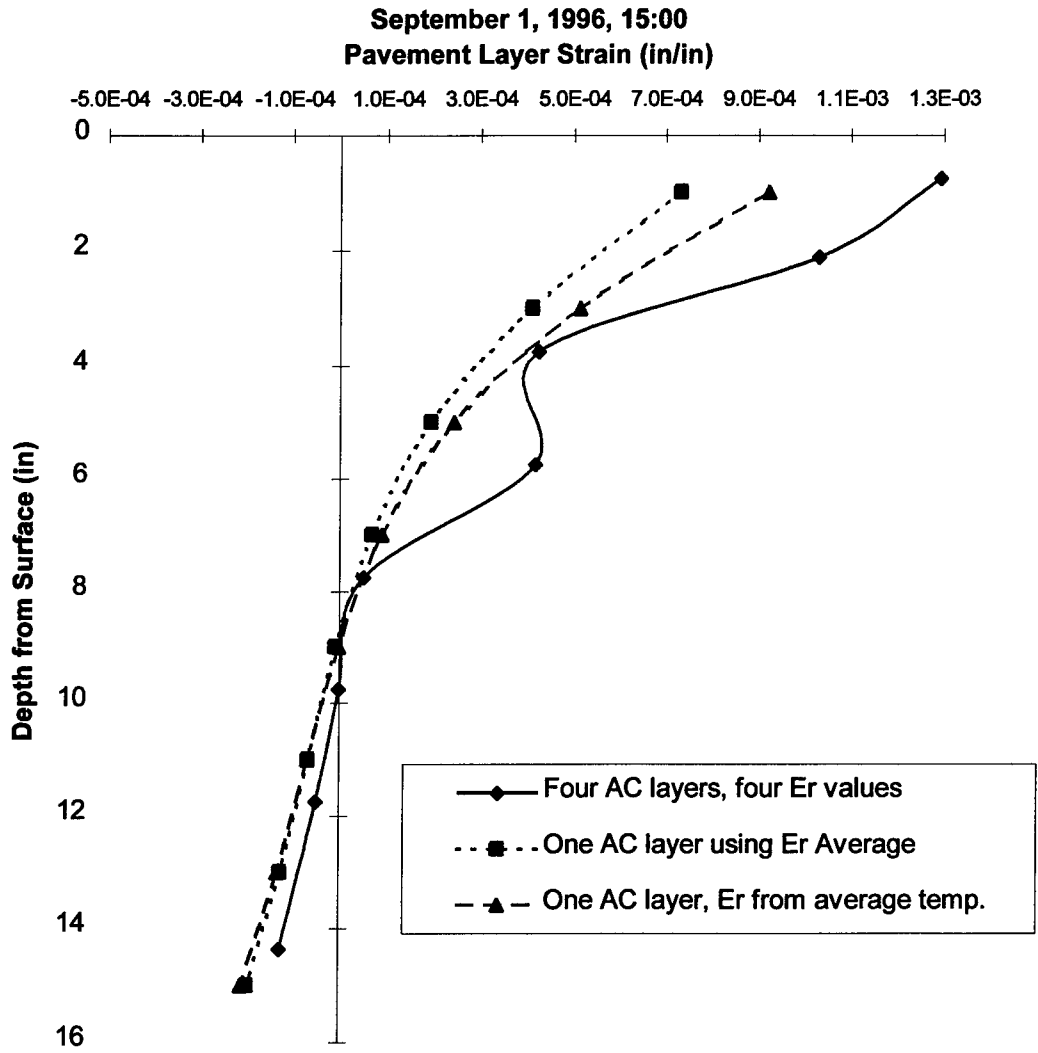


Figure A6. ILLIPAVE AC Radial Strain, 9/1/96 at 3:00 p.m.

January 11, 1997, 8:00 a.m.

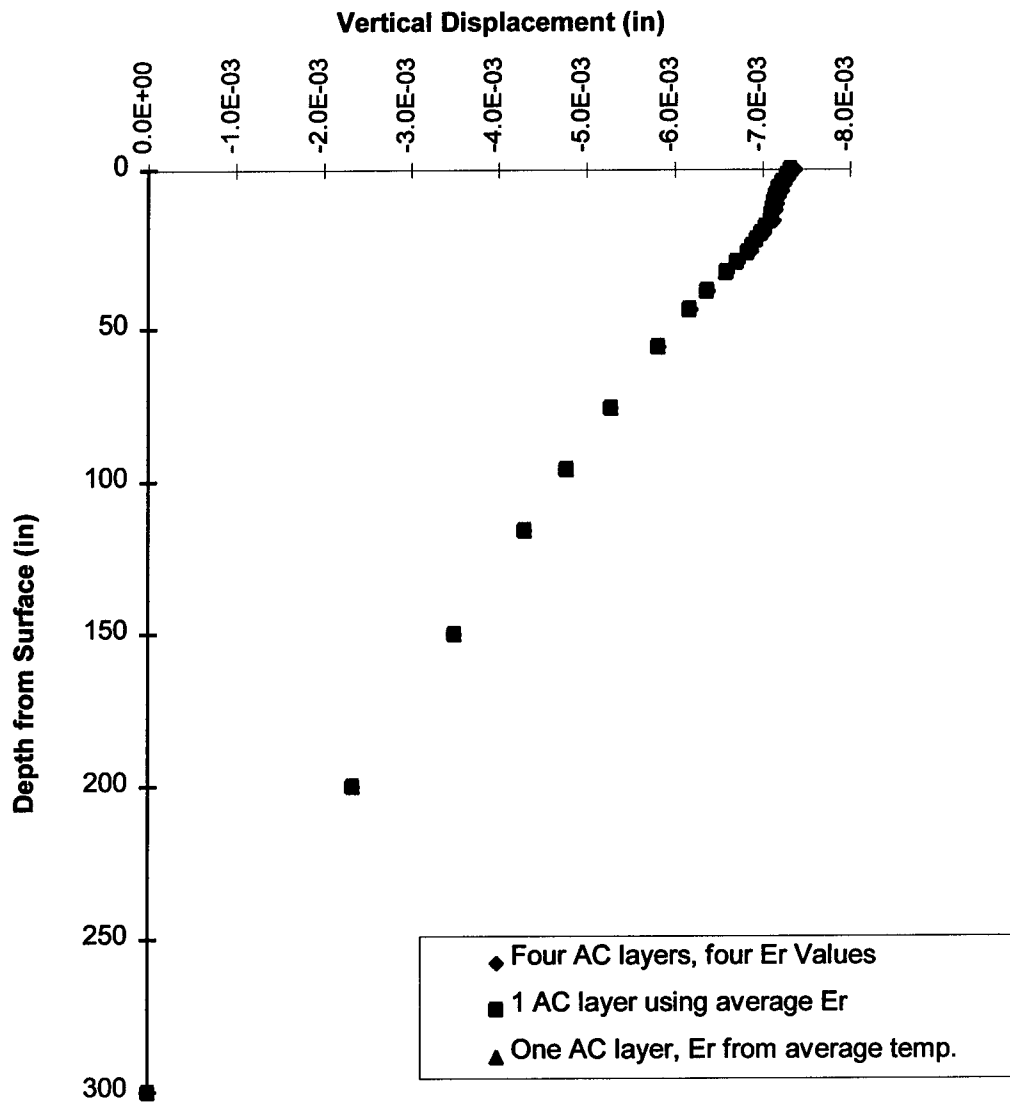


Figure A7. ILLIPAVE Vertical Displacement, 1/11/97 at 8:00 a.m.

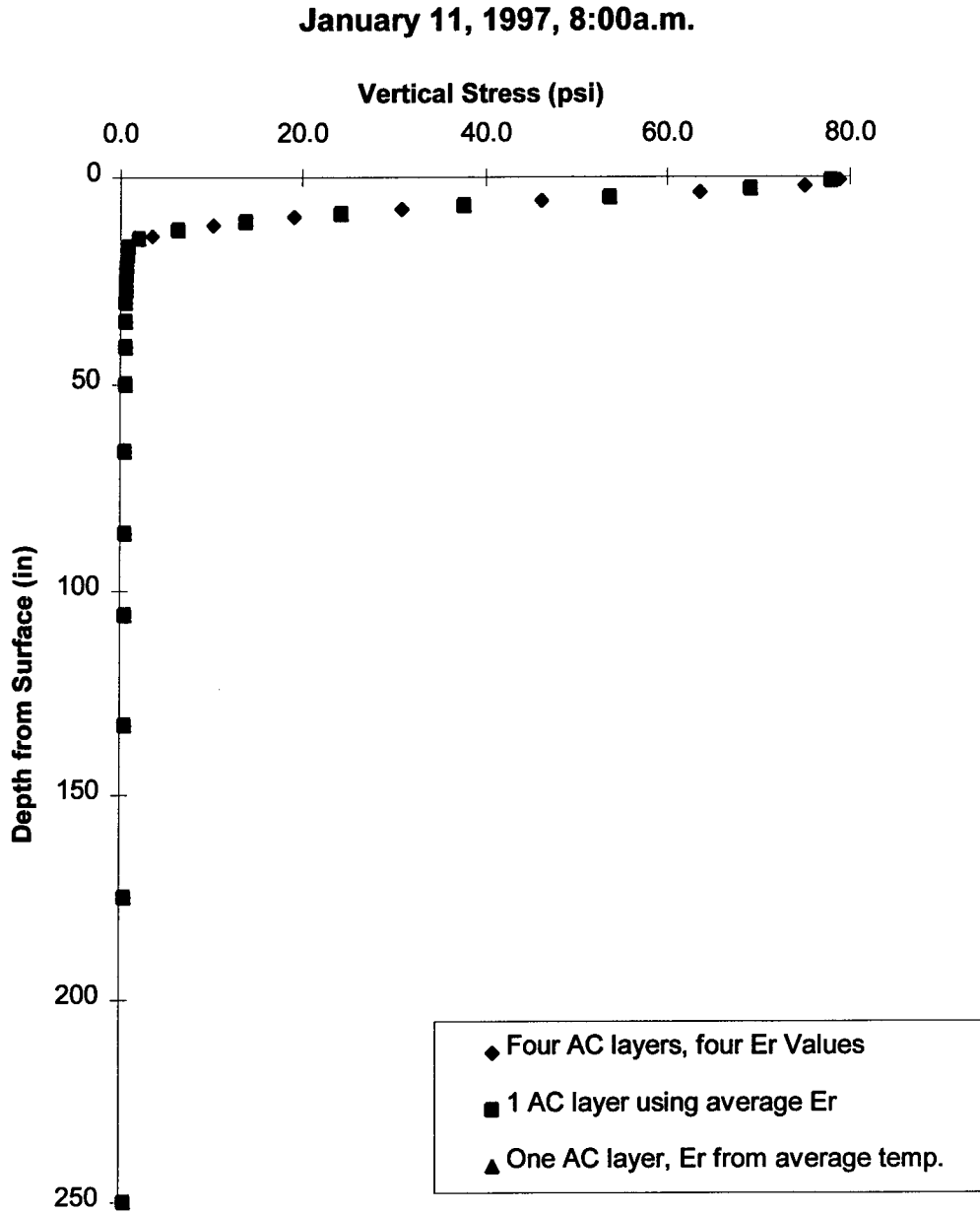


Figure A8. ILLIPAVE Vertical Stress, 1/11/97 at 8:00 a.m.

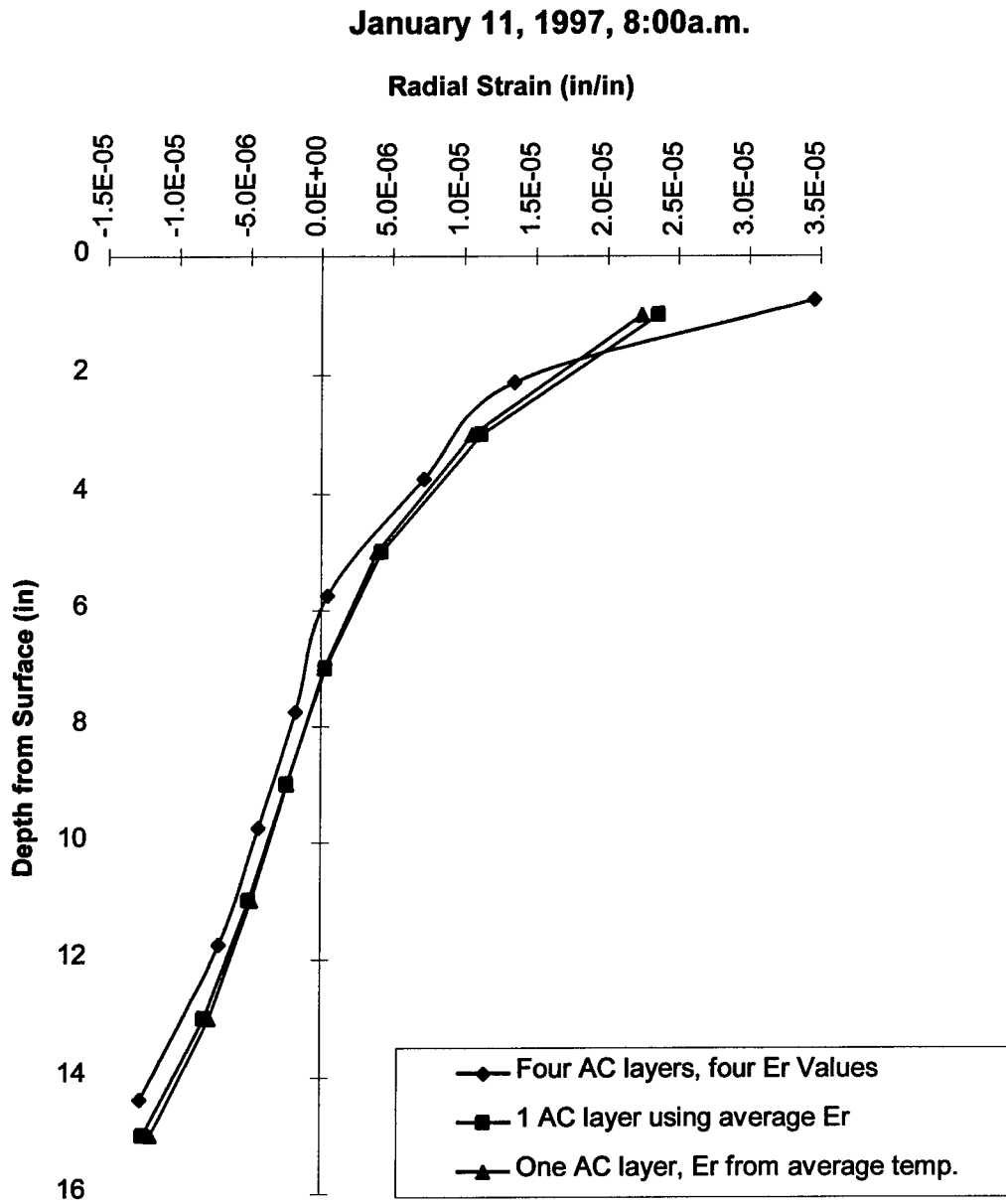


Figure A9. ILLIPAVE AC Radial Strain, 1/11/97 at 8:00 a.m.

January 11, 1997, 4:00p.m.

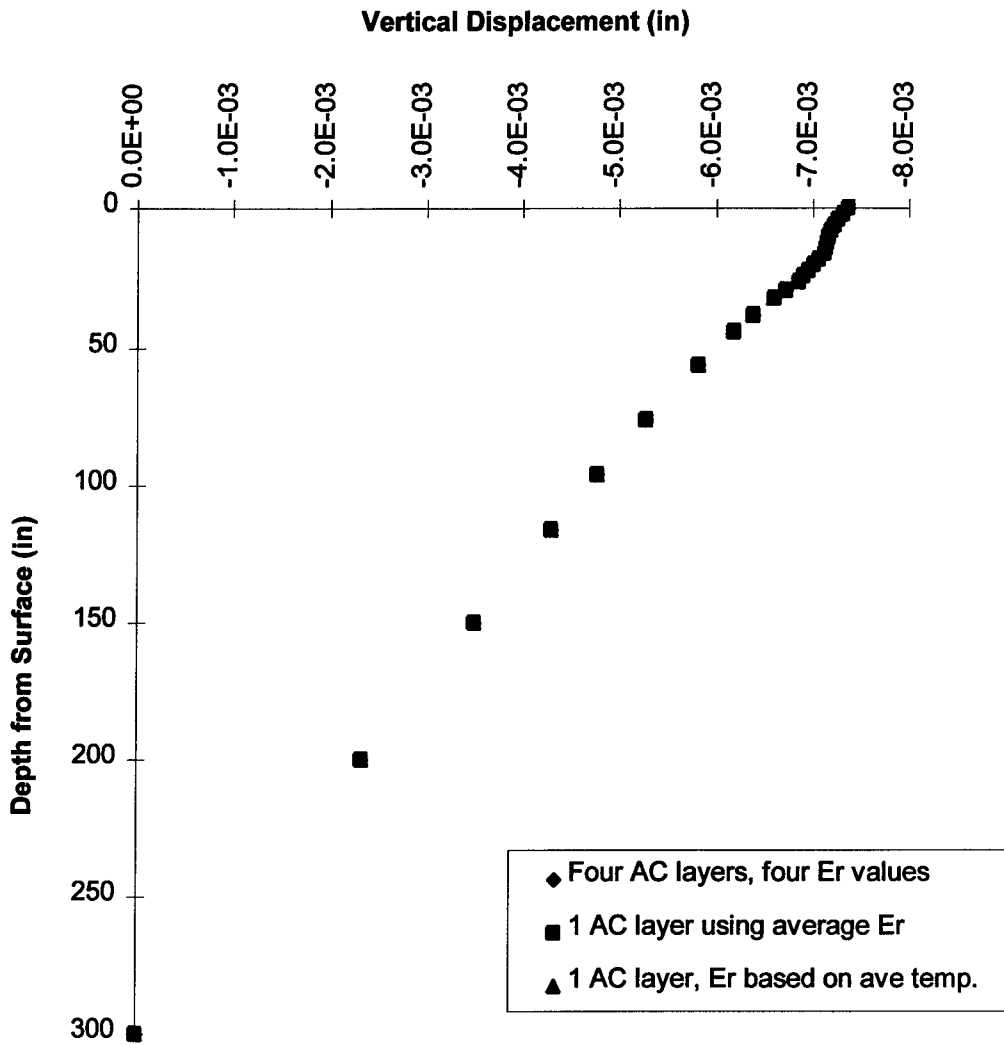


Figure A10. ILLIPAVE Vertical Displacement, 1/11/97 at 4:00 p.m.

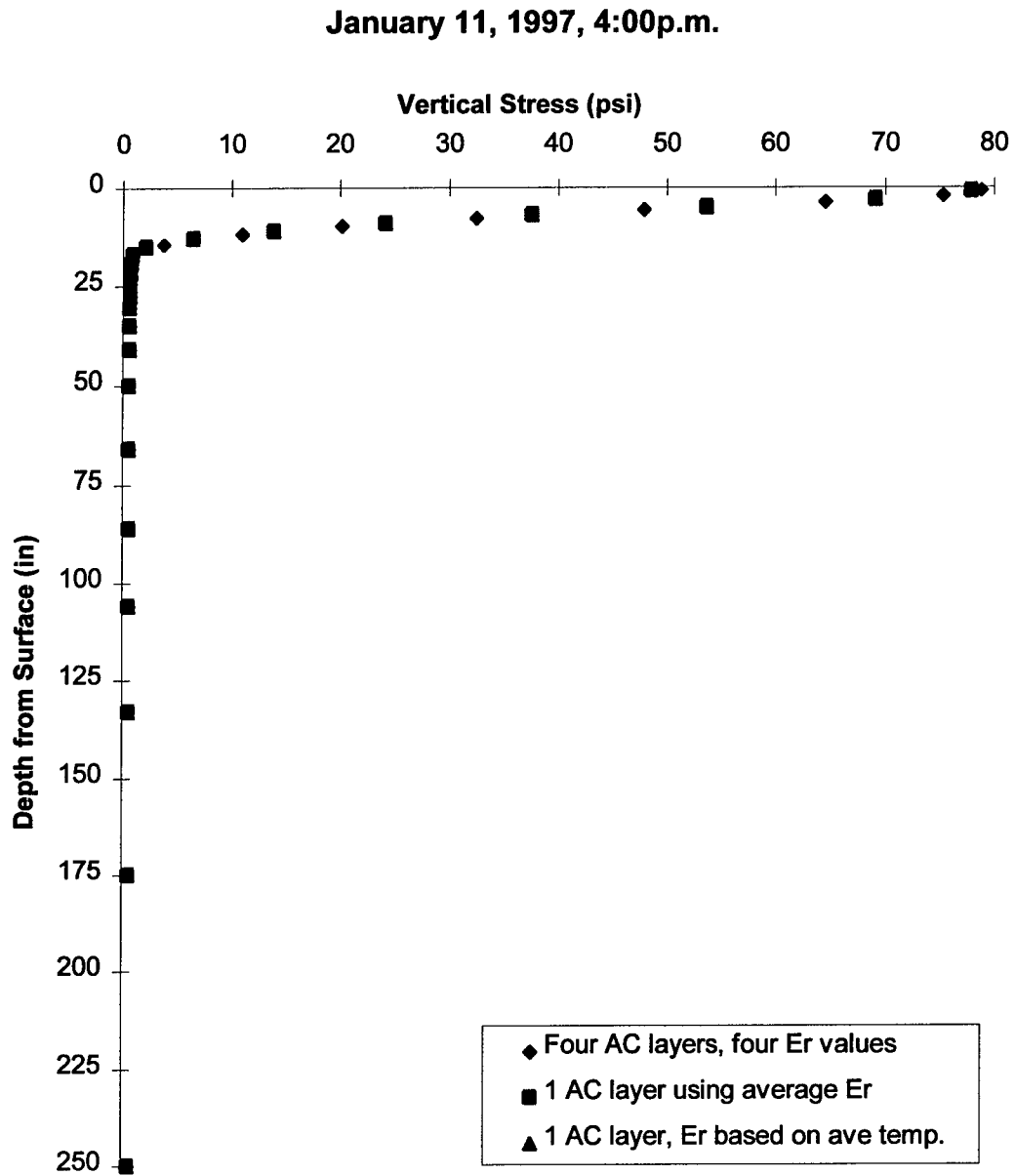


Figure A11. ILLIPAVE Vertical Stress, 1/11/97 at 4:00 p.m.

January 11, 1997, 4:00p.m.

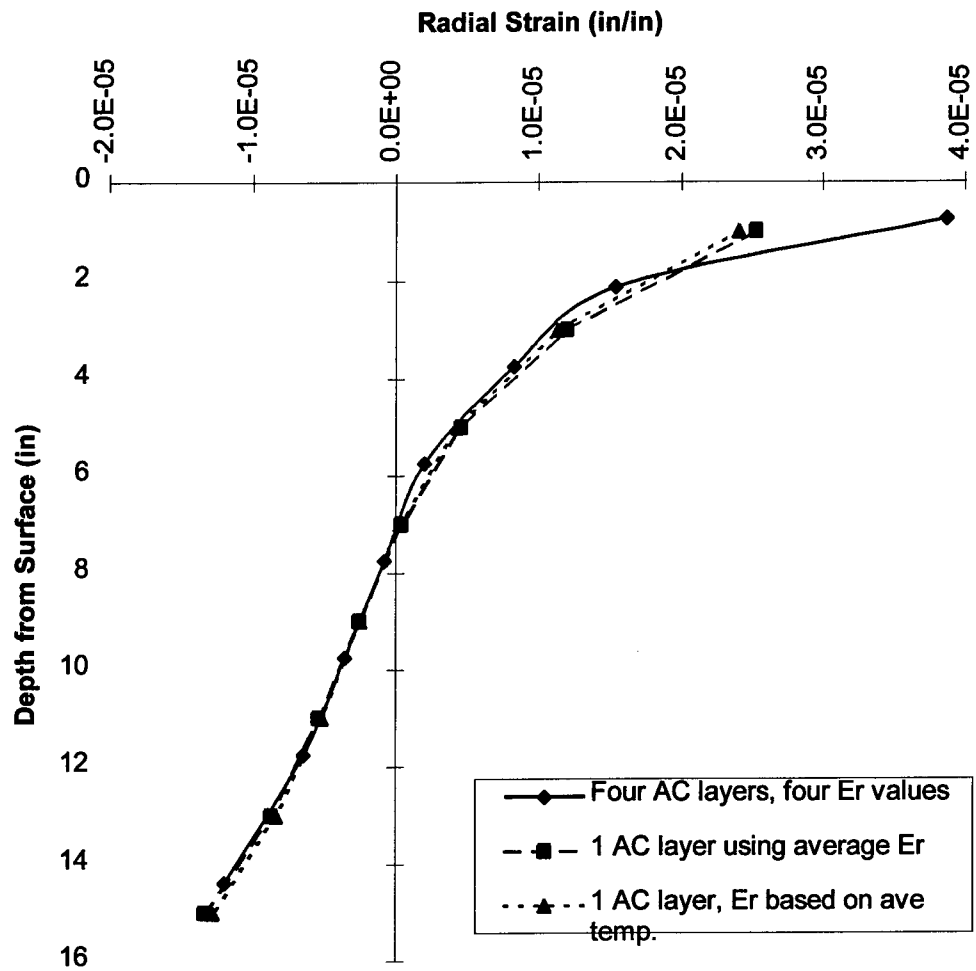


Figure A12. ILLIPAVE AC Radial Strain, 1/11/97 at 4:00 p.m.

APPENDIX B

SOIL MOISTURE CONTENT AND RAINFALL CORRELATIONS

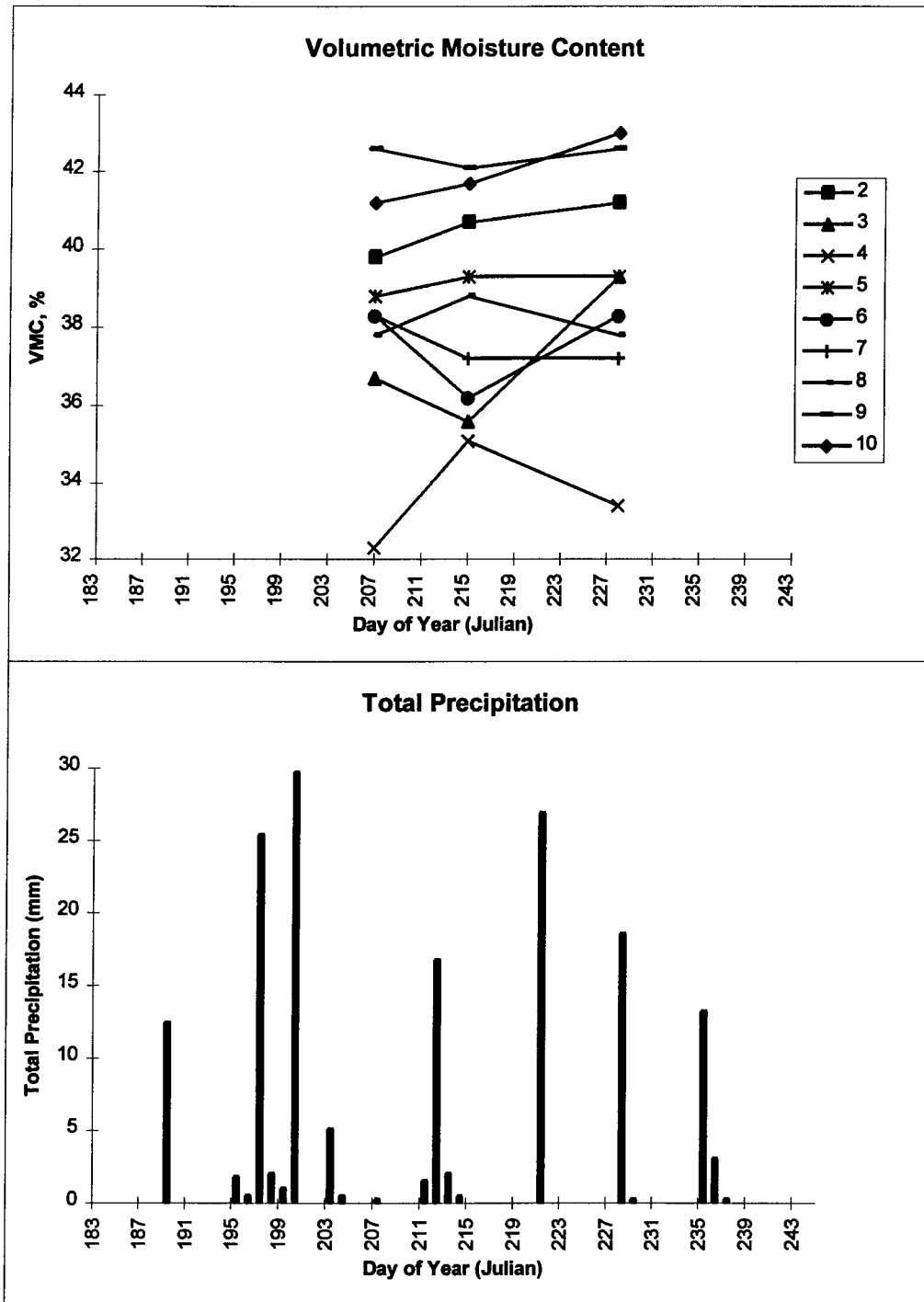


Figure B1. SPS1-J2 Soil Moisture Content and Rainfall Correlation

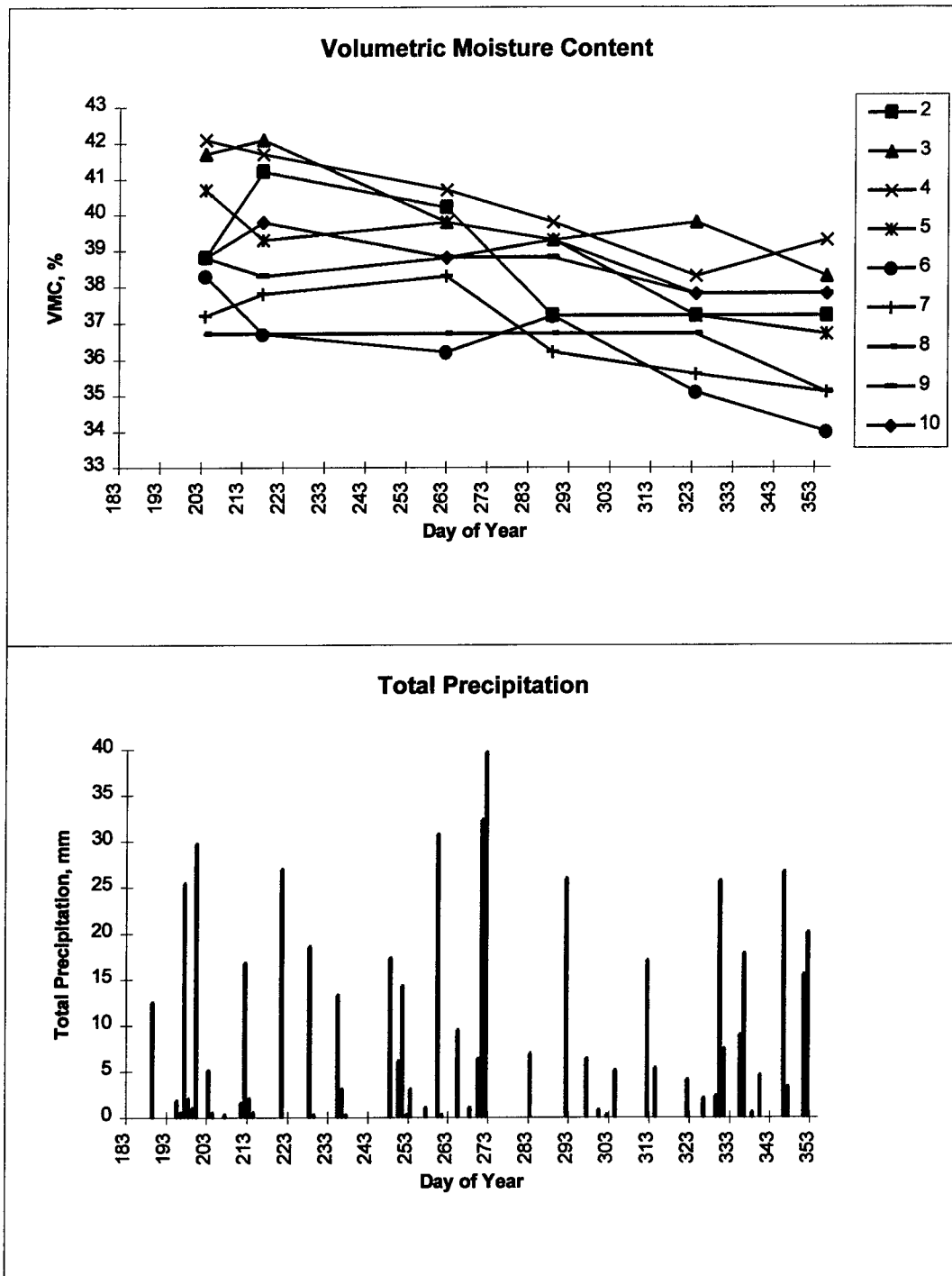


Figure B2. SPS2-J3 Soil Moisture Content and Rainfall Correlation

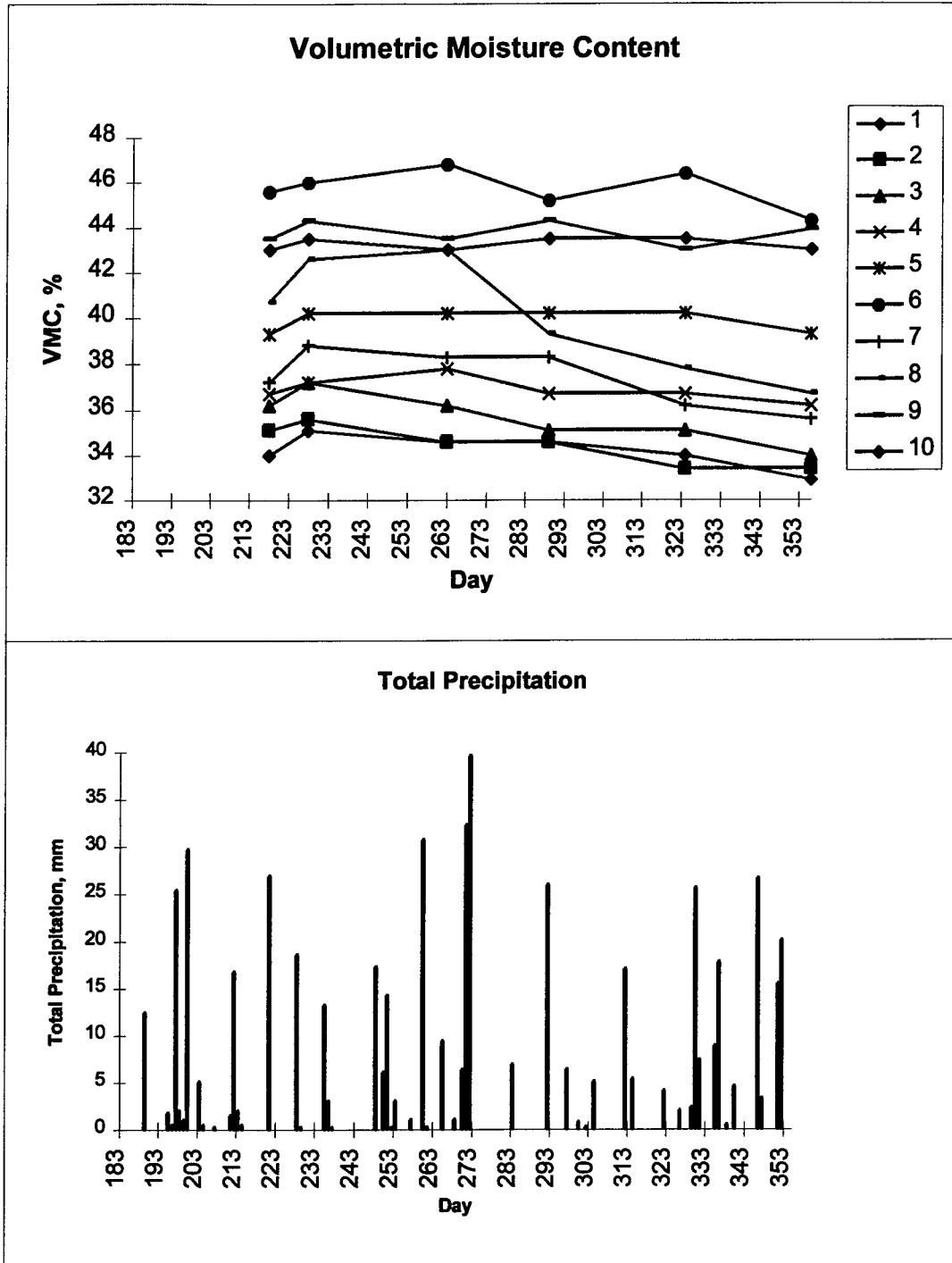


Figure B3. SPS2-J5 Soil Moisture Content and Rainfall Correlation

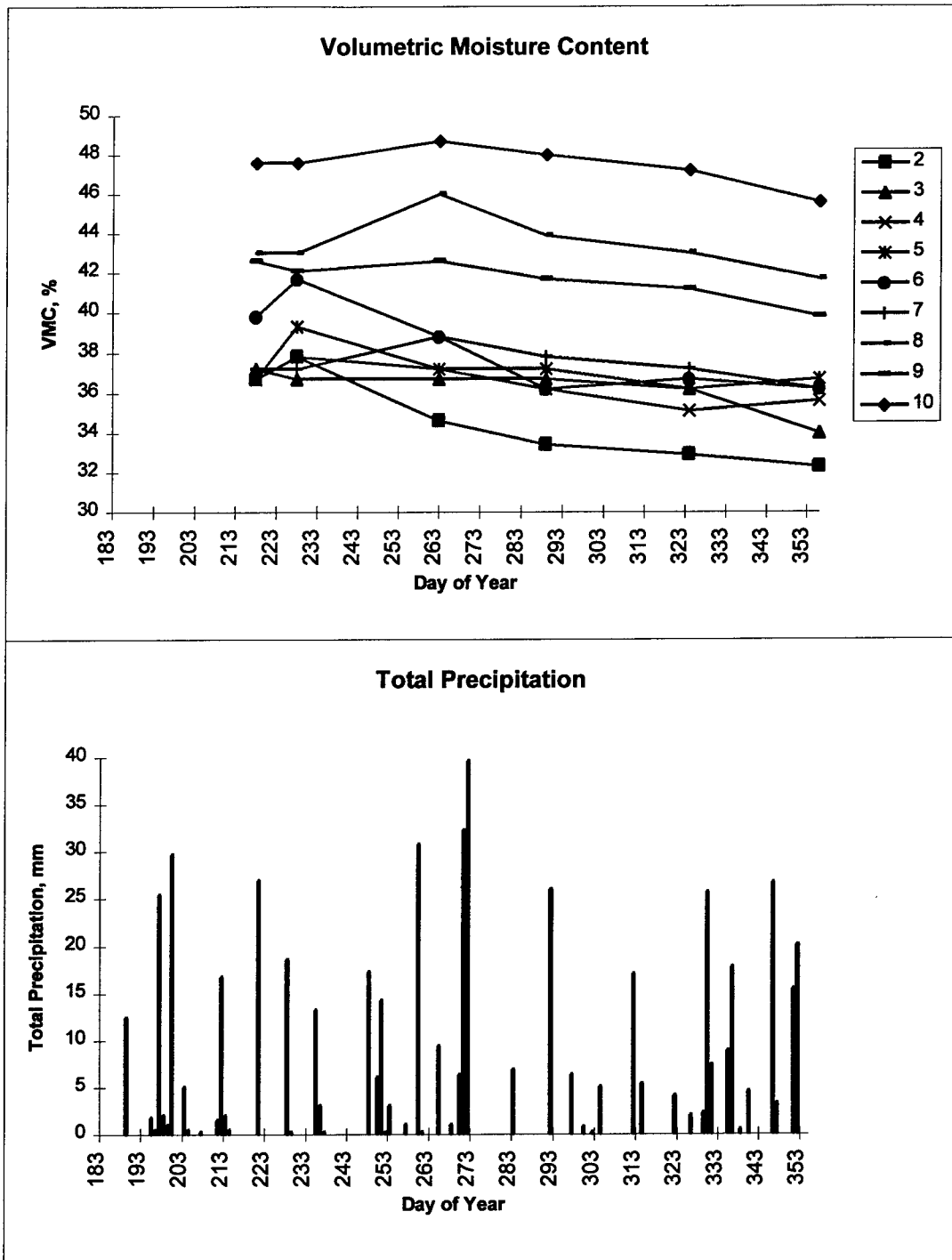


Figure B4. SPS2-J12 Soil Moisture Content and Rainfall Correlation

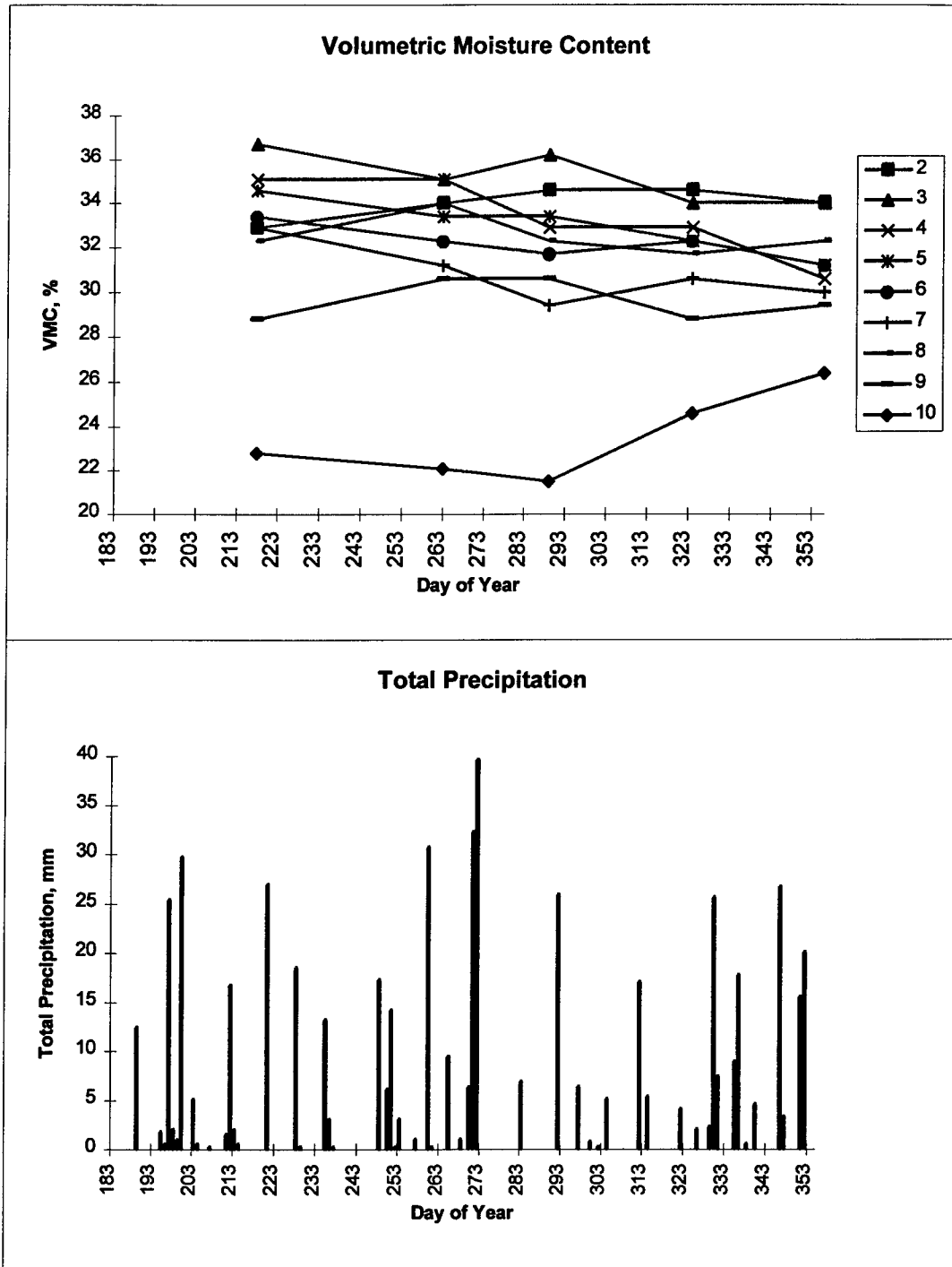


Figure B5. SPS9-J1 Soil Moisture Content and Rainfall Correlation

APPENDIX C

AIR AND ASPHALT CONCRETE TEMPERATURE CORRELATIONS

SPS9-ODOT -- Thermistor 1

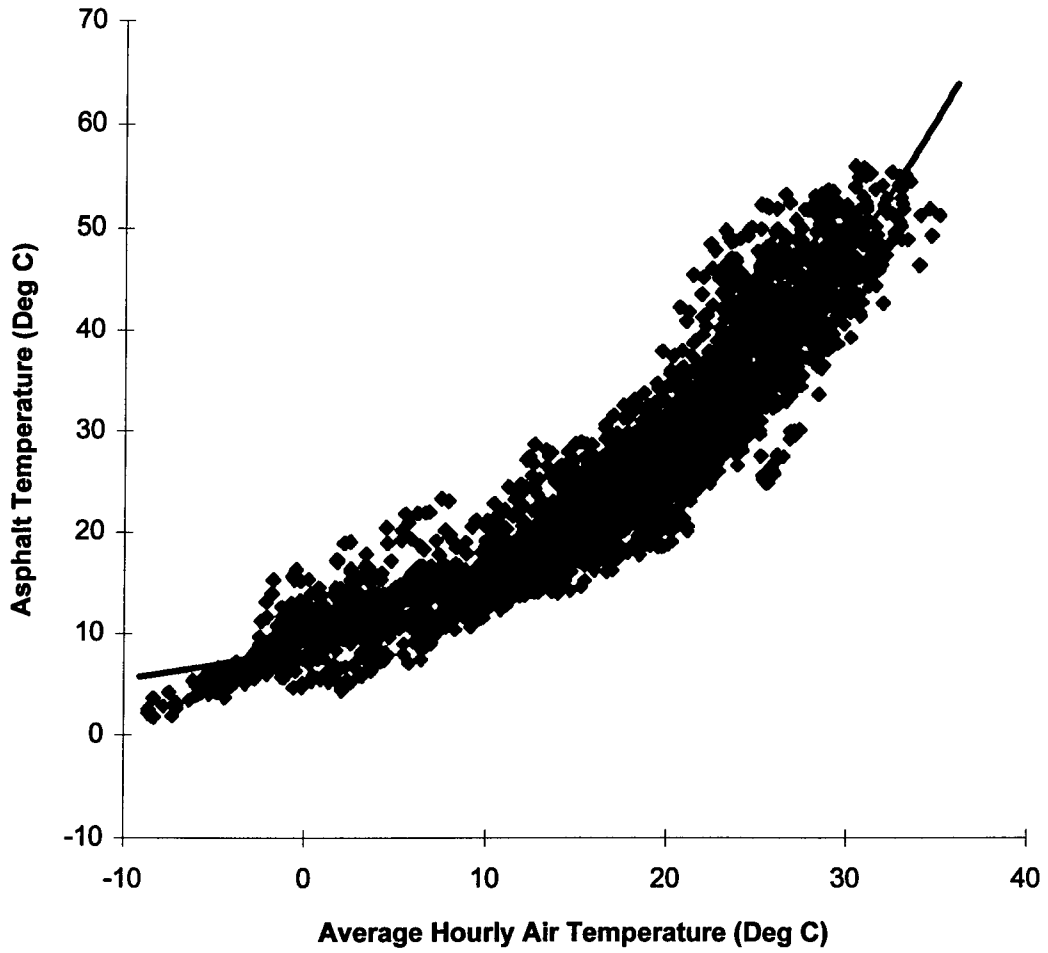


Figure C1. Asphalt Temp vs. Air Temp: SPS9-ODOT, Thermistor 1

SPS9-ODOT -- Thermistor 2

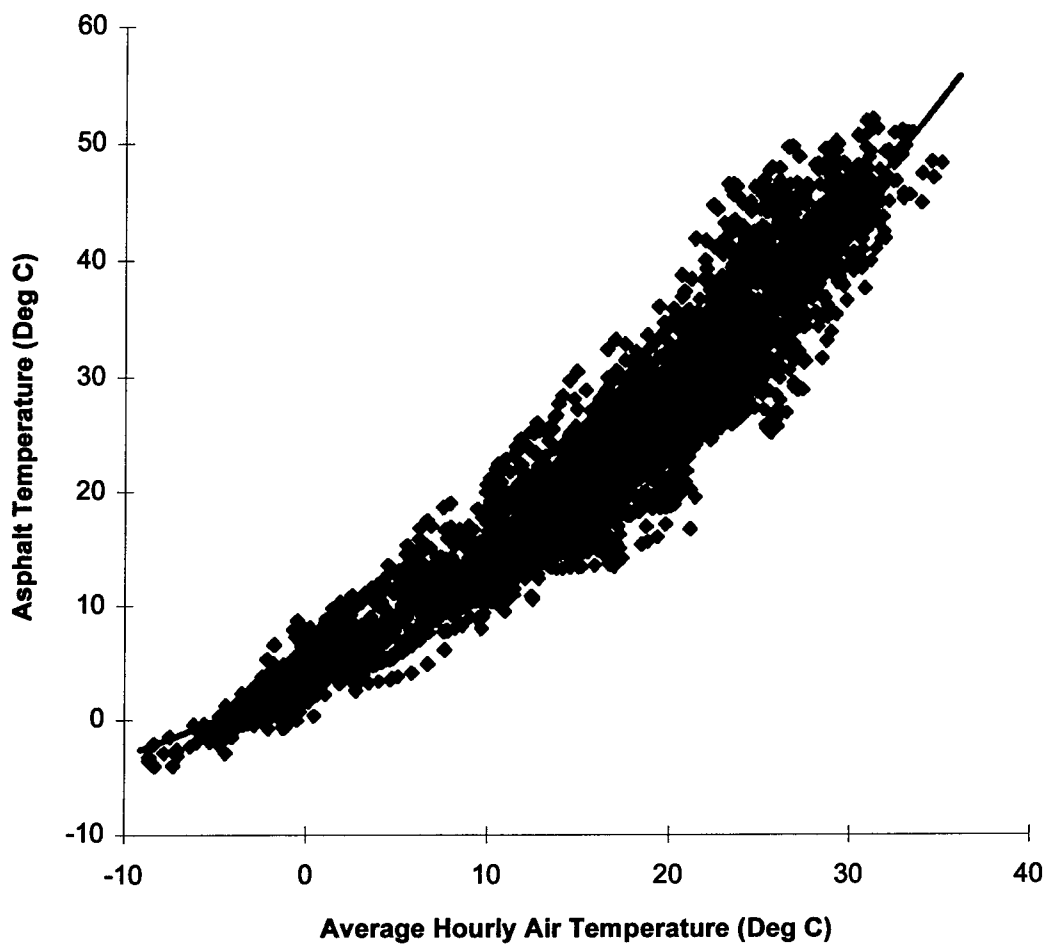


Figure C2. Asphalt Temp vs. Air Temp: SPS9-ODOT, Thermistor 2

SPS9-ODOT -- Thermistor 3

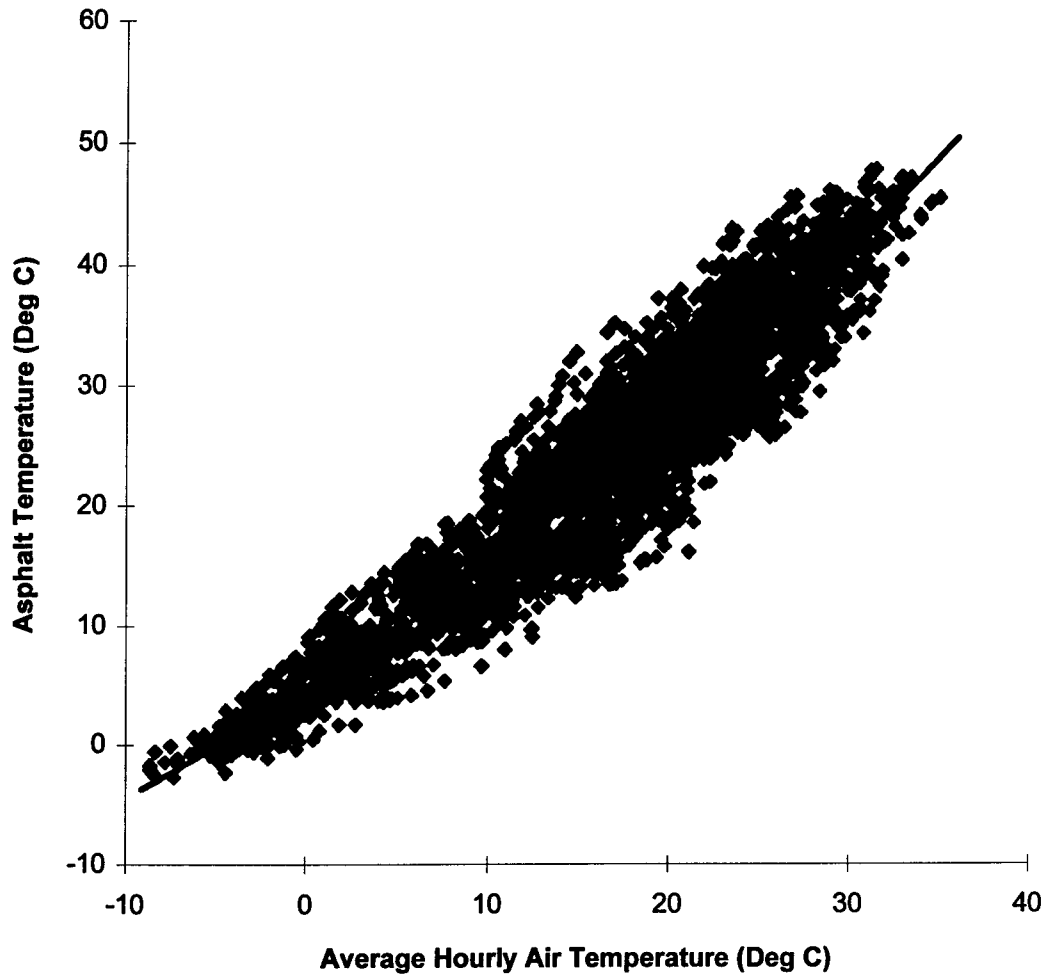


Figure C3. Asphalt Temp vs. Air Temp: SPS9-ODOT, Thermistor 3

SPS9-ODOT
Average Pavement Temperature

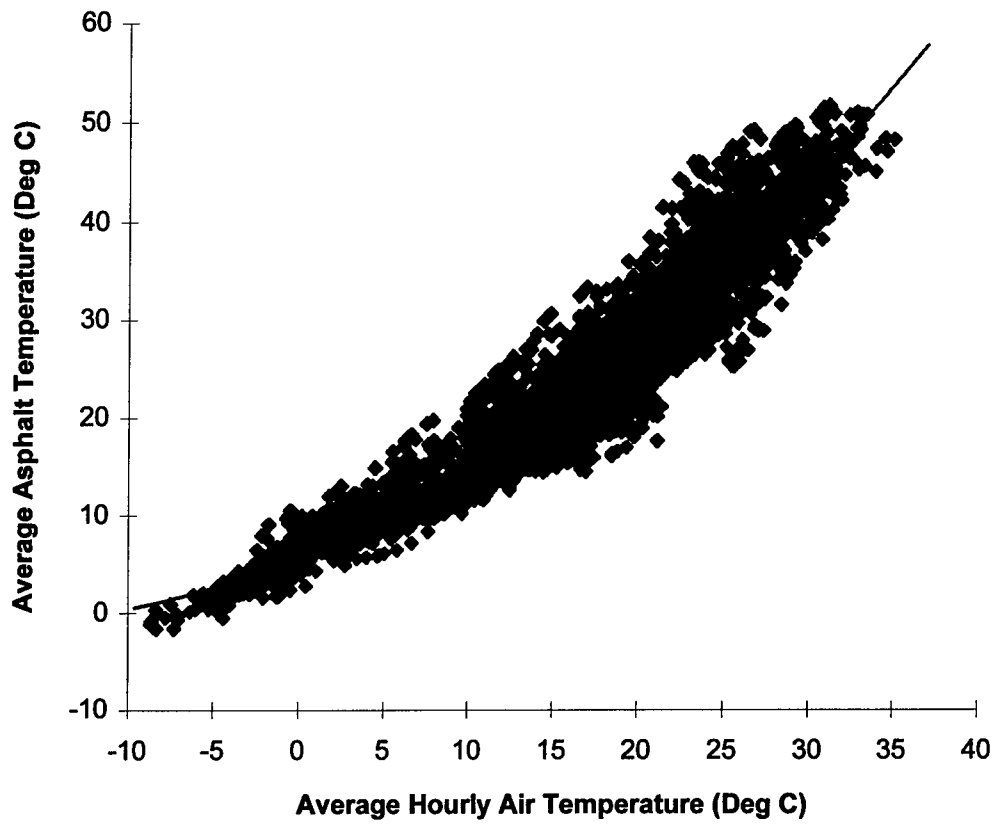


Figure C4. Average Asphalt Temp vs. Air Temp: SPS9-ODOT

SPS1-J2 – Thermistor 1

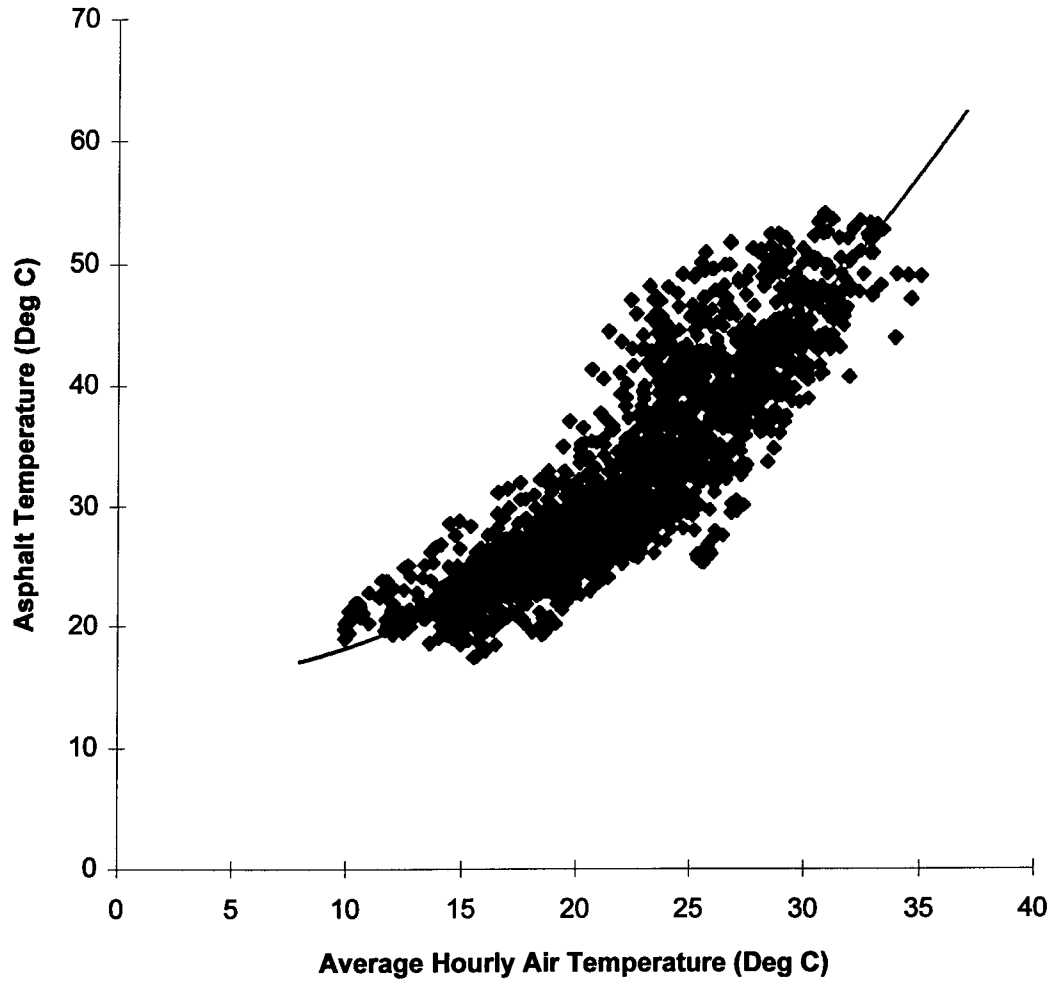


Figure C5. Asphalt Temp vs. Air Temp: SPS1-J2, Thermistor 1

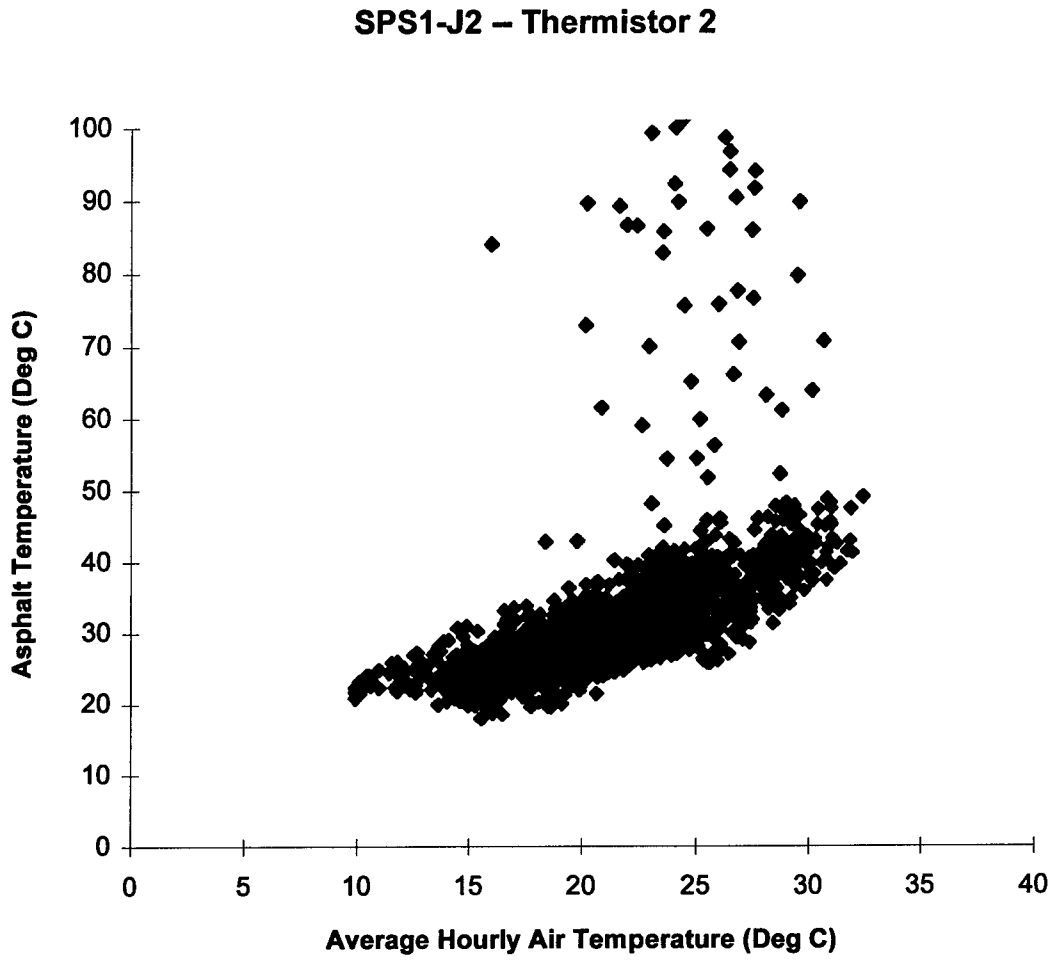


Figure C6. Asphalt Temp vs. Air Temp: SPS1-J2, Thermistor 2

SPS1-J2 – Thermistor 3

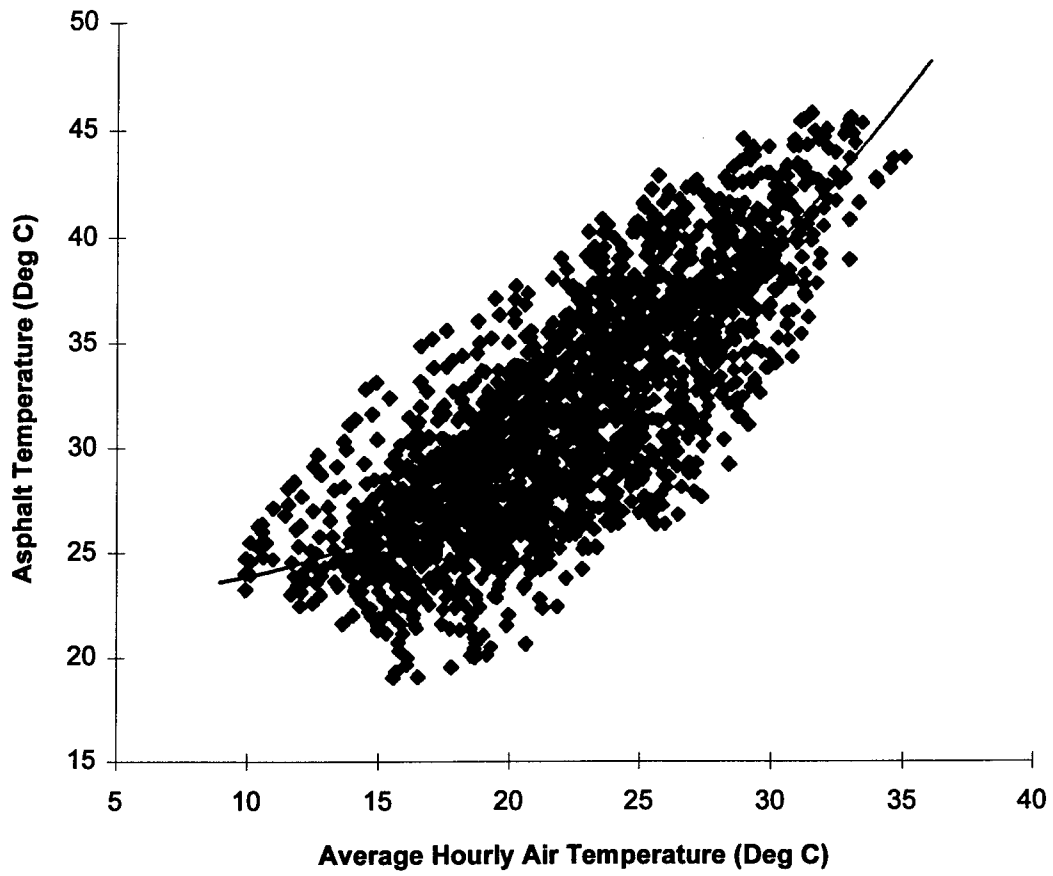
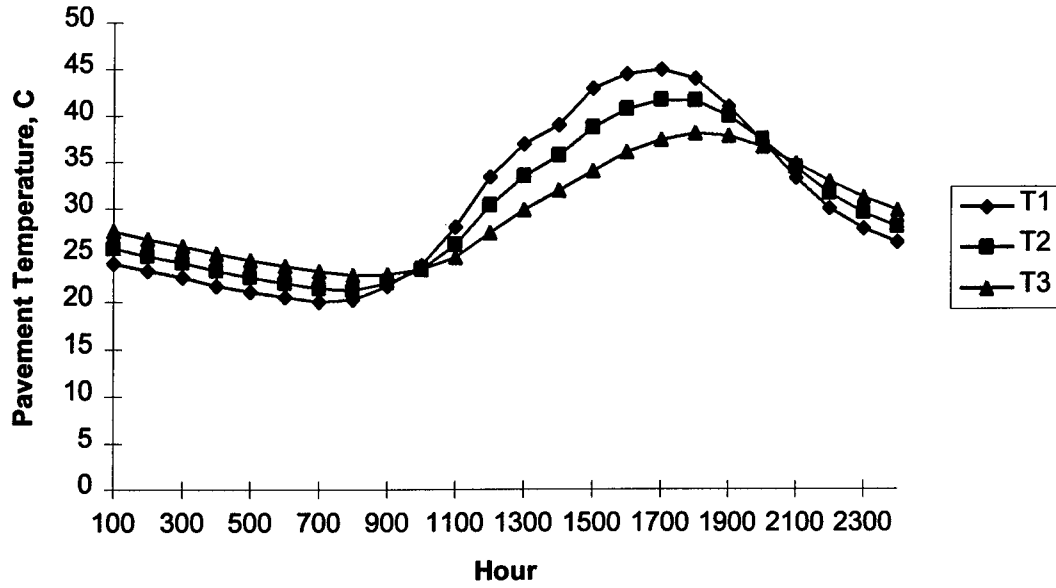


Figure C7. Asphalt Temp vs. Air Temp: SPS1-J2, Thermistor 3

APPENDIX D

HOURLY PAVEMENT TEMPERATURE VARIATIONS

**SPS1-J2
August 1, 1996**



**SPS1-J2
September 1, 1996**

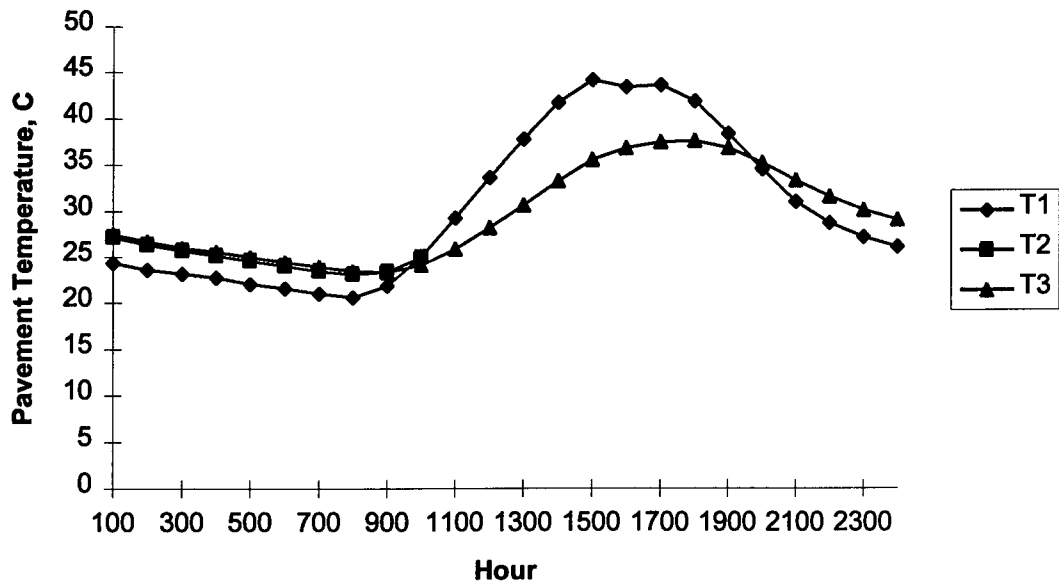
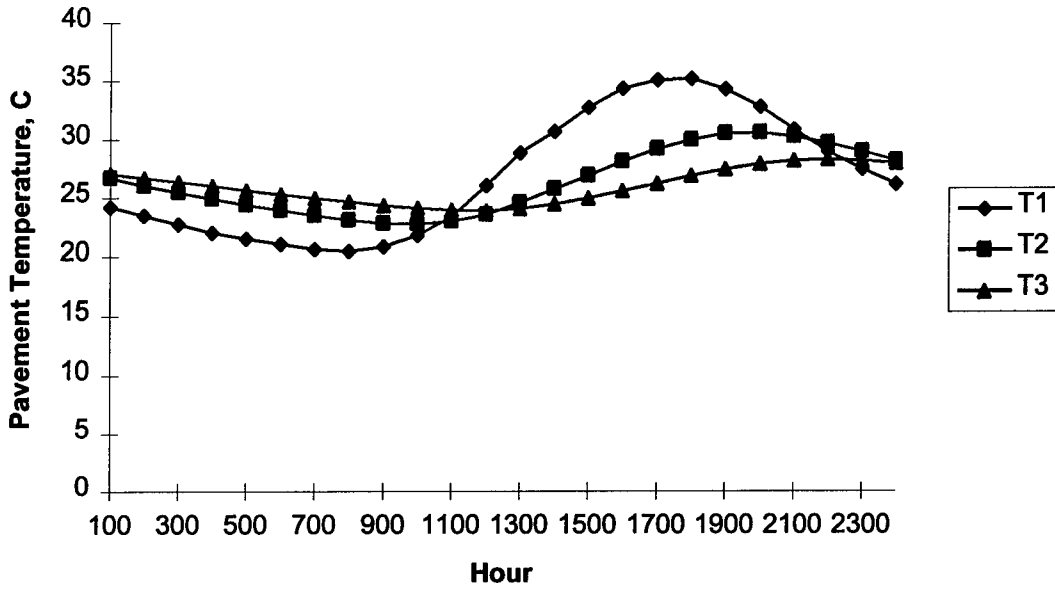


Figure D1. Pavement Temperature, SPS1-J2, August 1 and September 1, 1996

**SPS2-J3
August 1, 1996**



**SPS2-J3
September 1, 1996**

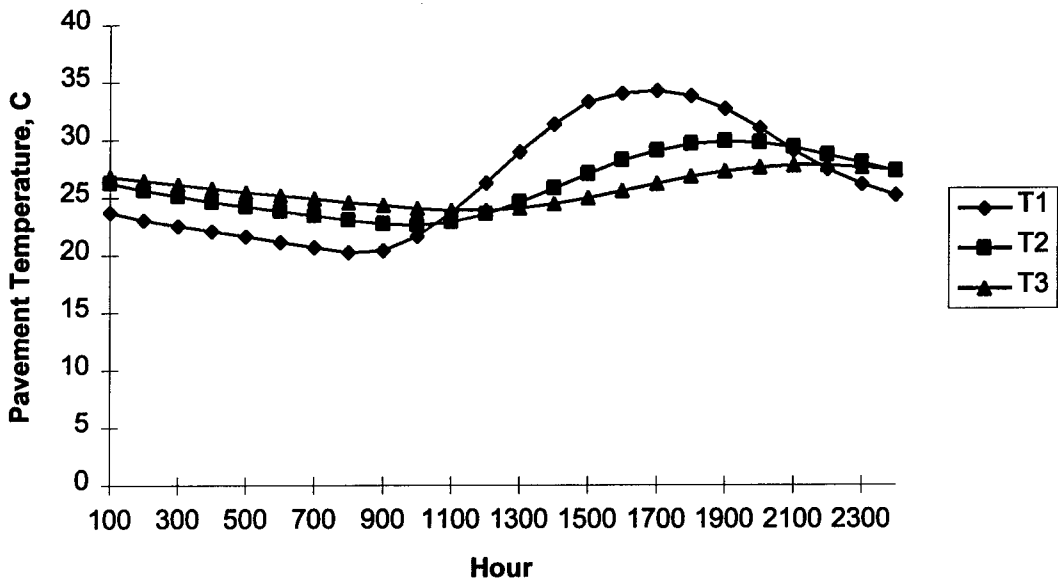
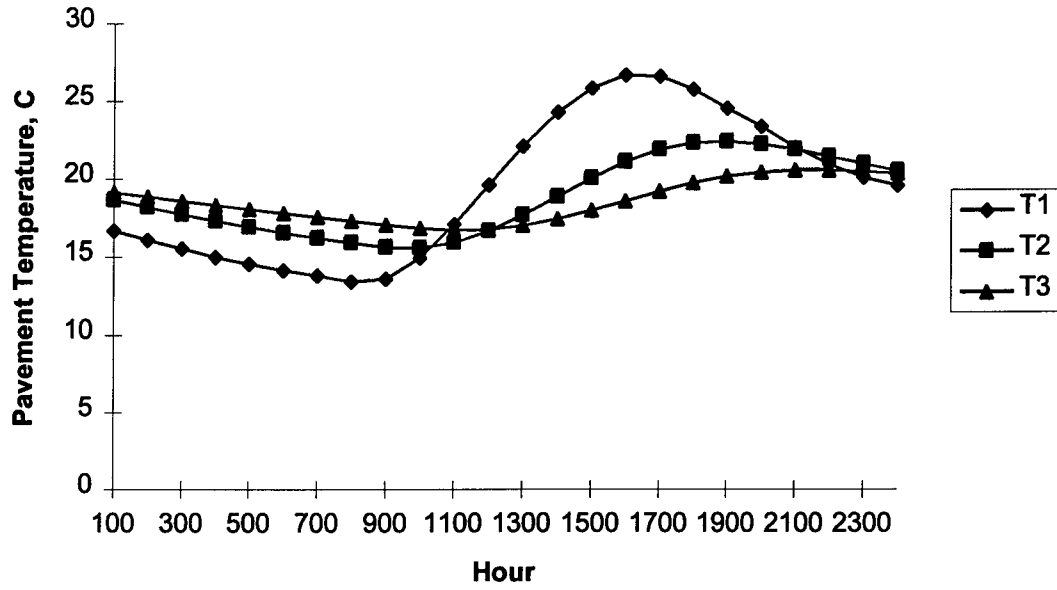


Figure D2. Pavement Temperature, SPS2-J3, August 1 and September 1, 1996

**SPS2-J3
October 1, 1996**



**SPS2-J3
November 1, 1996**

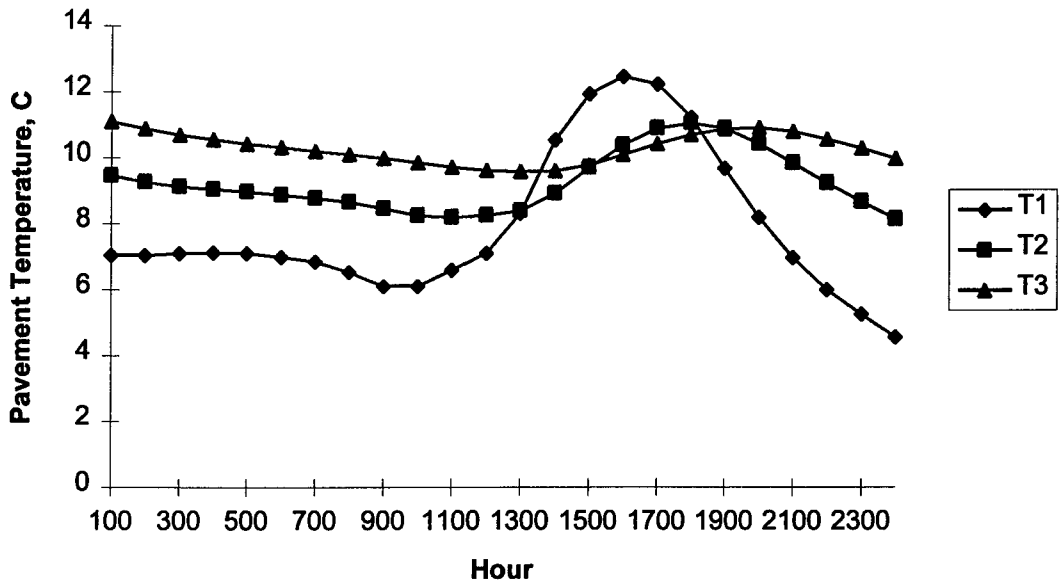
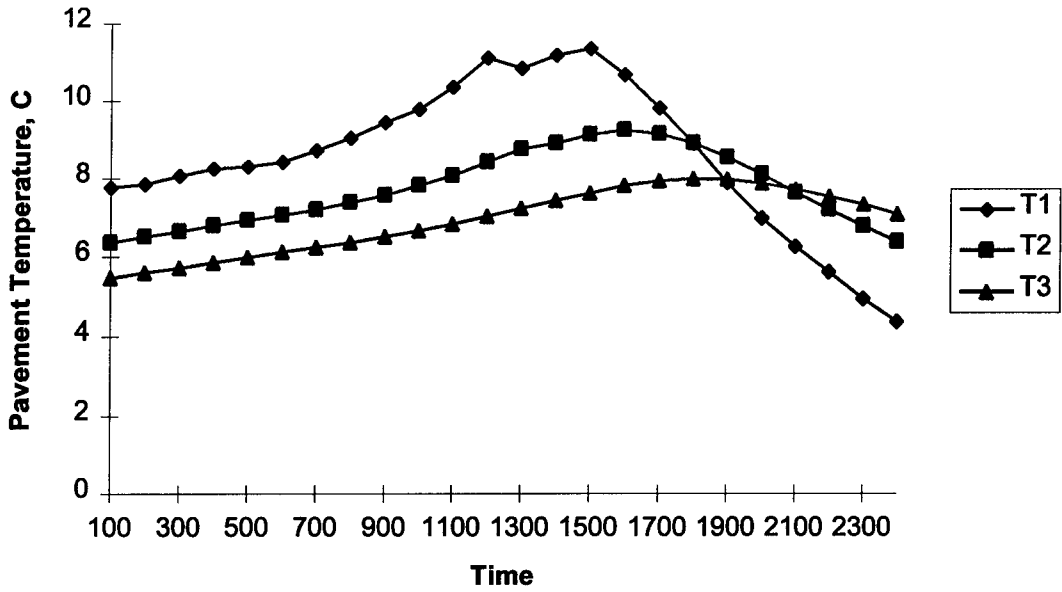


Figure D3. Pavement Temperature, SPS2-J3, October 1 and November 1, 1996

**SPS2-J3
December 1, 1996**



**SPS2-J3
January 1, 1997**

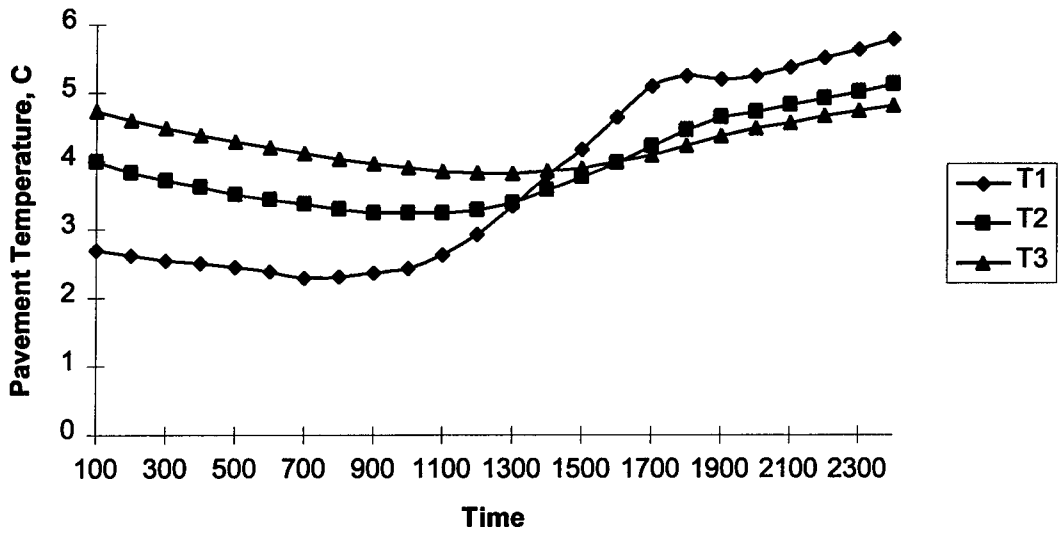
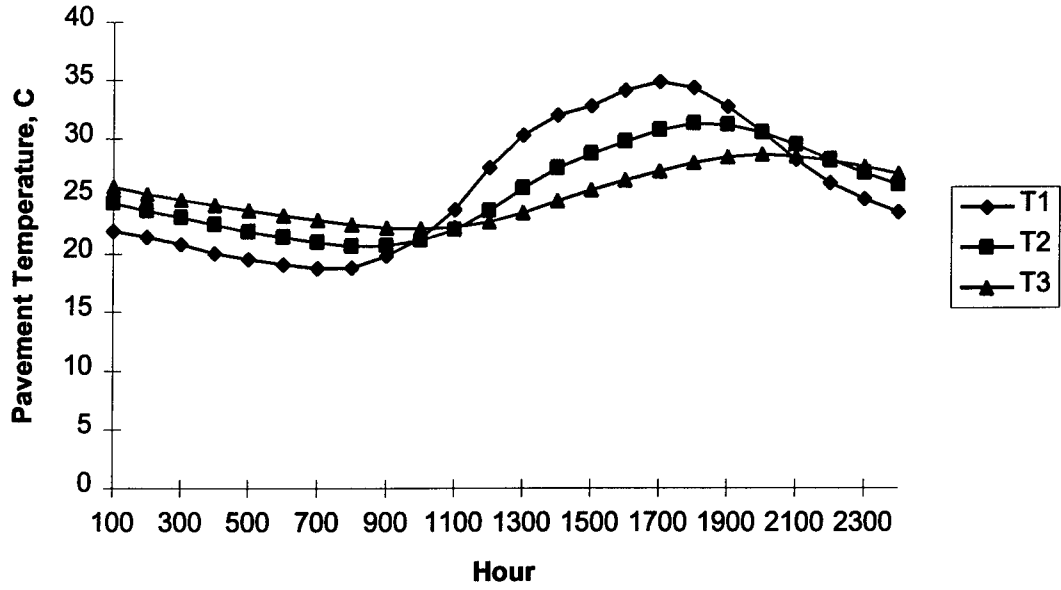


Figure D4. Pavement Temperature, SPS2-J3, Dec. 1, '96 and Jan. 1, '97

**SPS2-J5
August 1, 1996**



**SPS2-J5
September 1, 1996**

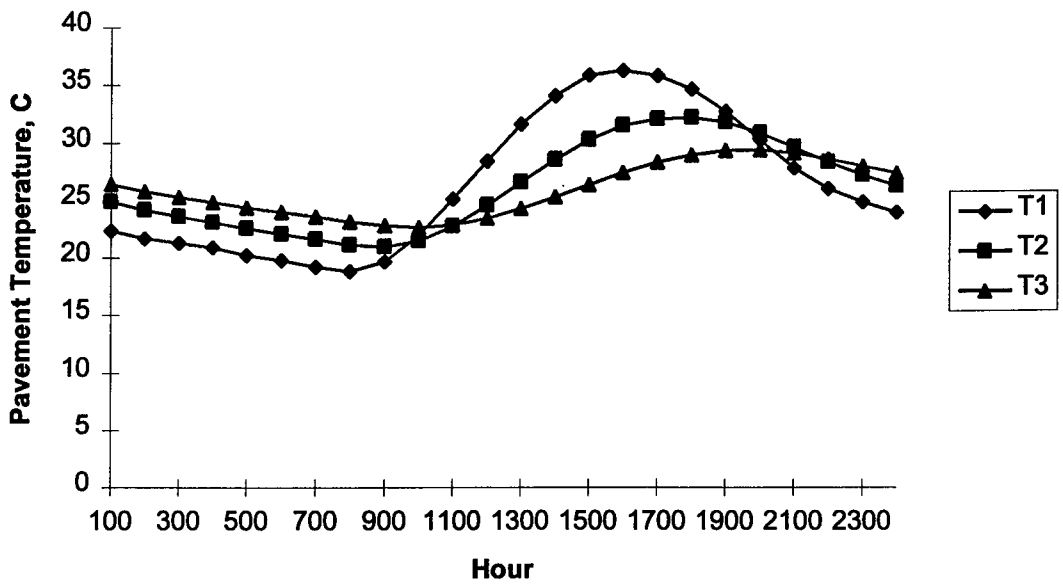
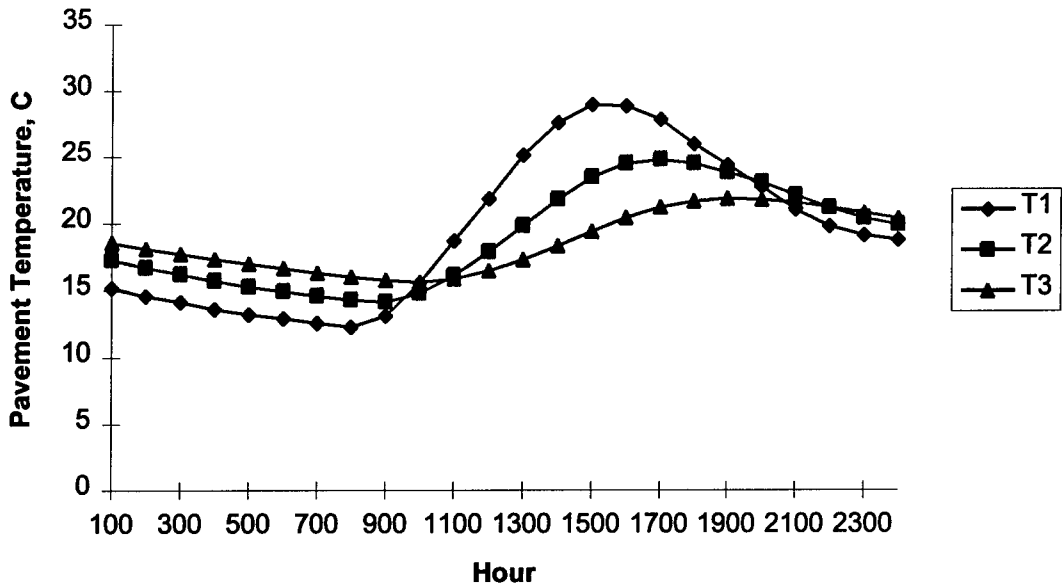


Figure D5. Pavement Temperature, SPS2-J5, August 1 and September 1, 1996

**SPS2-J5
October 1, 1996**



**SPS2-J5
November 1, 1996**

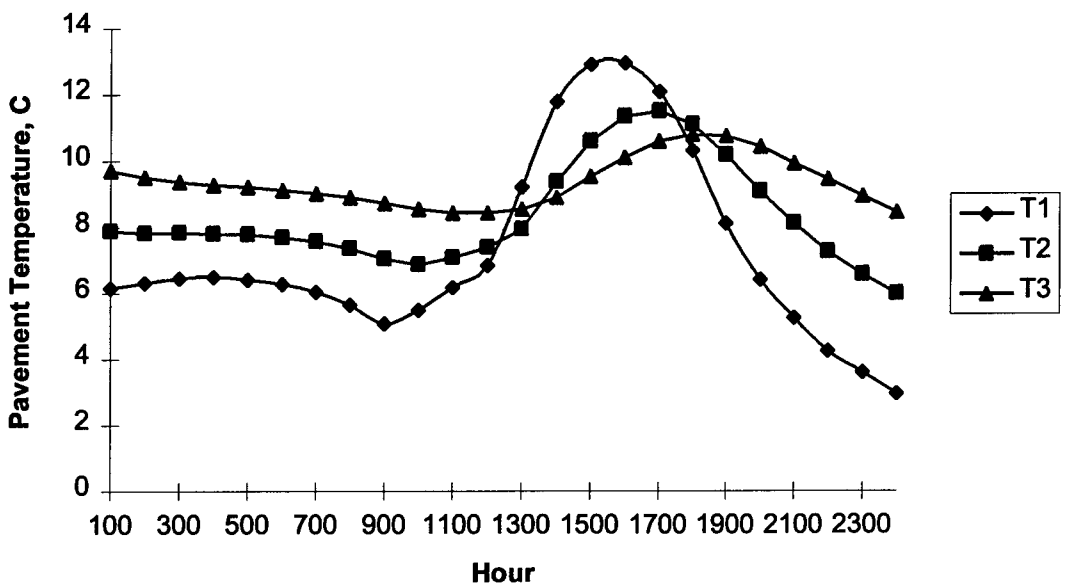
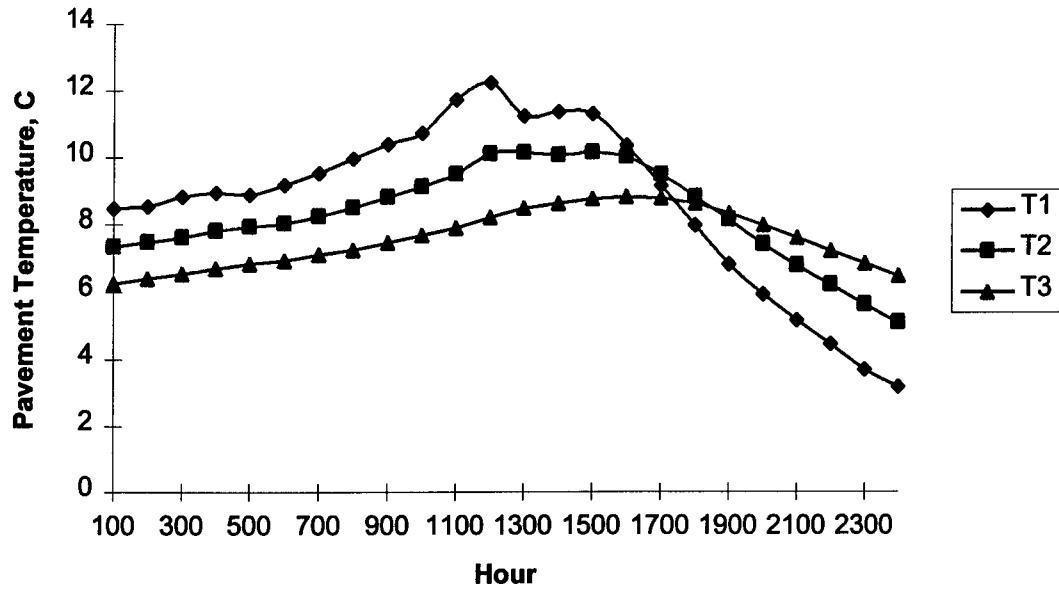


Figure D6. Pavement Temperature, SPS2-J5, October 1 and November 1, 1996

**SPS2-J5
December 1, 1996**



**SPS2-J5
January 1, 1997**

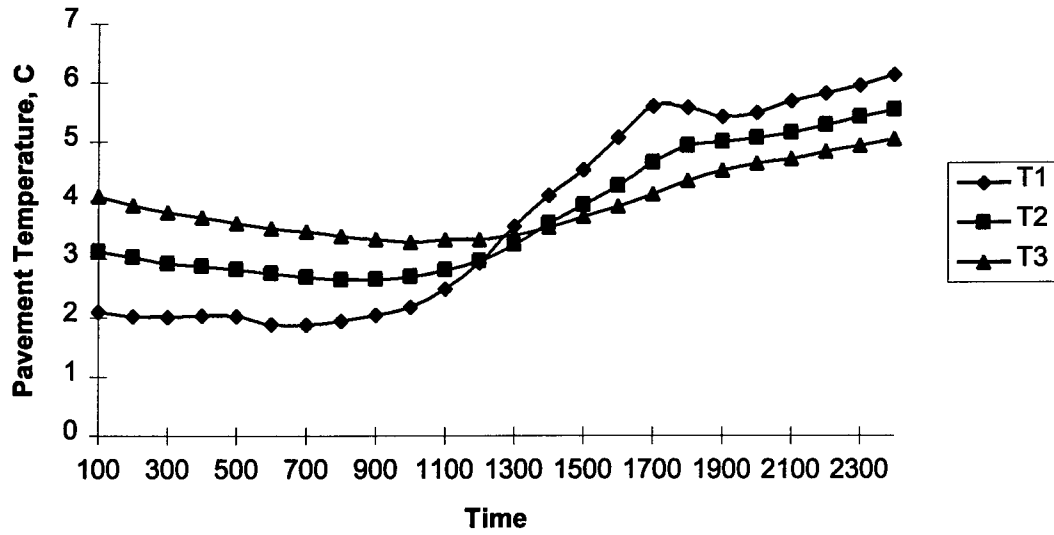
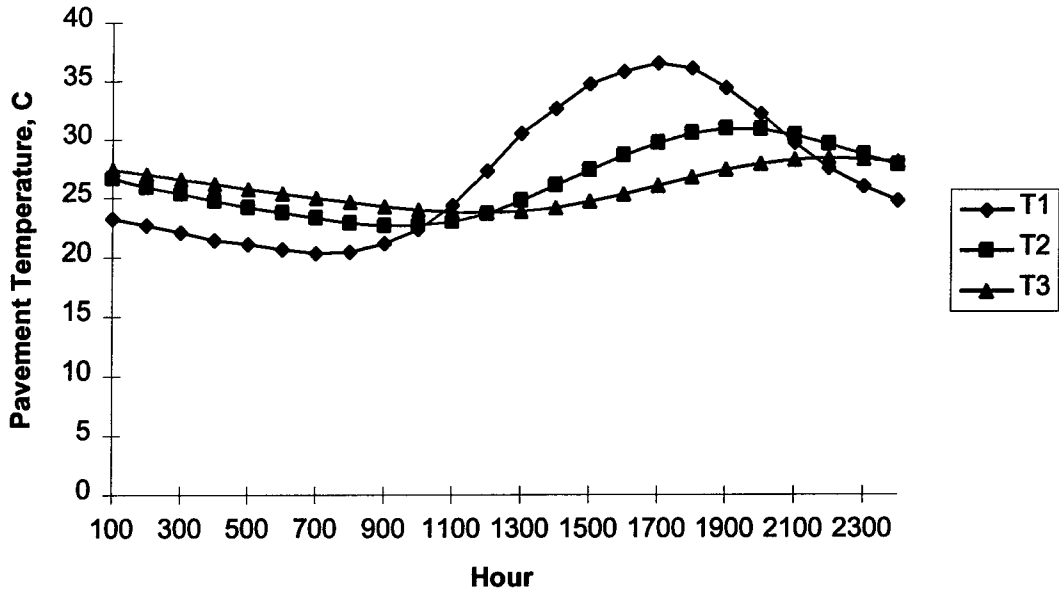


Figure D7. Pavement Temperature, SPS2-J5, Dec. 1, 1996 and Jan. 1, 1997

**SPS2-J12
August 1, 1996**



**SPS2-J12
September 1, 1996**

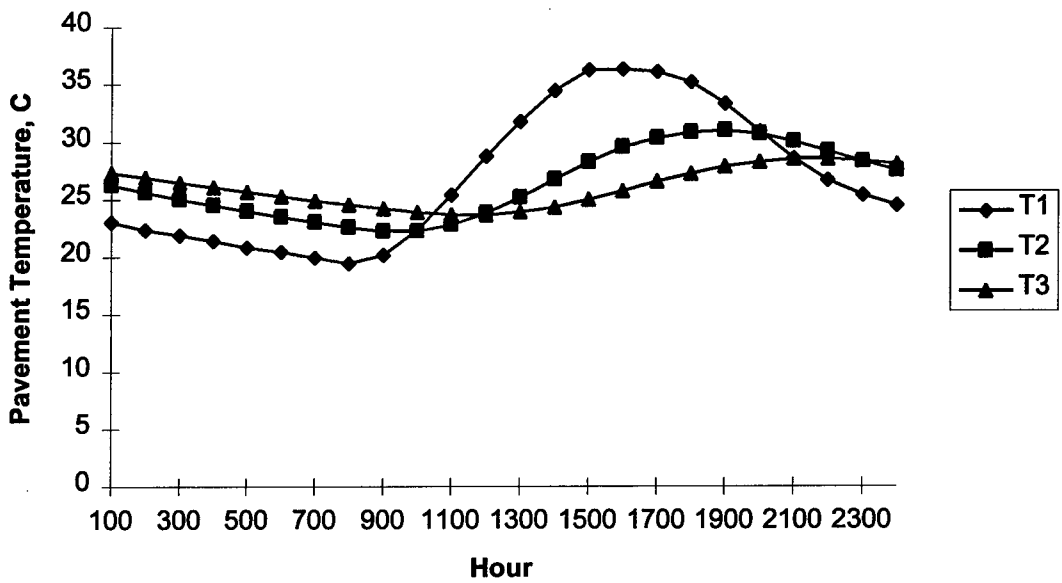
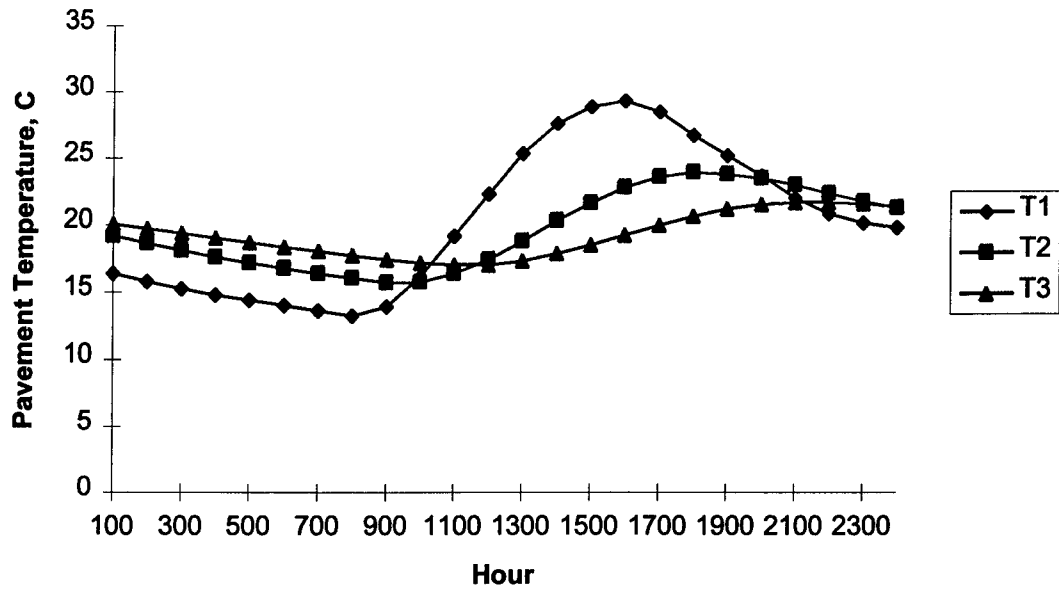


Figure D8. Pavement Temperature, SPS2-J12, August 1 and September 1, 1996

**SPS2-J12
October 1, 1996**



**SPS2-J12
November 1, 1996**

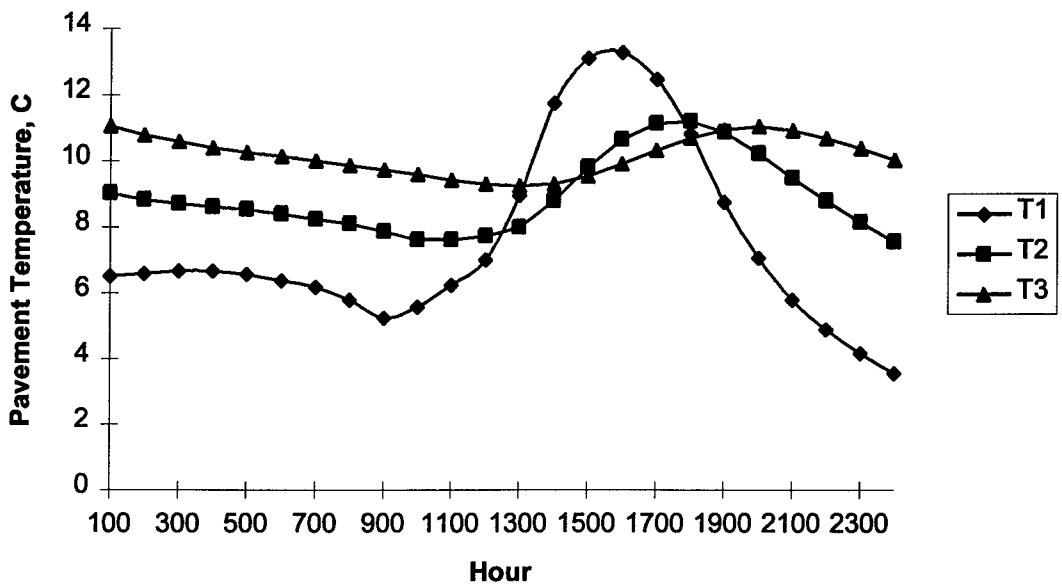
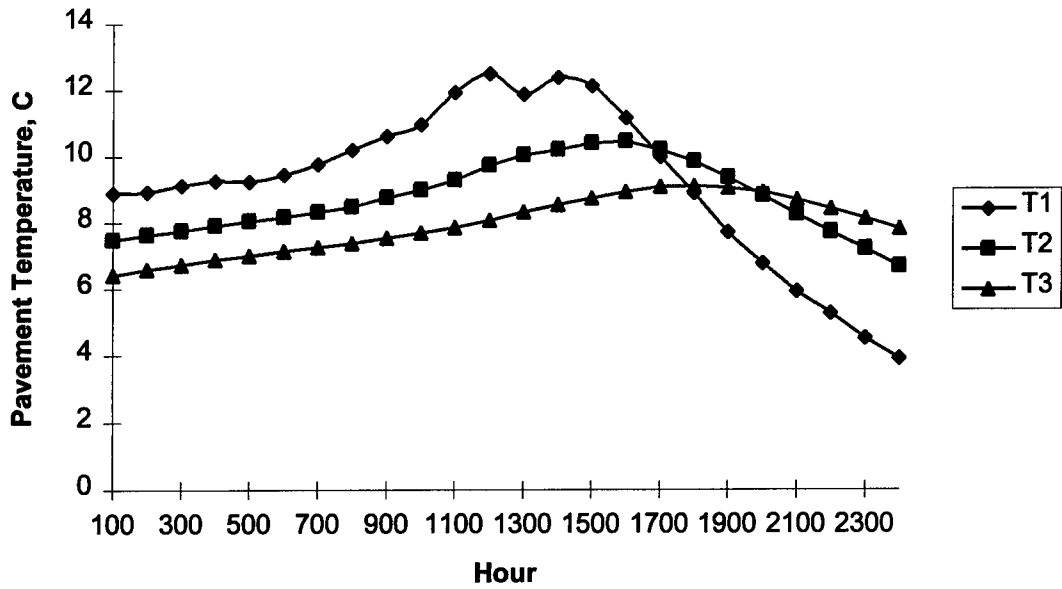


Figure D9. Pavement Temperature, SPS2-J12, October 1 and November 1, 1996

**SPS2-J12
December 1, 1996**



**SPS2-J12
January 1, 1997**

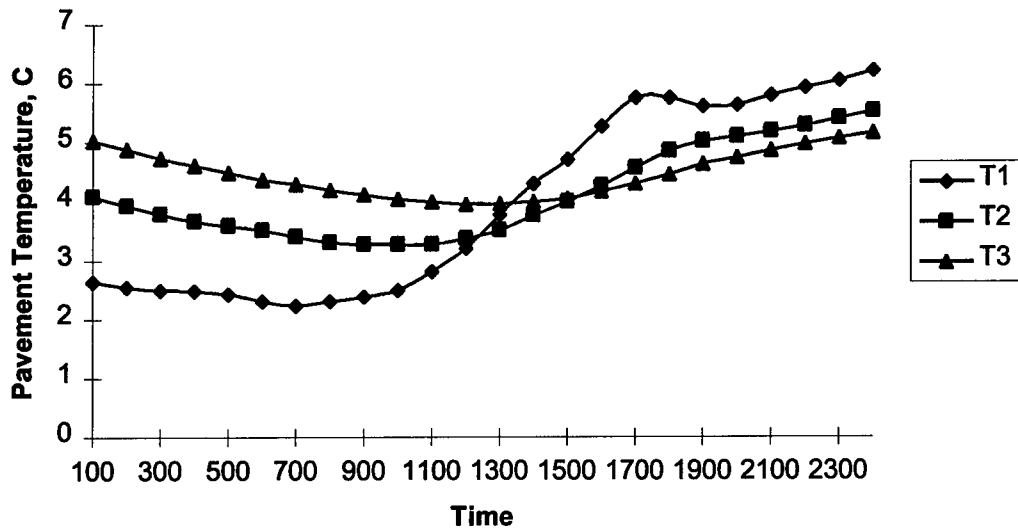
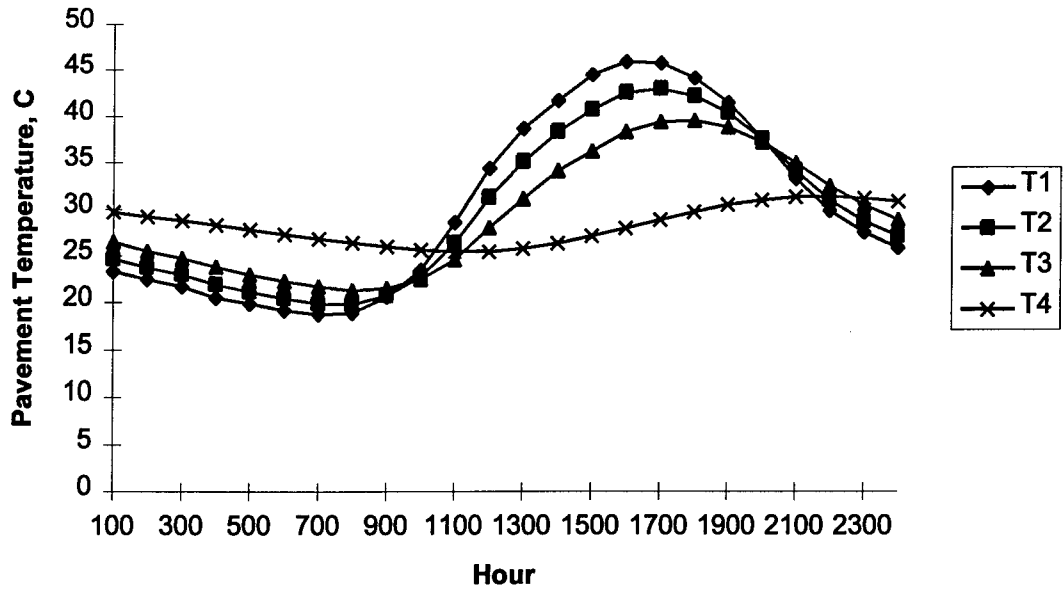


Figure D10. Pavement Temperature, SPS2-J12, Dec. 1, '96 and Jan. 1, '97

**SPS9-ODOT
August 1, 1996**



**SPS9-ODOT
September 1, 1996**

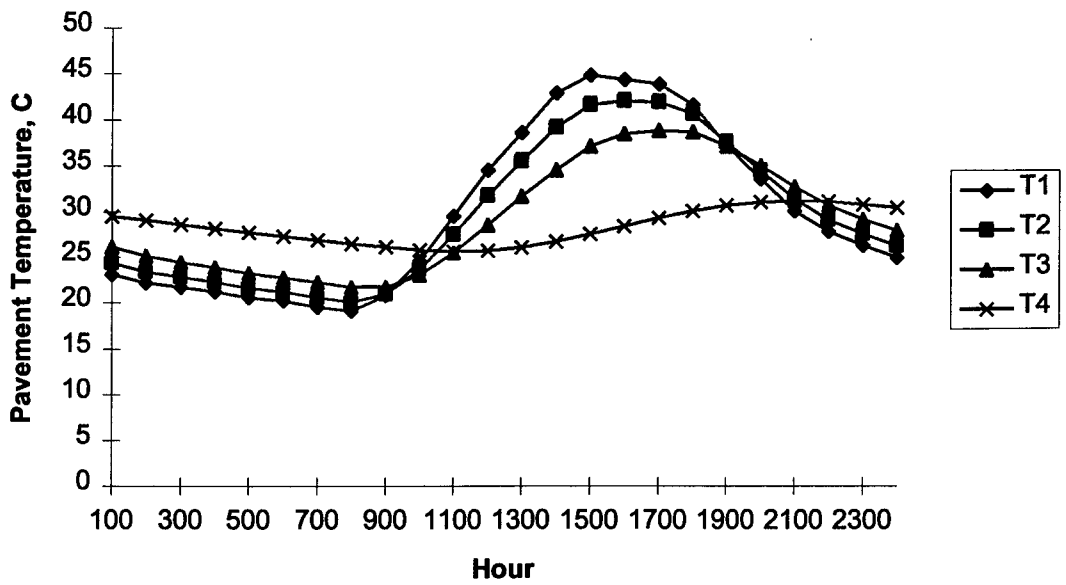
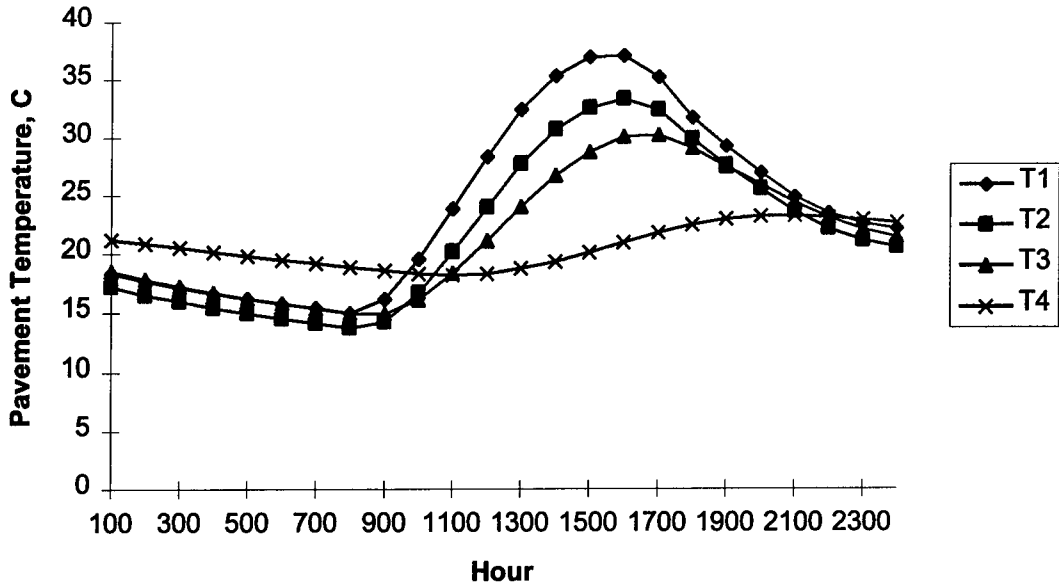


Figure D11. Pavement Temperature, SPS9-ODOT, August 1 and Sept. 1, 1996

**SPS9-ODOT
October 1, 1996**



**SPS9-ODOT
November 1, 1996**

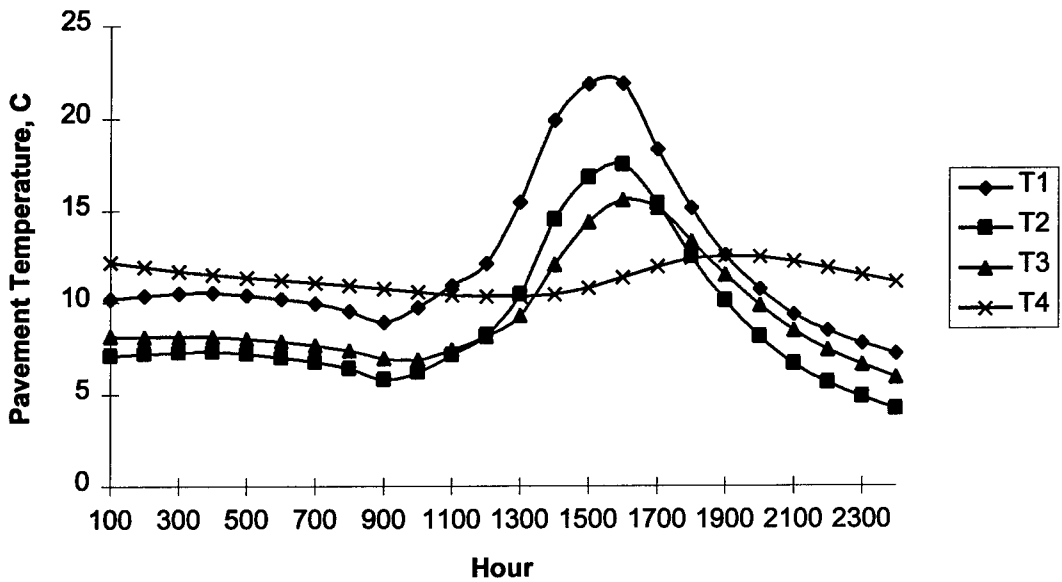
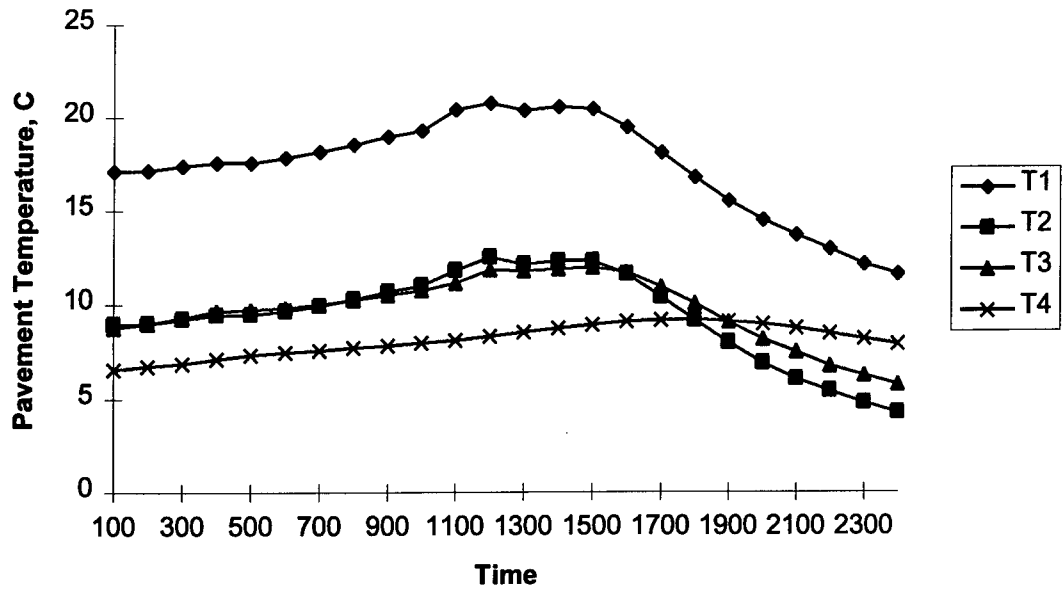


Figure D12. Pavement Temperature, SPS9-ODOT, October 1 and Nov. 1, '96

**SPS9-ODOT
December 1, 1996**



**SPS9-ODOT
January 1, 1997**

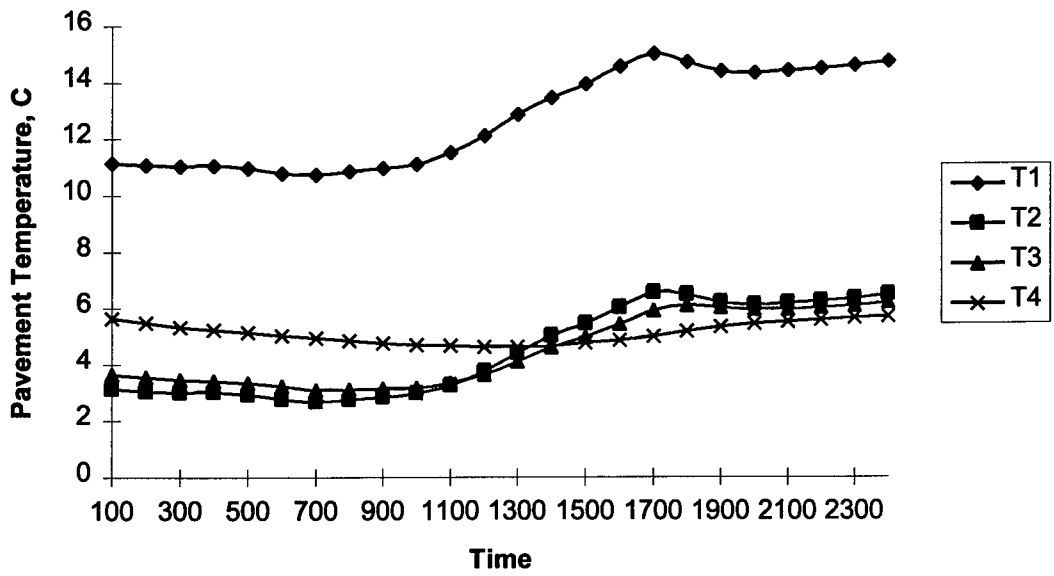


Figure D13. Pavement Temperature, SPS9-ODOT, Dec. 1, '96 and Jan. 1, '97

